

**The Regulation of Vascular Smooth Muscle Cell Phenotype and Function by Nitrite and
Mitofusin-1**

by

Christopher Ryan Reyes

Bachelor of Science, The Ohio State University, 2014

Submitted to the Graduate Faculty of the
Swanson School of Engineering in partial fulfillment
of the requirements for the degree of
Doctor of Philosophy

University of Pittsburgh

2020

UNIVERSITY OF PITTSBURGH

SWANSON SCHOOL OF ENGINEERING

This dissertation was presented

by

Christopher Ryan Reyes

It was defended on

July 8, 2020

and approved by

Partha Roy, Ph.D., Associate Professor, Department of Bioengineering and Department of Pathology

Sanjeev Shroff, Ph.D., Distinguished Professor and Gerald E. McGinnis Chair in Bioengineering, Department of Bioengineering

Adam Straub, Ph.D., Associate Professor, Department of Pharmacology and Chemical Biology

Prithu Sundd, Ph.D., Assistant Professor, Pulmonary, Allergy, and Critical Care Medicine and Department of Bioengineering

Dissertation Director: Sruti Shiva, Ph.D., Associate Professor, Department of Pharmacology and Chemical Biology

Copyright © by Christopher Ryan Reyes

2020

The Regulation of Vascular Smooth Muscle Cell Phenotype and Function by Nitrite and Mitofusin-1

Christopher Ryan Reyes, PhD

University of Pittsburgh, 2020

Restenosis is a clinical complication affecting 20% of people who undergo balloon angioplasty to treat atherosclerotic plaques. Restenosis is driven by vascular smooth muscle cell (VSMC) dysfunction. Physiologically, VSMC are the primary mediators of vessel tone, which respond to molecular and biomechanical cues to modulate blood flow. During restenosis, the endothelium is disrupted resulting in a local inflammatory response; consequently, VSMC transition from a highly-specialized contractile cell to a proliferative, synthetic phenotype. This results in increased migration to the intimal layer of the vessel where VSMC aberrantly proliferate (neointimal hyperplasia), decreasing lumen diameter and potentiating future infarct. Nitrite, an endogenously generated oxidation product of nitric oxide and regulator of mitochondrial function, has recently been suggested to attenuate restenosis after vascular injury. However, the mechanisms by which nitrite modulates VSMC proliferation and phenotypic switching remains unknown. Herein, we demonstrate nitrite has opposing effects on cellular proliferation versus phenotypic switching. First, we show that nitrite inhibits growth factor stimulated-proliferation of rat aortic smooth muscle cells (RASMC). This effect is dependent on inhibition of E3 ubiquitin ligase March5, which leads to upregulation of mitochondrial dynamics protein mitofusin-1 (Mfn1) and subsequent cell cycle arrest. In contrast, our data reveal that nitrite promotes RASMC migration and decreases contractile gene expression, consistent with switching from contractile to synthetic

phenotype. Notably, nitrite's effects on phenotypic switching were independent of Mfn1. To further investigate the interaction between nitrite and Mfn1 and its role in VSMC function *in vivo*, a smooth muscle cell-specific Mfn1 knockout (KO) mouse was generated. In a carotid artery ligation model to mimic restenosis after balloon angioplasty, Mfn1 KO mice exhibited significantly increased neointimal hyperplasia in response to injury compared to control animals. Oral administration of nitrite attenuated neointimal hyperplasia in Mfn1 KO mice but not wildtype mice. In sum, these data demonstrate that nitrite is a regulator of VSMC function both through the modulation of Mfn1 (for proliferation) and independent of this protein (for phenotypic switching). The implications of these data for nitrite as a potential therapeutic agent for neointimal hyperplasia as well as Mfn1 as a putative therapeutic target will be discussed.

Table of Contents

Preface..... xiv

1.0 Introduction.....1

1.1 Vascular Smooth Muscle Cells in Cardiovascular Diseases 1

1.1.1 Restenosis1

1.1.2 Vascular Smooth Muscle Cell Origin and Development3

1.1.3 Homeostatic Function of the Vascular Smooth Muscle Cell4

1.1.4 VSMC-Mediated Vasodilation by sGC/PKG Signaling.....7

**1.1.5 Vascular Smooth Muscle Cell Phenotypic Switching, Proliferation, and Cell
Cycle Regulation.....11**

1.2 Mitochondrial Dynamics..... 14

1.2.1 Fission Machinery14

1.2.2 Fusion Machinery.....16

1.2.3 Dynamics Crosstalk: Metabolism and the Cell Cycle20

1.2.4 Targeting Mitochondrial Dynamics in Cardiovascular Diseases.....23

1.3 NO and Nitrite: Physiological Functions and Role in Disease 25

1.3.1 NO: eNOS-dependent Enzymatic Production and Reduction of Nitrite.....25

1.3.2 Therapeutic Role of Nitrite in the Cardiovascular System30

**2.0 Mitofusin-1 is Upregulated by Nitrite to Inhibit Vascular Smooth Muscle Cell
Proliferation.....33**

2.1 Introduction 33

2.2 Materials & Methods 35

2.2.1 Reagents	35
2.2.2 Cell Culture.....	35
2.2.3 Transfection	36
2.2.4 Tritiated Thymidine Incorporation.....	36
2.2.5 Plasmid Purification & Transient Transfection	37
2.2.6 Protein Extraction & Western Blot Analysis.....	38
2.2.7 Immunoprecipitation	40
2.2.8 RNA Isolation and Real-Time PCR with TaqMan Reagents.....	41
2.2.9 Cell Cycle Analysis by Flow Cytometry	41
2.2.10 Confocal Microscopy.....	42
2.2.11 Statistics.....	43
2.3 Results.....	44
2.3.1 Nitrite Inhibits RASMC PDGF-Induced Proliferation through Mfn1 Upregulation	44
2.3.2 Nitrite Inhibits March5-Mediated Ubiquitination of Mfn1 to Upregulate its Protein Expression	52
2.4 Discussion	58
3.0 Nitrite and Mitofusin-1 Regulate Smooth Muscle Cell Phenotype	63
3.1 Introduction	63
3.2 Material & Methods	65
3.2.1 Reagents	65
3.2.2 Cell Culture.....	66
3.2.3 Transfection	66

3.2.4 RNA Isolation and Real-Time PCR.....	66
3.2.5 Scratch Assay	69
3.2.6 Measurement of Cellular ROS.....	69
3.2.7 Measurement of Cellular Energetics by XFe96 Extracellular Flux Bioanalyzer.....	70
3.2.8 Statistics.....	73
3.3 Results.....	73
3.3.1 Nitrite Promotes RASMC Phenotypic Switching.....	73
3.3.2 Nitrite-mediated VSMC Migration and Phenotypic Switching is Not Dependent on Mfn1	77
3.3.3 Nitrite and Mfn1 Alter RASMC Bioenergetics	81
3.3.4 Nitrite Promotes RASMC Phenotypic Switching by Increasing ROS Production.....	85
3.4 Discussion	91
4.0 Mitofusin-1 Regulates Smooth Muscle Cell Vasoreactivity and Proliferation <i>In</i> <i>Vivo</i>	97
4.1 Introduction	97
4.2 Materials & Methods	99
4.2.1 Reagents	99
4.2.2 Cell Culture.....	100
4.2.3 Transfection	100
4.2.4 Murine Model Generation	100

4.2.5 Cryosectioning and Tissue Preparation for IHC of OCT Embedded Tissue	103
4.2.6 Wire Myography	104
4.2.7 Radio Telemetry	105
4.2.8 Carotid Ligation Model	105
4.2.9 Deparaffinization and Immunofluorescence Staining	106
4.2.10 Confocal Microscopy.....	107
4.2.11 Masson’s Trichrome Staining	107
4.2.12 Light Microscopy.....	108
4.2.13 Nitrite Measurement	108
4.2.14 Protein Extraction & Western Blot Analysis.....	108
4.2.15 Measurement of cGMP	109
4.2.16 Measurement of Cellular ROS.....	110
4.2.17 Statistics.....	110
4.3 Results.....	111
4.3.1 Verifying Smooth Muscle Cell-specific KO of Mfn1.....	111
4.3.2 The Effects of SMC-specific Deletion of Mfn1 on Systemic Blood Pressure	113
4.3.3 SMC-specific KO of Mfn1 Alters Resistance but not Conduit Artery Vascular Function.....	116
4.3.4 Alterations in Response to Vascular Injury with SMC-specific KO of Mfn1	121
4.4 Discussion	126

5.0 General Discussion.....	132
5.1 Conclusions	132
5.2 Future Directions.....	133
5.2.1 How does nitrite inhibit March5-mediated ubiquitination to upregulate Mfn1?.....	133
5.2.2 How do nitrite and Mfn1 regulate VSMC phenotypic switching?	135
5.2.3 What are the roles of nitrite and Mfn1 in other vasculopathies?	136
Appendix A Supplemental Figures.....	139
Appendix A.1 Chapter 2.0	139
Appendix A.2 Chapter 3.0	141
Appendix A.3 Chapter 4.0	142
Appendix A.3.1 Mouse Model of Pulmonary Hypertension.....	145
Bibliography	146

List of Tables

Table 1: Primers for Plasmid Sequencing	37
Table 2: Antibodies used for Western blot analysis	39
Table 3: TaqMan Probes.....	41
Table 4: Antibodies for immunofluorescence microscopy	43
Table 5: Primers for Real-Time PCR	68
Table 6: Genotyping Primers.....	102
Table 7: Primary Antibodies for IHC of OCT Embedded Tissue.....	103
Table 8: Secondary Antibodies for IHC of OCT Embedded Tissue	104
Table 9: Primary Antibodies for IHC	106
Table 10: Secondary Antibodies for IHC	107
Table 11: Antibodies used for Western blot analysis	109

List of Figures

Figure 1: Regulation of Vascular Smooth Muscle Cell Contraction and Relaxation.....	6
Figure 2: Activation of sGC by Nitric Oxide, Stimulators, and Activators.....	10
Figure 3: Mitochondrial Dynamics Machinery.....	15
Figure 4: ATP Production through OXPHOS and Other Functions of Mitochondria.....	21
Figure 5: NO-Nitrite Cycle.....	27
Figure 6: Nitrite inhibits PDGF-induced proliferation	45
Figure 7: Nitrite stimulates mitochondrial fusion in RASMC.....	46
Figure 8: Nitrite upregulates Mfn1	48
Figure 9: Nitrite-mediated upregulation of Mfn1 is required to inhibit proliferation.....	50
Figure 10: Nitrite treatment arrests RASMC in G1-S phase progression	51
Figure 11: Nitrite upregulates Mfn1 by inhibiting its degradation.....	53
Figure 12: Nitrite inhibits ubiquitination of Mfn1.....	55
Figure 13: Nitrite inhibits March5 E3 activity to increase Mfn1 expression	57
Figure 14: Mechanism by which nitrite inhibits VSMC proliferation.....	59
Figure 15: Measuring mitochondrial respiration	72
Figure 16: Nitrite promotes RASMC migration	74
Figure 17: Nitrite decreases markers of contractile phenotype in RASMC.....	76
Figure 18: Nitrite promotes RASMC migration independent of Mfn1	78
Figure 19: Nitrite regulates contractile gene expression in RASMC independent of Mfn1	80
Figure 20: Nitrite and Mfn1 alter RASMC bioenergetics.....	84
Figure 21: Nitrite increases cellular ROS production.....	86

Figure 22: Nitrite requires oxidative enzyme activity to stimulate ROS production.....	88
Figure 23: Nitrite is dependent on ROS production to promote RASMC phenotypic switching	90
Figure 24: Nitrite promotes phenotypic switching by stimulating ROS production.....	91
Figure 25: Generation of smooth muscle-specific Mfn1 knockout mouse.....	101
Figure 26: Verification of efficient deletion of Mfn1 in SMC.....	112
Figure 27: Deletion of Mfn1 does not alter blood pressure	113
Figure 28: Blood pressure lowering effects of nitrite are unaffected by Mfn1 deletion.....	115
Figure 29: Conduit artery reactivity is unchanged with Mfn1 KO.....	117
Figure 30: cGMP production is not regulated by Mfn1	120
Figure 31: Nitrite attenuates neointimal hyperplasia in SMC-Mfn1^{-/-} mice	123
Figure 32: Nitrite increases vascular proliferation after carotid ligation <i>in vivo</i>	125
Figure 33: Mfn1^{-/-} mice are more susceptible to hypoxia-induced PH.....	138
Appendix Figure 1: Nitrite does not inhibit PDGF-induced cell cycle progression after serum starvation	139
Appendix Figure 2: Anti-proliferative effects of nitrite in normoxia are NO-dependent..	140
Appendix Figure 3: Nitrite does not prevent PDGF-induced decrease of RASMC contractile genes	141
Appendix Figure 4: Increase in Bay 58-stimulated mesenteric artery dilation in Mfn1^{-/-} mice is dependent on mitochondrial ROS	142
Appendix Figure 5: Deletion of smooth muscle Mfn1 alters MAP and HR.....	143
Appendix Figure 6: Tissue Nitrite Concentrations.....	144

Preface

I would like to acknowledge assistance from the University of Pittsburgh Center for Biological Imaging in all microscopy experiments, specifically in collaboration with Dr. Claudette St. Croix with help from Morgan Jessup and Katherine Helfrich. Additionally, I would like to acknowledge our collaborations with investigators at the University of Pittsburgh Vascular Medicine Institute, including Dr. Adam Straub with assistance from Scott Hahn who performed wire myography and radio telemetry as well as Dr. Delphine Gomez with assistance from Sidney Mahan who performed carotid ligation surgeries and assisted in tissue preparation. The work presented in this dissertation would not have been possible without the expertise of these individuals. Finally, I would like to thank Dr. Sruti Shiva for her mentorship as well as all members of her lab throughout my candidacy. It was the help from these people who supported me in my career endeavors and have prepared me to be an independent scientific investigator.

This work was supported by the University of Pittsburgh Berenfield Graduate Fellowship in Cardiovascular Bioengineering as well as the predoctoral NIH T32 Cardiovascular Bioengineering Training Program Fellowship.

1.0 Introduction

1.1 Vascular Smooth Muscle Cells in Cardiovascular Diseases

1.1.1 Restenosis

Restenosis is a clinical complication occurring in 20% of patients who undergo balloon angioplasty for the treatment of atherosclerotic plaques (Kim and Dean). Once a patient with coronary artery disease (CAD) has a plaque occluding >70% of the vessel, angioplasty is recommended per guidelines from the American College of Cardiology Foundation and the American Heart Association (Levine et al.). Angioplasty may also be implemented in patients presenting with symptomatic carotid artery stenosis size of >50% (Brott et al.). In either case, comorbidities such as diabetes mellitus or acute kidney injury as well as anatomical limitations of the stenotic artery may alter clinical decision making to alternative revascularization procedures, such as coronary artery bypass graft or carotid endarterectomy.

During an angioplasty procedure, a balloon catheter is placed into the circulation, typically through the femoral artery, and threaded through, until it reaches the stenosis. Once near the stenotic area, the catheter is expanded, thereby compressing the plaque and restoring luminal blood flow. In some instances, stenting is used in addition to balloon angioplasty. This is a situation in which a metal or polymer-based stent surrounding the balloon catheter is applied to the plaque upon balloon expansion and is left indefinitely over the stenosis, suppressing any future growth or plaque rupture (Kim and Dean; Borhani et al.). The advent of angioplasty has improved clinical outcomes significantly, with over 90% success rate of patients undergoing the procedure as defined

by <50% stenosis occlusion of the vessel (Savage et al.). However, restenosis can occur following the procedure, in which vessel remodeling causes stenotic growth, potentiating thrombus formation and vessel occlusion. The additional utilization of stents during angioplasty has significantly reduced incidence of restenosis from 60% to between 10% and 20%. Even accounting for the significant impact from stent technology, approximately 200,000 patients experience restenosis annually in the United States and it thus remains a significant clinical problem (Wassif and Welt).

Pathogenesis of restenosis is initiated by vessel damage incurred during and following procedures due to disruption of the luminal endothelium and exposure of the underlying extracellular matrix (ECM), vascular recoil, and in some instances thrombus formation (Wassif and Welt). This vascular injury initiates a natural wound healing process, in which platelets localize to the site of injury by binding to the ECM. Once platelets become activated and adhere to the injury site, surface P-selectin presented by platelets recruits circulating leukocytes to the stenosis, which migrate into the plaque site and recruit additional inflammatory cells (Inoue et al.). All of these cells secrete a number of inflammatory signaling molecules, such as platelet-derived growth factor (PDGF), vascular endothelial growth factor (VEGF), tumor necrosis factor alpha (TNF- α), and interleukin-6 (IL-6), creating a local milieu of inflammatory signaling molecules (Ahanchi et al.). These initial inflammatory events occur rapidly after vessel injury, on the order of hours to days, however cytokines release remains sustained for a year or more (Marx et al.; Jukema et al.; Wasser et al.). In response to cytokines, vascular smooth muscle cells (VSMC) within the medial layer of the vessel wall migrate to the intimal layer where they aberrantly proliferate in a process called neointimal hyperplasia, effectively decreasing luminal diameter. This constrictive remodeling, beginning at approximately 3 to 5 weeks after angioplasty,

potentiates future risk of stroke or myocardial infarction in these patients. By understanding the underlying mechanisms of neointimal hyperplasia due to VSMC migration and proliferation, the hallmark of restenosis, new therapies can be developed to reduce the risk of cardiovascular events after balloon angioplasty and any other disorders involving smooth muscle cell proliferation including atherosclerosis and hypertension (Frismantiene et al.).

1.1.2 Vascular Smooth Muscle Cell Origin and Development

Vascular smooth muscle cells arise beginning in week 4 of human embryogenesis (day 8.5 in mice) from multiple origins. VSMC derive primarily from the mesoderm with partial contribution from the ectoderm of the neural crest (Bacakova et al.). Many of the signals that drive differentiation of VSMC during development emanate from endothelial cells (EC), which originate earlier in development (Takahashi et al.). In the initial stages of embryogenesis, ECs exist as progenitor cells, or angioblasts, which form nascent tubes that will ultimately develop into fully formed blood vessels. ECs secrete factors such as VEGF and PDGF which recruit VSMC to form new vessels (vasculogenesis) or sprout from existing vessels (angiogenesis) (Lilly; Adams and Eichmann). Conversely, VSMC secrete factors like angiopoietin 1, which binds Tie2 receptors of neighboring ECs, suppressing further recruitment of additional VSMC. In addition, ECs recruit mural cells including pericytes, which further stabilize nascent vessels.

Once a nascent vessel is formed, VSMC differentiation is required for the contractile function observed in mature vessels. The differentiation of smooth muscle cells into a highly-specialized, functioning cell type is tightly regulated by a number of factors, the majority of which involve transcriptional events initiated by signaling molecules from the local microenvironment, as well as the surrounding mechanical forces. Endothelial-smooth muscle cell crosstalk remains

crucial to VSMC differentiation and vessel maturation. One example of this cross-talk is Notch signaling between neighboring ECs and VSMCs, whereby ECs present transmembrane ligands Jagged1/2 and Delta like 1,3, and 4 which bind to Notch1-4 on VSMCs (Boucher et al.; Lilly). This leads to translocation of Notch to the nucleus where it is able to initiate transcription of many genes, including those regulating VSMC phenotype. This transcriptional regulation coordinating maturation of VSMC into a functional, contracting phenotype occurs primarily at CArG *cis*-elements. In addition to Notch, factors such as serum response factor (SRF) and members of the SMAD and FOXO families also regulate transcription at these sites (Mack). Many of the downstream targets of these signaling pathways are master regulator transcription factors of VSMC plasticity, such as Myocardin and Ten-Eleven Translocation-2 (TET2) (Z. Xu et al.; R. Liu et al.). These master regulators induce expression of contractile genes such as Acta2 and Myh11, driving VSMC differentiation into a functional cell type which is able to perform its physiological function of vessel contraction (Gomez, Swiatlowska, et al.; Manabe and Owens).

1.1.3 Homeostatic Function of the Vascular Smooth Muscle Cell

Once formed, VSMC are the cells responsible for preserving vascular homeostasis, providing structural integrity and mediating contraction and dilation of the vessel wall. The primary physiological function of VSMC is to maintain vascular tone within the vessel wall of large arteries and arterioles. Extracellular signaling molecules and environmental cues may modulate either contraction or relaxation of muscle fibers in these cells, eliciting changes in blood pressure. Contraction within the smooth muscle layers of blood vessels are mediated by actin-myosin bundles (**Figure 1**). However, they lack the organizational sarcomeric reticulum found in skeletal and cardiac muscle (Herrera et al.). Briefly, myosin binds ATP and hydrolyzes it to ADP

and P_i , inducing a conformational change into a high force generating state of the myosin head that favorably binds actin filaments (Brozovich et al.). Upon actin binding and release of ADP and P_i , a power stroke occurs that pulls actin filaments, contracting the cell and decreasing lumen diameter. As blood pressure (BP) is the product of cardiac output (CO) and vascular resistance (VR), systemic blood pressure then increases. A subunit of myosin, myosin light chain (MLC), is a target for phosphorylation by myosin light chain kinase (MLCK) and dephosphorylation by myosin light chain phosphatase (MLCP) (Frismantiene et al.; Kamm and Stull; ALESSI et al.). When MLC is phosphorylated, myosin ATP hydrolysis rate increases 1000-fold, allowing for rapid contraction within a cell (Sellers and Adelstein). Thus, the phosphorylation status of myosin determines the contractility of the cell at a given state.

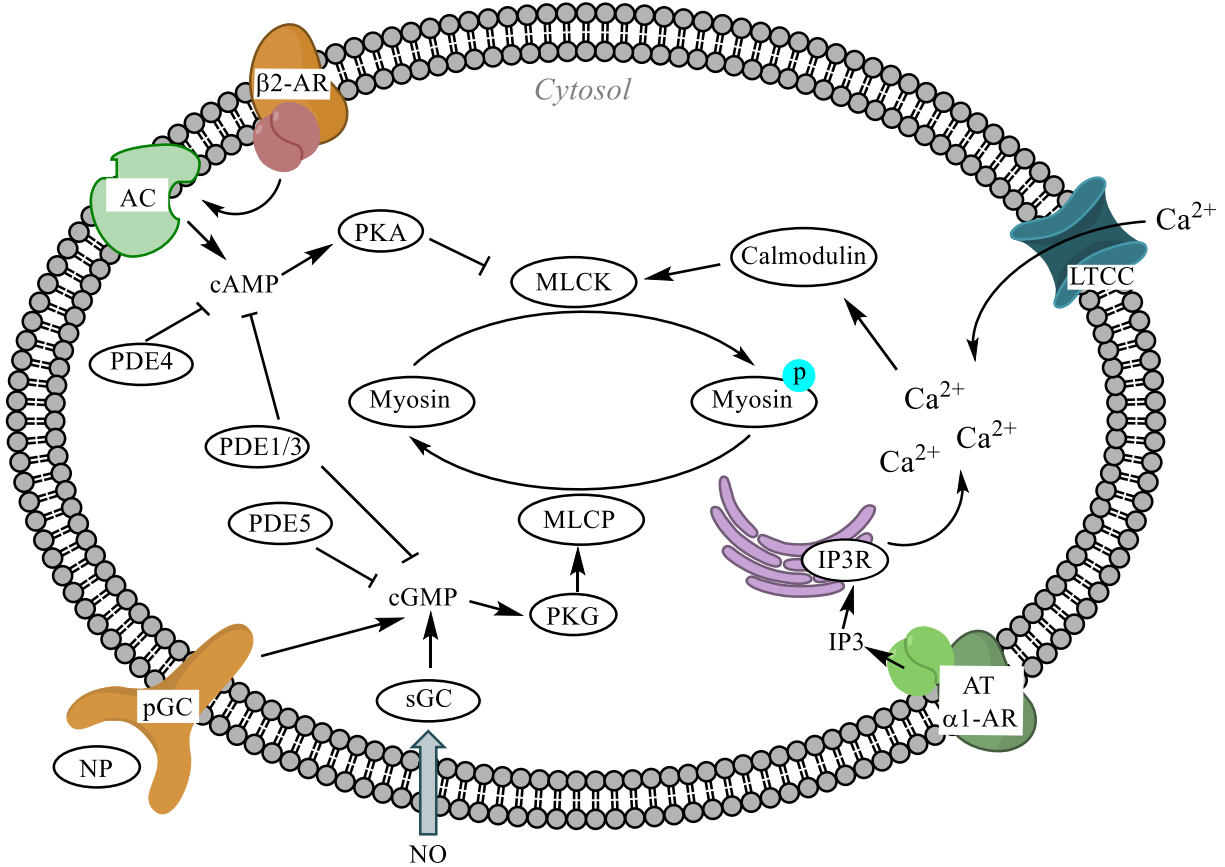


Figure 1: Regulation of Vascular Smooth Muscle Cell Contraction and Relaxation. Schematic of the molecular machinery in VSMC that regulate contractility. Myosin light chain kinase (MLCK) phosphorylates myosin to increase contractile activity, whereas myosin light chain phosphatase (MLCP) dephosphorylates myosin to promote VSMC relaxation. Many upstream signaling events lead to activation of PKA and PKG through production of secondary messengers cAMP and cGMP respectively, which under most physiological conditions promote VSMC relaxation. When adenylate cyclase (AC) is activated, such as by beta-2 adrenergic receptor ($\beta 2$ -AR), it produces cAMP which can be degraded by phosphodiesterase (PDE) 1, 3, and 4. Production of cGMP is performed by the guanylate cyclases (GC), which may be hydrolyzed by PDE1/3 or PDE5. Membrane-bound particulate GC (pGC) is activated upon binding of natriuretic peptides (NP), while soluble GC (sGC) is activated upon binding (termed nitrosylation) by nitric oxide (NO) which diffuses across the cell membrane. Contraction is promoted by the presence of increased cytosolic concentrations of calcium (Ca^{2+}) which may enter the cell through L-type calcium channels (LTCC) or be released from the ER through inositol

triphosphate (IP₃) signaling upon activation of receptors such as angiotensin receptor (AT) or alpha-1 adrenergic receptor (α 1-AR).

Many factors contribute to VSMC contractility, such as external signaling molecules, actin availability, activity of MLCK and MLCP, and ATP levels. Akin to other types of muscle, vascular smooth muscle also relies heavily on calcium influx for initiating contraction. Specifically, one of the canonical signaling pathways for muscle contraction in VSMC is mediated by calcium/calmodulin-dependent activation of MLCK (Kamm and Stull). Numerous molecules are involved in regulating cytosolic calcium in VSMC, such as angiotensin, adrenergic receptor agonists, and L-type calcium channels. At high calcium concentrations, calmodulin binds calcium resulting in an “open” conformation that increases probability of calmodulin interacting with other proteins (Chin and Means). This complex binds MLCK, resulting in a conformational change that removes an autoinhibitory domain on MLCK, leading to activation of MLCK phosphorylation activity (Mizuno et al.). MLCK then phosphorylates myosin to induce muscle contraction. Calcium-independent pathways leading to muscle contraction also exist in smooth muscle, such as RhoA/ROCK mediated phosphorylation of MLCP (Brozovich et al.). This inhibits phosphatase activity of MLCP, thereby maintaining the phosphorylation status of MLC and muscle contraction.

1.1.4 VSMC-Mediated Vasodilation by sGC/PKG Signaling

In addition to contraction, VSMC are also able to relax in order to dilate blood vessels. There are a number of signaling pathways leading to smooth muscle relaxation, the majority of which rely on the nucleotides cyclic adenoside monophosphate (cAMP) and cyclic guanosine monophosphate (cGMP). In VSMC, cAMP induces relaxation in VSMC through activation of

cAMP-dependent protein kinase (PKA) which phosphorylates and inhibits MLKC (Horman et al.). Alternatively, cGMP binds cGMP-dependent protein kinase (PKG) (Hofmann). Upon binding, PKG is activated as its autoinhibitory domain is released to reveal the catalytic domain. PKG then phosphorylates many protein targets, including MLCP. This phosphorylation increases MLCP phosphatase activity, resulting in increased dephosphorylation of MLC and VSMC relaxation.

In order to properly maintain vessel tone, the relative levels of these nucleotides are tightly regulated. The conversion of GTP to cGMP is performed by guanylate cyclases (GCs), of which there are two forms: transmembrane bound or particulate GC (pGC) and soluble GC (sGC) (Kuhn). A number of natriuretic peptide hormones bind to pGC to mediate intracellular cGMP and perform physiological vasodilation (Sharma and Duda). More related to the contents of this dissertation is sGC, the primary receptor for nitric oxide (NO) *in vivo*. Soluble GC is a dimeric guanylate cyclase that contains a heme prosthetic group to which NO coordinates (Montfort et al.). Redox state of the heme-iron is essential to sGC activity (Shah et al.). Specifically, the binding of NO to ferrous [Fe(II)] sGC is remarkably sensitive, with concentrations in the picomolar range eliciting cGMP production (Batchelor et al.). This is due to release of the proximal histidine of heme which results in a planar geometry and conformational change of sGC. Upon NO binding, sGC activity increases 100 to 200-fold, allowing rapid cGMP production and downstream signaling to elicit PKG-dependent relaxation (Louis J. Ignarro et al.; Francis et al.). Ferric heme [Fe(III)] may also bind NO, however its affinity is greatly reduced (Zhao et al.). In this way, NO-sGC signaling promotes VSMC relaxation and vasodilation.

A number of pharmacological agents have been developed to target cGMP-PKG signaling to promote physiological vasodilation, especially in the context of cardiovascular disease (**Figure 2**). As a signaling molecule at the nexus of NO-mediated vasodilation, sGC has been a target of

these pharmaceuticals. Soluble guanylate cyclase stimulator and activator molecules are the main classes of drugs that have been developed to increase sGC activity (Evgenov et al.). Stimulator molecules, such as Bay 41-2272, are dependent on the presence of reduced heme of sGC. Recent insights from structural studies reveal that these compounds bind the H-NOX domain of the sGC β 1 subunit containing the heme pocket where binding to gaseous molecules occurs, resulting in activation of the enzyme (Wales et al.). Additionally, it has been proposed that stimulators either bind preferentially to or induce a sGC folding confirmation with increased NO-binding affinity. Thus in the presence of both stimulator and NO, sGC exhibits a synergistic increase in cGMP production. As opposed to stimulators, activator molecules such as Bay 58-2667 act independently of the oxidation state of sGC and preferentially activate either oxidized or heme-free sGC (Stasch et al.). Recent crystallization and structure determination of H-NOX bound to Bay 58-2667 provide evidence that these compounds actually displace heme and non-covalently bind to sGC (Martin et al.). Currently, a number of stimulators and activators are undergoing clinical trials for various indications. As proof of concept for pharmacological targeting of sGC, the stimulator Riociguat has been approved for treatment of pulmonary arterial hypertension (PAH) (Sandner et al.).

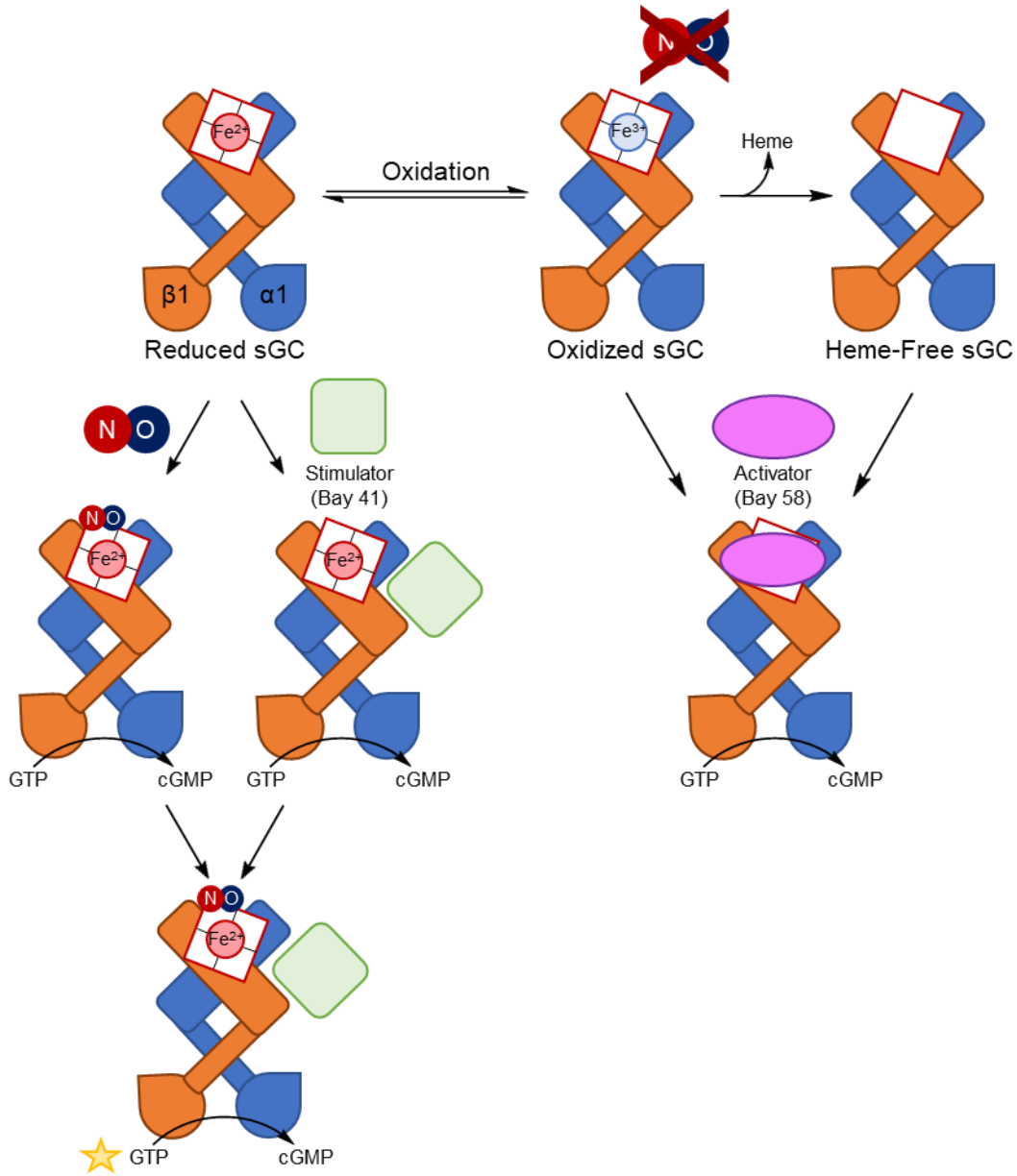


Figure 2: Activation of sGC by Nitric Oxide, Stimulators, and Activators. Soluble GC exists as a heterodimer comprised of α and β subunits. When the heme bound to the H-NOX domain of the β subunit is in its reduced form (Fe^{2+}), NO binds the iron resulting in dissociation of the distal histidine causing a conformational change that increases cyclase activity. Stimulator molecules such as Bay 41 bind allosterically which induces a similar conformational change and activate of the enzyme. Additionally, stimulator binding increases sGC affinity for NO resulting in a synergistic increase in cGMP production when both NO and stimulator are present.

Alternatively, sGC can be oxidized (Fe^{3+}) under certain physiological conditions and in this state, sGC is desensitized to NO. Additionally, oxidization of sGC causes a conformational change resulting in an open heme binding pocket, eventually leading to dissociation of the heme prosthetic group (Pan et al.). Activator molecules such as Bay 58 increase cGMP production through activation of either the oxidized or heme-free form of sGC by replacing the heme group.

In addition to strategies to promote production of cGMP, a number of therapeutics have been developed to inhibit hydrolysis of cGMP. Degradation of cAMP and cGMP are regulated by phosphodiesterases (PDEs), which hydrolyze cAMP and cGMP to AMP and GMP respectively (Lehners et al.). The isoforms of PDE known to be expressed in VSMC include PDE1 and PDE3 which hydrolyze both cAMP and cGMP, PDE4 which is specific to cAMP, and cGMP-specific PDE5 (Rybalkin et al.; Zhai et al.). Specifically, sildenafil and other agents targeting cGMP hydrolysis by PDE5 have been successful clinically, notably in the treatment of erectile dysfunction (ED) and pulmonary arterial hypertension (PAH) (Jeremy et al.; Francis and Corbin; Ramani and Park). These data demonstrate that studying mechanism of VSMC function is essential to understanding vascular biology and modulation of VSMC function can play a significant role in modifying disease pathologies.

1.1.5 Vascular Smooth Muscle Cell Phenotypic Switching, Proliferation, and Cell Cycle Regulation

Although VSMC play a specific physiological role in vascular homeostasis and are highly differentiated to perform this task, VSMC may undergo a phenotypic switch, shifting from this contractile phenotype to what is termed a synthetic phenotype. VSMC synthetic phenotype is

characterized by secretion of extracellular matrix components, expression of metalloproteinases and adhesion factors, loss of contractile protein expression and function, and increased rates of migration and proliferation (Frismantiene et al.; Allahverdian et al.; House et al.). VSMC may occupy any point on the spectrum from contractile to synthetic phenotype depending on mechanical and biochemical cues, with recent evidence suggesting this is the result of chromatin remodeling via epigenetic regulation (Gomez, Swiatlowska, et al.; Bennett et al.). Furthermore, the VSMC are able to transition to other cell types of varying characteristics, adopting macrophage-like, mesenchymal-like, and even osteochondrogenic-like qualities (Durham et al.; Liu and Gomez). In atherosclerosis, monocytes and macrophages secrete inflammatory signaling molecules such as IL-1, IL-6, TGF- β , and PDGF which induce phenotypic-switching in VSMC (Libby). Uptake of high concentrations of free cholesterol and oxidized lipids by either macrophages or VSMC themselves leads to foam cell formation which secrete additional inflammatory molecules and expedite this process. Atherosclerotic lesions form locally at sites of inflammation and are characterized by VSMC migration and proliferation (Allahverdian et al.).

During angioplasty, the vascular injury and downstream mechanisms can lead to restenosis as described in **Section 1.1.1**, further contributing to the pathogenesis of atherosclerosis. However, the exact mechanisms leading to VSMC phenotypic switching and proliferation remain unclear. Recent evidence using lineage tracing techniques suggests that regulation of phenotypic plasticity, migration, and proliferation may be independently controlled processes which can occur either simultaneously or independent of each of each (Chappell et al.). Data from this publication and others also suggest that VSMC phenotypic switching and proliferation may be drive by clonal expansion, with individual VSMC contributing to propagation of lesion growth (Feil et al.; Chappell et al.; Liu and Gomez). Although knowledge gaps still remain in our understanding of

VSMC phenotypic switching and proliferation in atherosclerosis and restenosis, these processes undoubtedly play a significant role in maintaining physiological homeostasis and can significantly impact disease pathogenesis. By further understanding the endogenous mediators and processes that govern VSMC phenotype and proliferation, new therapeutic strategies may be developed.

Evidence from drug-eluting stents (DES) has proven that inhibition of cellular migration and proliferation at the sight of injury is successful in reducing rate of restenosis occurrence (Marx et al.). VSMC proliferation is governed by cell cycle progression, during which cyclins bind their respective cyclin-dependent kinases (CDKs) at specific phases of the cell cycle to activate necessary cellular machinery. During G₁ phase, synthesis of transcriptional machinery need for DNA replication in S phase occurs (Chaabane et al.). After S phase, cells enter G₂ phase, expressing proteins required for mitosis (M phase). The major cell cycle checkpoints occur at G₁-S phase and G₂-M phase, as these steps are significant commitments in terms of resource expenditure by the cell. Endogenous cell cycle inhibitors (CKIs), such as p21^{Cip1} and p27^{Kip1}, repress CDKs, thereby inhibiting cellular proliferation at these checkpoints. Under homeostasis, VSMC reside in a quiescent, G₀ phase of the cell cycle. Cytokines and mitogens such as PDGF or IL-6 activate VSMC to initiate cell cycle entry into G₁ phase. In atherosclerosis and other models of vascular injury, CKI expression is decreased within the vessel wall (Boehm et al.). Localized overexpression of p21^{Cip1} has also been shown to inhibit neointimal hyperplasia after vessel injury, demonstrating the protective role of CKIs in restenosis pathogenesis (Chang et al.). The pharmacological agents incorporated in DES specifically inhibit cellular proliferation through regulation of cell cycle machinery. Rapamycin, also known as Sirolimus, binds mTOR, inhibiting many Akt-mediated phosphorylation events leading to cell cycle entry, progression, and proliferation while also increasing levels of p27^{Kip1} (Marx et al.). Paclitaxel, another commonly

used drug in DES, binds to β -tubulin to inhibit microtubule dynamics, a process required for mitotic division of the cell (Borhani et al.).

These pharmacological agents illustrate the effectiveness of targeting cell cycle progression in restenosis and potentially other diseases involving hyperproliferative VSMC. Although DES have greatly reduced restenosis occurrence, complications such as late-stage thrombosis still occur (Borhani et al.). Additionally, the exact endogenous mediators that regulate VSMC phenotypic switching and increased proliferation are still not entirely understood. The mitochondrion is a cellular organelle responsible for numerous functions, including oxidative phosphorylation through the electron transport chain (ETC) and initiation of apoptosis via cytochrome *c* release. Recent evidence has emerged suggesting that mitochondria and, specifically, the process of mitochondrial dynamics, are intimately linked to cell cycle progression and proliferation in VSMC. In the next section, I will describe mitochondrial dynamics, its role in regulation of the cell cycle, and its potential as a therapeutic target in restenosis and other cardiovascular-related disorders.

1.2 Mitochondrial Dynamics

1.2.1 Fission Machinery

Over the past few decades, mitochondrial dynamics has emerged as a key regulator of mitochondrial function and overall cellular homeostasis. Dynamics is defined collectively as the processes by which mitochondrial networks form (fusion) and break apart (fission) in the cell.

Over the past few decades, the essential molecular machinery involved in mitochondrial dynamics have been discovered (**Figure 3**).

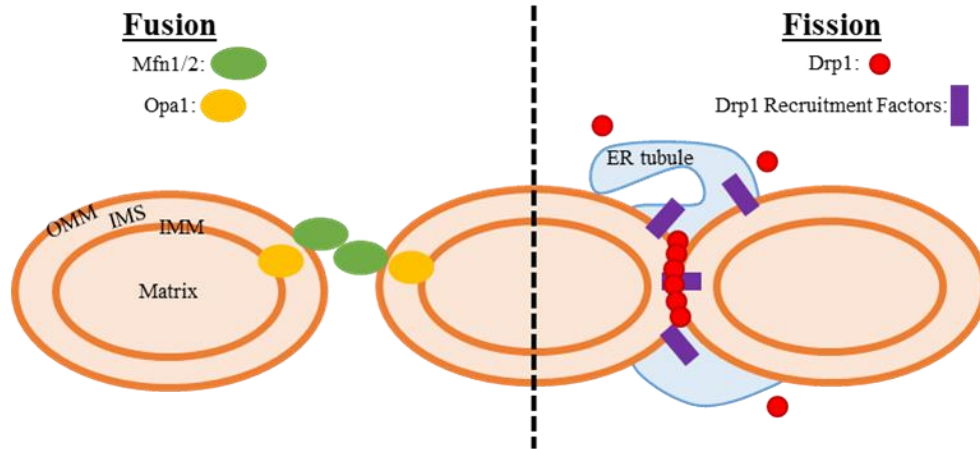


Figure 3: Mitochondrial Dynamics Machinery. Schematic of proteins involved in molecular regulation of mitochondrial morphology adapted from van der Bliek et al. Mitofusin 1 and 2 (Mfn1/2) regulate fusion of the outer mitochondrial membrane (OMM) while optic atrophy 1 (Opa1) is responsible for inner mitochondrial membrane (IMM) fusion. Fission is mediated by the cytosolic protein dynamin-related protein 1 (Drp1) which is recruited to the OMM by various factors such as Fis1 or Mff. Recent evidence has show that constriction by endoplasmic reticulum (ER) tubules at sites of localized Drp1 oligomerization is required for fission of mitochondria to occur.

Mitochondrial fission is coordinated primarily by the cytosolic protein Dynamin-related protein 1 (Drp1). For fission to occur, mitochondria are first pre-constricted by endoplasmic reticulum (ER) tubules (Friedman et al.). In response to certain stimuli, Drp1 is recruited to the outer mitochondrial membrane (OMM) at ER contacts by binding to one or more of its OMM bound binding partners, which include Fis1, Mff, MiD49, and MiD51 (Losón et al.; Otera et al.;

Palmer et al.). This increased avidity of Drp1 localized to ER-mitochondria contact sites and potentiates the oligomerization of Drp1 dimers. Following assembly of high-order oligomers, it has been proposed that these Drp1 filaments encircle the mitochondrial membrane and constrict, resulting in budding off of two new mitochondrial fragments which results in mitochondrial fission (Fröhlich et al.). While Drp1 is known as the predominant mitochondrial fission protein, recent work suggests the protein Dnm2 actually catalyzes the final step of fission through its membrane scission activity (Tilokani et al.).

Nevertheless, modulation of Drp1 activity can drastically alter mitochondrial morphology. Drp1 is primarily regulated via multiple post-translational modifications, including phosphorylation. A number of kinases phosphorylate Drp1 at serine 616, including CDK1, ERK2, and PKC (Marsboom et al.; Kashatus et al.; Lim et al.). This results in Drp1 translocation to the mitochondria, promoting mitochondrial fission (Breitzig et al.). Of note, Drp1 may react with NO and undergo *S*-nitrosation (see **Section 1.3.1** for definition) at cysteine 644 (Soonpaa et al.). It has recently been shown that *S*-nitrosation at this residue increases the phosphorylation of Drp1 at serine 616, thereby promoting mitochondrial fission (Lee and Kim; Bossy et al.). Alternatively, Drp1 may be phosphorylated at serine 637 by a number of kinases, such as protein kinase A (PKA), which inhibits Drp1 fission activity thereby promoting fusion (Chang and Blackstone). Thus, the phosphorylation state of Drp1 is a major determinant of the overall mitochondrial morphology within a cell.

1.2.2 Fusion Machinery

Less understood than fission is the process of mitochondrial fusion. Mitofusin-1 (Mfn1) and mitofusin-2 (Mfn2) are the predominant mediators of OMM fusion, while optic atrophy-1

(Opa1) mediates inner mitochondrial membrane (IMM) fusion. The structures of Mfn1 and Mfn2 consist of an N-terminal GTPase domain and heptad-repeat domain both residing in the cytosol (Cohen and Tareste). This is followed by a transmembrane region which spans the OMM. Recent evidence suggests that a C-terminal, second heptad-repeat region resides in the mitochondrial intermembrane space, as opposed to folding back into the cytosol as previously theorized (Mattie et al.). Mfn1 and Mfn2 monomers may bind either one another (homodimers) or the other paralog (heterodimers) on either the same mitochondrial membrane or on adjacent mitochondria. Of note, both paralog must perform GTP hydrolysis which results in a conformational change that favors dimerization (Cao et al.). In a test tube, Mfn1 GTPase activity has been reported to be 8-fold higher than Mfn2 (Ishihara). Furthermore, mitochondrial fusion via Mfn1 has a 100-fold higher rate than Mfn2, suggesting Mfn1 is the primary mediator of membrane fusion. In addition to its role in mediating OMM fusion, Mfn2 (but not Mfn1) has been proposed to be a mediator of mitochondrial tethering to the ER, however recent evidence suggests it may actually act as an antagonist to ER tethering (de Brito and Scorrano; Filadi et al.). Although GTPase activity has shown to be required for mitochondrial fusion, the exact mechanism of membrane fusion remains unknown. One theory is that the region heptad-repeat region may actually destabilize the lipid membrane, promoting the fusion of adjacent lipid membranes, while another theory has suggested that OMMs fuse through large, circular docking complexes consisting of Mfn1/2 (Daste et al.; Brandt et al.).

In general, modulation of OMM fusion facilitated by Mfn1 and Mfn2 is regulated through post-translational modifications. These modifications to Mfn1 and Mfn2 regulate mitochondrial dynamics by either modulating their fusion activity or changing their relative protein levels. ERK phosphorylates Mfn1 at threonine 562, which results in mitochondrial fragmentation and increased apoptosis (Pyakurel et al.). Mfn1 also contains an acetylation site at lysine 491. Although the

acetyl-transferase which acetylates Mfn1 has not been determined, SIRT1 and HDAC6 has been identified as a potential deacetylases at this site (J.-Y. Lee et al.; Oanh et al.). The acetylated form of Mfn1 preferentially binds E3 ligase March5, which polyubiquitinates Mfn1 but not Mfn2 (Y-Y Park et al.; Yong-Yea Park, Lee, et al.). Polyubiquitination of a protein results in its translocation to the proteasome, where it undergoes degradation via proteolysis. Mfn2, while not a target of ERK, is phosphorylated by Jnk which promotes ubiquitination by E3 ligase Huwe1, targeting Mfn2 for degradation (Leboucher et al.). Mfn2 may also be phosphorylated by PKA at serine 442, however phosphorylation has effects on cell proliferation and function independent of mitochondrial morphology (Zhou et al.). Recent evidence has also highlighted the presence of redox sensitive cysteines on both Mfn1 and Mfn2 located on the heptad-repeat region within the intermembrane space which, upon oxidation, results in disulfide bridge formation with adjacent mitofusins (Mattie et al.). This covalent linkage induces fusion, suggesting that Mfn1 and Mfn2 may act as cellular redox sensors through a post-translational modification to modulate mitochondrial reactive species (ROS) production in response to oxidative stress. Finally, both Mfn1 and Mfn2 are targets for E3 ligase Parkin, which polyubiquitinates both Mfn1 and Mfn2 to promote degradation (Gegg et al.).

Downstream of OMM fusion is IMM fusion, which is mediated by Opa1. Opa1, also a GTPase, resides on the IMM. Similar to the other prominent mitochondrial dynamics protein, GTP hydrolysis is required to perform fusion efficiently (Ban et al.). Once OMM fusion is complete, the IMMs of two adjacent mitochondria are exposed to each other within the intermembrane space. Opa1 is able join the IMMs, either by *trans*-complex formation with Opa1 (homotypic) or binding to IMM-bound lipids (heterotypic) such as cardiolipin (Ban et al.; Ge et al.). Both homotypic and heterotypic binding allow for membrane lipid exchange between mitochondria. However,

exchange of contents within the mitochondrial matrices occurs only with homotypic binding (Ge et al.). Opa1 regulation is complex, with 8 known splice variants identified to date. Additionally, its fusion activity is regulated via proteolytic cleavage by OMA and YME1L to two distinct forms, L-Opa1 and S-Opa1 respectively (Tilokani et al.). L-Opa1, the membrane bound form, promotes mitochondrial fusion and is required for lipid merging, while the soluble S-Opa1 is unable to fuse lipids in the absence of L-Opa1. Instead, evidence suggests the primary function of S-Opa1 is to maintain cristae formation (H. Lee et al.). Differential activity and expression of each of fusion proteins and their balance with Drp1 expression and activity regulates the mitochondrial morphology and function of the cell.

1.2.3 Dynamics Crosstalk: Metabolism and the Cell Cycle

Mitochondrial dynamics have been implicated in numerous cellular processes, including metabolism, ROS production, and apoptosis (Westermann, “Mitochondrial Fusion and Fission in Cell Life and Death.”). Maybe most directly, dynamics are crucial for maintenance of overall mitochondrial health. Mitochondria produce ATP via oxidative phosphorylation (OXPHOS) through the electron transport chain (ETC), which is composed of 5 protein complexes that span the IMM (see **Figure 4** for in-depth summary). Electrons enter the ETC at complexes I and II from reducing equivalents produced via the TCA cycle. Electrons travel through the ETC until they reach complex IV, which catalyzes the transfer of electrons from reduced cytochrome *c* to the terminal electron acceptor, molecular oxygen, resulting in oxygen consumption and its reduction to form water. The transfer of electrons through the ETC is coupled to proton shuttling from the mitochondrial matrix to the inner membrane space, creating an electrical potential and proton gradient. Protons then travel down their electrochemical gradient through complex V of the ETC, ATP synthase, which utilizes this protonmotive force to convert ADP to ATP through oxidative phosphorylation.

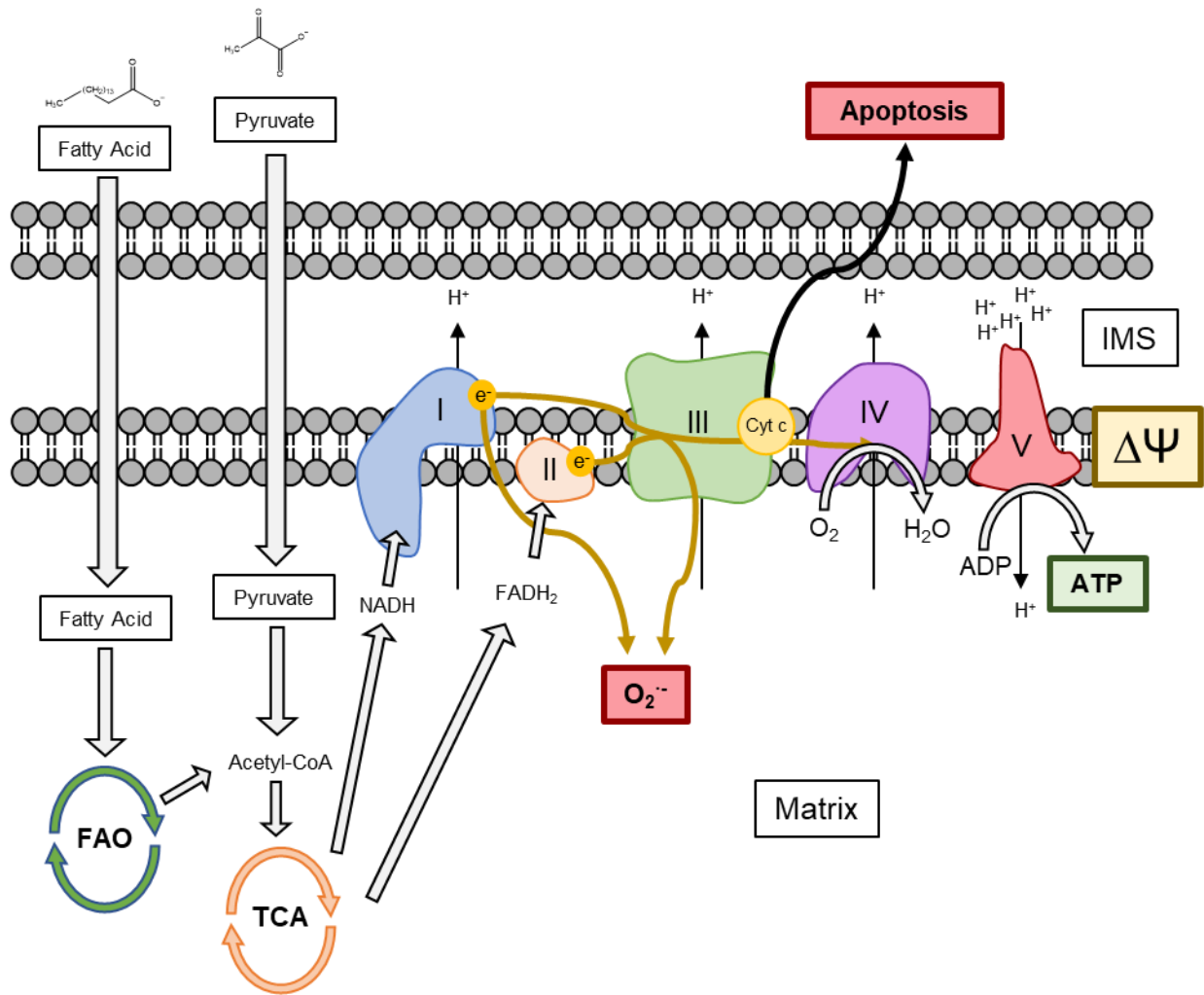


Figure 4: ATP Production through OXPHOS and Other Functions of Mitochondria. Acetyl coenzyme A (Acetyl-CoA) is produced from energy sources such as fatty acids broken down through fatty acid oxidation (FAO) or converted from pyruvate originating from cytosolic glycolysis. Acetyl-CoA then enters the tricarboxylic acid (TCA) cycle, during which NADH and FADH₂ are generated. NADH and FADH₂ donate electrons to complex I and II of the ETC respectively. These electrons are shuttled to complex III, which transfers electrons to cytochrome *c* (cyt *c*). Cytochrome *c* carries electrons to complex IV, which catalyzes the transfer of electrons from cytochrome *c* to oxygen, resulting in oxygen consumption and water formation. This series of electron transfer reactions is coupled to proton shuttling from the mitochondrial matrix to the IMS by complexes I, III, and IV, creating a proton gradient and electrochemical potential ($\Delta\Psi$). Complex V then catalyzes the formation of ATP from ADP using this proton motive force as protons travel down their gradient

into the matrix. Electrons within the ETC can leak from complexes I and III and reduce molecular oxygen to form superoxide, which can perform physiological signaling or cause oxidative stress if overproduced. Additionally, cytochrome *c* can be released by mitochondria into the cytosol and lead to apoptosome formation initiating apoptosis.

The overall health of mitochondria can thus be assessed as a function of mitochondrial membrane potential. Generally, an increase in membrane potential is favorable, as this allows for increased ATP synthesis. However, high membrane potential can increase ROS production which, in excessive quantities, may cause protein oxidation or DNA damage (Zorova et al.; Willems et al.). When mitochondrial membrane potential decreases, the protein kinase PINK1 is stabilized on the OMM, which then recruits the E3 ubiquitin ligase Parkin (Youle and Narendra). Parkin ubiquitinates proteins on the OMM, which bind ubiquitin-adaptor protein p62. This accumulated pool of p62 on the OMM then interact with LC3 bound to phagophores, which eventually form autophagosomes that engulf and degrade dysfunctional mitochondria (Ashrafi and Schwarz). This autophagy of dysfunctional mitochondria, termed mitophagy, ensures that a healthy population of mitochondria is maintained in the cell. While dysfunctional mitochondria can be culled through mitophagy, they may also undergo fusion with healthier mitochondria to allow for transmission of membrane potential, akin to an electrical circuit (Skulachev; Westermann, “Bioenergetic Role of Mitochondrial Fusion and Fission”). Additionally, mitochondria may also share their molecular contents, such as mitochondrial DNA, which can also improve mitochondrial health (Chan).

As suggested above, mitochondrial dynamics is tightly associated with metabolism and energy production. In general, mitochondrial morphology adapts to meet the bioenergetic demands of the cell. Mitochondrial fusion is broadly associated with increased ATP production, OXPHOS, and mitochondrial membrane potential (Schrepfer and Scorrano). Fission, on the other hand, is

associated with increased glycolysis and associated decrease in oxygen consumption and fatty acid oxidation (Schrepfer and Scorrano). In response to stress conditions such as nutrient deprivation, mitochondria elongate presumably to increase ATP synthesis (Gomes et al.). Conversely, mitochondrial fission is associated with nutrient excess, ROS overproduction, and membrane depolarization (Liesa and Shirihai; Yu et al.). Recent literature highlights the link between mitochondrial dynamics and the energy demanding process of cell cycle progression. Fusion is associated with regulation of the G₁ to S phase transition in the cell cycle, as fusion increases ATP generation which is required for the buildup of critical mediators such as cyclin E (Mitra et al.). Furthermore, mitochondrial hyperfusion has been linked to cell cycle arrest and inhibition of cellular proliferation (Mitra). Conversely, mitochondrial fission is required in early phases of mitosis, with degradation of Mfn1 by March5 being linked to G₂/M phase progression (Yong-Yea Park, Cho, et al.). Drp1-mediated fission also allows for equal segregation of mitochondria following mitosis and is thus required for cellular proliferation (Qian et al.). Taken together, mitochondrial dynamics is crucial in the maintenance of mitochondrial function as well as cellular homeostasis. In relation to restenosis and other cardiovascular diseases, mitochondrial dynamics could also serve as a potential therapeutic target and aid in the development of new treatment options.

1.2.4 Targeting Mitochondrial Dynamics in Cardiovascular Diseases

Mitochondria comprise 3-5% of total volume within VSMCs (S.-Y. Park et al.). In native VSMC, mitochondria exhibit parallel, elongated rod shapes with low rates of inter-mitochondrial fusion events (Chalmers et al.). However, after 24 hours in culture, VSMC begin to display mitochondria of mixed shape and size due to an increase in mitochondrial motility. These

mitochondria appear scattered throughout the cytosol as perinuclear, elongated networks as well as smaller fragments that vary from rod-shaped to punctate spheres (McCarron et al.). Recent evidence suggests that inhibiting mitochondrial motility promotes fusion, resulting in cell cycle arrest of VSMC (Chalmers et al.; Nguyen et al.). Furthermore, others have shown that fusion and fission within VSMC can play a role in disease progression. Pulmonary arterial SMC derived from idiopathic PAH patients exhibit a proliferative phenotype with fragmented mitochondrial network and depleted Mfn2 levels (Marsboom et al.). With regards to atherosclerosis, it has been observed that ApoE-KO mice fed an atherogenic diet have reduced Mfn2 expression within VSMC of the aorta, however it is unclear whether this contributes to disease pathogenesis (Soriano et al.). Therapeutically, overexpression of Mfn2 via adenovirus-mediated expression has been shown to be protective against atherosclerotic lesion growth as well as VSMC proliferation (K.-H. Chen et al.). Additionally, overexpression of Mfn2 has been shown to inhibit VSMC proliferation as adenovirus transfection in the adventitia of carotid artery injured with a balloon catheter prevents neointimal growth (K.-H. Chen et al.). Also, the mitochondrial fission inhibitor Mdivi-1 has been shown to prevent VSMC cyclin D1 expression and G₁ progression *in vitro* as well as VSMC proliferation of intact resistance arteries in culture *ex vivo* (Salabei et al.; Chalmers et al.). Altogether, these data demonstrate that mitochondrial dynamics are involved in the pathogenesis of vascular disease.

As fusion has been shown to inhibit VSMC proliferation and be protective against oxidative stress, both of which can contribute to cardiovascular disorders, therapeutic agents which promote fusion might be promising. A number of compounds have been developed that promote mitochondrial fusion by increasing Mfn1/2 activity, showing that fusion can be promoted pharmacologically (Franco et al.; Rocha et al.). However, these peptides are not commercially

available and have not been tested in the context of cardiovascular-related disorders. In the next section, I will highlight the molecule nitrite as a potential therapy that inhibits neointimal hyperplasia through stimulation of mitochondrial fusion.

1.3 NO and Nitrite: Physiological Functions and Role in Disease

1.3.1 NO: eNOS-dependent Enzymatic Production and Reduction of Nitrite

As early as the 1970's, it was known that exogenous NO could activate sGC to increase cGMP production, however this was not recognized as a physiologically relevant pathway (Arnold et al.). In 1988, it was uncovered that the identity of the endogenously generated endothelium-derived relaxation factor was NO and endogenous production of this molecule was able to relax rat aortic rings in response to acetylcholine, an effect inhibited by the presence of hemoglobin (Furchgott et al.). It is now well established that endothelial nitric oxide synthase (eNOS) catalyzes the conversion of L-arginine with oxygen to L-citrulline, generating a molecule of NO that can elicit vasodilation of the vasculature (Moncada and Higgs). All three forms of NOS (including neuronal NOS and inducible NOS) operate as obligate homodimers, containing a reductase and oxidase domain. Electrons are donated from NADPH to the cofactor flavin adenine dinucleotide (FAD) in the reductase domain, however this reaction occurs only when calmodulin is bound to NOS (Förstermann and Sessa). Electrons are then transferred from FAD to flavin mononucleotide (FMN) which eventually reduces heme in the oxygenase domain. Reduced heme is then able to bind molecular oxygen (O_2) which is activated through reduction by cofactor tetrahydrobiopterin (BH_4) or NADPH (Stuehr). When L-arginine also binds the oxygenase domain of NOS, this

activated heme-peroxo complex oxidizes L-arginine to N-hydroxy-L-arginine (NHA). NOS catalyzes this reaction a second time, resulting in oxidative cleavage of NHA to L-citrulline and NO. In the absence of BH₄, this two-step reaction becomes uncoupled resulting in NOS monomerization which can alternatively liberate superoxide (Gebhart et al.). In the vasculature, NO then diffuses from the endothelium to the medial layer, where it activates sGC within VSMC to mediate cGMP production and downstream vasodilation (Ignarro). While NO is a relatively stable free radical in oxygen and metal-free environments, it has a half-life in blood of approximately 2 ms (DeMartino et al.).

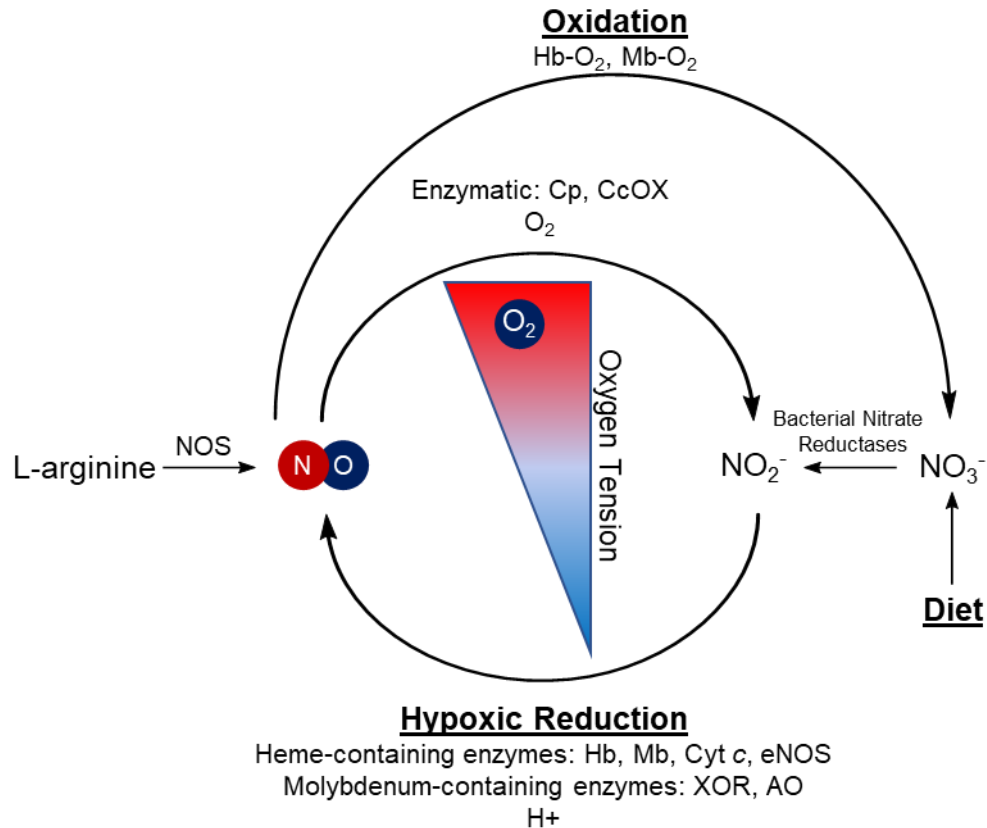


Figure 5: NO-Nitrite Cycle. Nitrate (NO_3^-) enters the body through the diet, which is reduced by bacterial nitrate reductases to nitrite (NO_2^-). The 1 electron reduction of nitrite to NO may be performed by many pathways, such as under acidic conditions (H^+) or through enzymatic reduction. A number of heme-containing enzymes are known to have nitrite reductase activity, such as hemoglobin (Hb), myoglobin (Mb), cytochrome *c* (Cyt *c*), and eNOS. Molybdenum-containing enzymes such as xanthine oxidoreductase (XOR) and aldehyde oxidase (AO) are also able to reduce nitrite to NO. NO is also produced by nitric oxide synthase (NOS), which requires the presence of oxygen to convert L-arginine to NO and L-citrulline. NO can be oxidized to nitrite through autooxidation with O_2 or through catalysis by such proteins as ceruloplasmin (Cp) or cytochrome *c* oxidase (CcOX). Additionally, NO can be further oxidized directly to nitrate by oxy-heme enzymes such as Hb- O_2 and Mb- O_2 . Thus, under low oxygen tension and acidic conditions, nitrite reduction to NO is most favorable.

Notably, enzymatic production of NO requires not only the many cofactors mentioned above but also oxygen as a substrate, thus leading to the question of how NO is generated in conditions of hypoxia (see **Figure 5** for a visualized NO-nitrite cycle). In the last two decades, it has emerged that nitrite (NO_2^-), is a singly charged inorganic anion that was previously thought to be the biologically inert oxidation product of NO, serves as a source of NO in hypoxic conditions. This bioactivation of nitrite to NO is catalyzed by a myriad of metal containing proteins (Kim-Shapiro and Gladwin). These proteins include those with heme prosthetic groups such as hemoglobin, myoglobin, cytoglobin, and eNOS (Shiva, Rassaf, et al.; U. B. Hendgen-Cotta et al.; Alzawahra et al.; Vanin et al.). Nitrite reductase proteins reduce nitrite rapidly when in their deoxygenated forms to produce one molecule of NO which also results in oxidation of the catalytic metal center. Of note, hemoglobin nitrosylation results in relaxation of hemoglobin to its R-state, akin to its coordination with oxygen, and thus exhibits cooperative binding. In circulation, oxygen levels at the transition from arteriole to capillary are ideal for R-state hemoglobin to have open, deoxygenated heme sites for optimized nitrite reduction (Gladwin et al.). In addition to heme proteins, a number of molybdenum containing enzymes such as xanthine oxidoreductase (XOR), aldehyde oxidation, and enzymes within the mitochondrion are able to reduce nitrite to NO (Ghosh et al.; Zhang et al.; Walters and Taylor; Dungal et al.; Kim-Shapiro and Gladwin). In addition to catalytic reduction to NO, nitrite can be converted to NO via acidification, such as by gastric fluids or during tissue acidosis (Jon O Lundberg et al.; Feelisch, Fernandez, et al.). Thus, nitrite reduction to NO is potentiated under scenarios of hypoxia and low pH.

Nitrite is ubiquitous in all tissues and in the blood. In plasma, the concentration of nitrite ranges from 100 to 250 nM, while in tissue levels can reach 1 to 20 μM (Dejam et al.; Bryan et al.). Approximately 60% of the nitrite in the human body derives from oxidation of endogenous

NO, while the remainder originates from the diet (Dejam et al.). NO can undergo auto-oxidation with aqueous oxygen at a rate of approximately $8 \times 10^6 \text{ M}^{-2} \cdot \text{s}^{-1}$ to form nitrite, however this reaction is relatively slow (L. J. Ignarro et al.). More physiologically relevant is likely the rapid oxidation of NO to nitrite by the NO oxidase activity of ceruloplasmin in plasma or by cytochrome *c* oxidase in tissue (Shiva, Wang, et al.; Sarti et al.). Nitrite can also be formed from nitrate (NO_3^-) which is found in our diet and converted to nitrite through reduction by commensal bacteria in the entero-salivary pathway (Weitzberg and Lundberg). In addition to introduction by the diet, nitrate can be formed through oxidation of either NO or nitrite by oxy-ferrous hemoglobin (Doyle and Hoekstra; DeMartino et al.; Keszler et al.).

Nitrite is now well established as a physiological signaling molecule that elicits biological effects through a number of mechanisms, the majority of which require its reduction to NO. Although not as well studied, nitrite may also modify molecules independent of reduction to NO. For example, the reaction of nitrite with hydrogen peroxide forms the radical nitrogen dioxide which is able to perform nitrate tyrosine residues (Van Der Vliet et al.; Monzani et al.; Radi). Tyrosine nitration can elicit changes in protein function, such as inactivation of MnSOD (Macmillan-Crow et al.). Nitrogen dioxides may also react with fatty acids, which results in formation of electrophilic nitro-fatty acids. These species can activate electrophile sensing transcription factors such as Nrf2, promoting nuclear translocation and transcription of downstream targets (DeMartino et al.).

Most studies over the past two decades have investigated the role of hypoxic nitrite reduction to NO in biological signaling. However, more recent work sheds light on potential signaling mechanisms mediated by nitrite in normoxic conditions. For example, in an *in vitro* model of airway epithelium wound injury, nitrite significantly improved wound healing under

normoxic cell culture conditions (Ling Wang et al.). This effect was dependent on increased ROS production and ERK1/2 activation but independent of cGMP production. Similarly in a model of skeletal muscle regeneration in normoxia, nitrite was shown to increase myocyte proliferation independent of NO and cGMP production (Totzeck et al.). Our lab has shown that nitrite pretreatment in normoxia can prevent ischemia/reperfusion (I/R) injury by activating PKA to inhibit Drp1-mediated fission (Pride et al.). Although these studies have begun to probe potential nitrite-mediated signaling mechanisms in normoxia, more work is required to elucidate the role of nitrite under physiological levels of oxygen.

1.3.2 Therapeutic Role of Nitrite in the Cardiovascular System

Over a decade ago, it was first demonstrated that oral nitrite supplementation decreases blood pressure in healthy volunteers (Larsen et al.). More recently, it has been shown that dietary nitrate can lower both systolic and diastolic blood pressure in hypertensive patients (Ghosh et al.). Nitrite is also currently in clinical trials for use in the setting of PAH, with preclinical data suggesting that nitrite activates AMPK through SIRT3 *in vivo* to decrease RVSP and vascular remodeling (Lai et al.; Bueno et al.). While the acute hypotensive effects of nitrite rely on NO/sGC signaling to mediate vasodilation, other mechanisms have been proposed to mediate vasodilation, including promoting PKG oxidation and activation (Feelisch, Akaike, et al.).

Nitrite and nitrate have also been used in a number of other therapeutic interventions. It is well established that in I/R injury, nitrite confers cytoprotection by S-nitrosation of complex I of the ETC, which decreases ROS generation (Baker et al.; Gonzalez et al.; Shiva, Sack, et al.; De Lima Portella et al.). In diabetes, it has been shown nitrites and nitrates reduce hyperglycemia through activation of AMPK (Jon O. Lundberg et al.). Nitrite/nitrate therapy has also been shown

to decrease high-fat diet induced inflammation and endothelial dysfunction (Stokes et al.; Peleli et al.). While the exact mechanism is unclear, leukocyte adhesion to the vessel wall was decreased with nitrite therapy, which likely plays a role in mitigating inflammation (Jädert et al.). Furthermore, nitrite has been shown to inhibit superoxide generation by NADPH oxidase in macrophages which could also contribute to decreasing inflammation (Zollbrecht et al.). More closely tied to cardiovascular diseases, nitrite was found to promote angiogenesis in a model of hind limb ischemia (Kumar et al.; Ulrike B. Hendgen-Cotta et al.). In ApoE KO mice modeling atherosclerosis, dietary nitrate was found to also inhibit inflammatory cell recruitment to the vessel wall (Khambata et al.). Nitrate also increased plaque stability in this study, thus conferring protection against future cardiovascular events.

Relevant to this thesis, our lab recently showed that nitrite administration potently attenuates neointimal hyperplasia in a model of restenosis (Mo et al.; Alef et al.). In these studies, Sprague-Dawley rats were subjected to carotid artery balloon injury and after 14 days, the animals were sacrificed and arteries were harvested. Nitrite administered either through intraperitoneal injection, inhalation, or oral administration in the drinking water (10.5 g/L) significantly reduced neointimal growth as measured by ratio of intimal thickness to thickness of the medial layer. Also, an increase in mitochondrial density was observed with nitrite treatment, suggesting nitrite may be regulating mitochondrial number or function to elicit these effects. One potential mechanism for this inhibition of proliferation is regulation of mitochondrial dynamics, as our lab has shown that nitrite stimulates mitochondrial fusion in cardiomyocytes and adipocytes (Pride et al.; Khoo et al.). Taken together, this led us to the hypothesis that nitrite stimulates mitochondrial dynamics to inhibit VSMC proliferation.

First, I proposed to elucidate the mechanism by which nitrite stimulates mitochondrial fusion and attenuates VSMC proliferation *in vitro*, demonstrating that nitrite mediates these effects through upregulation of Mitofusin-1 (Mfn1). Next, I sought to determine whether nitrite alters VSMC phenotype and migration *in vitro* also through an Mfn1-dependent mechanism, showing that nitrite promotes VSMC phenotypic switching and migration mostly independent of Mfn1. Finally, I investigated the role of Mfn1 expression in VSMC on vasoreactivity and proliferation after vascular injury through generation of novel smooth muscle cell-specific Mfn1 knockout mouse. Furthermore, I also examined the effects of nitrite on neointimal hyperplasia in these mice. In sum, the work in this dissertation explores the role nitrite plays in regulating mitochondrial dynamics, specifically through Mfn1, to regulate vascular smooth muscle proliferation, phenotype, and function both *in vitro* and *in vivo*. Herein, I demonstrate that nitrite regulates the vasculature through mechanisms both independent and dependent on modulation of mitochondrial dynamics and overall function. Additionally, I establish Mfn1 as a regulator of VSMC phenotype and vessel reactivity while also providing further evidence that Mfn1 is protective in disorders propagated by hyperproliferative VSMC.

2.0 Mitofusin-1 is Upregulated by Nitrite to Inhibit Vascular Smooth Muscle Cell Proliferation

2.1 Introduction

Intimal hyperplasia is a hallmark of vascular injury that is characterized by vessel wall thickening due to cellular accumulation in the intima, leading to subsequent vessel narrowing and occlusion of blood flow. While intimal hyperplasia is propagated by a number of factors, including platelet activation, inflammatory stimuli, and endothelial cell apoptosis, VSMC migration from the medial to intimal layer of the vessel and subsequent aberrant proliferation plays a central role (Chaabane et al.). This proliferation of VSMC is stimulated in pathological conditions by many factors including platelet-derived growth factor (PDGF), vascular endothelial growth factor (VEGF), and interleukin-6 (IL-6), as well as the loss of vasoprotective species including NO (Libby; Maleknia et al.; Alef et al.; Tourneau et al.).

Accumulating data implicates mitochondrial structure and function in regulating VSMC proliferation. Mitochondria are highly dynamic organelles that constantly undergo reversible alterations in morphology by joining through fusion or breaking apart via fission, a process coined mitochondrial dynamics (Westermann, "Mitochondrial Fusion and Fission in Cell Life and Death."). Dynamics is tightly regulated by several different proteins, notably mitofusin 1 (Mfn1), mitofusin 2 (Mfn2) and optic atrophy 1 (Opa1) which mediate fusion (Dorn). Alternatively, fission is mediated primarily by dynamin-related protein 1 (Drp1) and its adapter proteins such as mitochondrial fission factor (Mff) (Tilokani et al.). Changes in overall cellular mitochondrial morphology is governed by both the expression levels of these proteins as well as by their activities

via posttranslational modifications. For example, the fusion proteins Mfn1 and Mfn2 are targets for polyubiquitination by E3 ligases such as Parkin and March5, thereby signaling their proteolysis and promoting mitochondrial fission (Escobar-Henriques and Joaquim). Drp1 is targeted by a number of kinases, such as protein kinase A (PKA) and extracellular signaling-regulated kinase (ERK), which can either inhibit or promote its fission activity based on the site of phosphorylation (Tilokani et al.). Recent evidence has established mitochondrial dynamics as a regulator of the cell cycle (Mitra). Fusion is associated with regulation of the G₁ to S phase transition in the cell cycle, as fusion increases ATP generation which is required for the buildup of critical mediators such as cyclin E and DNA replication machinery (Mitra et al.; Parker et al.). Furthermore, mitochondrial hyperfusion has been linked to cell cycle arrest and inhibition of cellular proliferation (Mitra; Yong-Yea Park, Cho, et al.). It has also been shown that cells must undergo Drp1-dependent mitochondrial fission to progress through mitotic division (Taguchi et al.; Salabei and Hill)

Recently, it was shown that nitrite potently inhibits neointimal hyperplasia in a carotid wire injury model in rats, the mechanism of which remains elusive (Alef et al.). Our lab has also recently shown that nitrite increases mitochondrial density specifically in rat aortic smooth muscle cells (RASMC), suggesting that nitrite may regulate mitochondrial number or function to inhibit VSMC proliferation to attenuate neointimal hyperplasia. One potential mechanism for this inhibition of proliferation is regulation of mitochondrial dynamics. This is consistent with the fact that our lab has shown that nitrite stimulates mitochondrial fusion in cardiomyocytes and adipocytes (Pride et al.; Khoo et al.). However, the exact mechanism by which nitrite regulates mitochondrial dynamics in VSMC has not been explored. Taken together, this led us to the hypothesis that nitrite stimulates mitochondrial dynamics to inhibit VSMC proliferation. Herein, we show that nitrite promotes cell cycle arrests to inhibit RASMC proliferation through stimulation of mitochondrial fusion. We

demonstrate that nitrite's effects are dependent on upregulation of Mfn1. Furthermore, we show that nitrite reduces March5-mediated polyubiquitination and degradation of Mfn1, thereby increasing protein expression of Mfn1. These data illustrate a novel mechanism by which nitrite attenuates neointimal hyperplasia, provide evidence for the role of Mfn1 in the regulation of VSMC proliferation, and establish mitochondrial dynamics as a therapeutic target in the treatment of restenosis and other vasculopathies.

2.2 Materials & Methods

2.2.1 Reagents

Reagents were obtained from Sigma-Aldrich unless otherwise specified.

2.2.2 Cell Culture

Rat aortic smooth muscle cells (RASMC) were purchased from Lonza and used from passages 1 through 8. RASMC were plated on tissue-cultured treated plates (Corning) and cultured in growth media containing a 1:1 mixture of DMEM containing 1.0 g/L glyucose, sodium pyruvate, and L-glutamine (Thermo Fischer 11885076) and Ham's F-12 nutrient mixture containing sodium pyruvate and L-glutamine (Thermo Fisher 11765047) supplemented with 10% heat inactivated fetal bovine serum (FBS). Where specified, RASMC were serum starved by replacing growth media with the DMEM/Ham's F-12 basal media containing 10% FBS.

2.2.3 Transfection

RASMC were seeded and grown until approximately 60% confluency. Growth media in the dish was replaced 30 minutes before performing transfection. Either control non-targeting siRNA (Dharmacon D-001810-01-20) or Mfn1 targeting siRNA (Dharmacon L-099253-02-0010) was duplexed with transfection reagent TransIT-X2 (Mirus MIR 6004) with serum-free Opti-MEM (Thermo Fisher 31985088) for 20-30 minutes at room temperature, after which the siRNA-lipid-polymer duplex was added dropwise to the cells at a final concentration of 20 nM. 24 h after transfection, RASMC were either washed with warm PBS and grown in normal growth media or subjected to experimental manipulation. Sufficient knockdown was confirmed by Western blot analysis 48-72 h after transfection.

2.2.4 Tritiated Thymidine Incorporation

RASMC were plated either into 12 or 24 well plates. If undergoing transfection, cells were transfected at 60% confluency as described in **Section 2.2.3**. RASMC were then serum starved for 24 h, at which time cells were pretreated with or without 25 μ M nitrite followed by stimulated proliferation with various concentrations of PDGF (SIGMA). This was followed by the addition of 5 μ Ci/mL 3 H-thymidine to the medium. After 24 or 48 h, the media was aspirated and cells were wash with cold PBS. DNA was precipitated with the addition of cold 5% TCA for 30 minutes at 4°C. DNA was then washed sequentially with 5% TCA and PBS, after which it was dissolved into 0.2 M NaOH with shaking for 30 minutes at room temperature. 0.5 mL of dissolved DNA was added to 4 mL of Ultima Gold scintillation fluid (Perkin Elmer). Incorporation of 3 H-thymidine into DNA was measured via a scintillation counter.

2.2.5 Plasmid Purification & Transient Transfection

Plasmid pcDNA3-EGFP encoding eGFP was purchased as bacterial stab from Addgene (plasmid #13031). Plasmid pcDNA3.1D-March5-V5-His was a kind gift from Dr. Bill Chen at the University of Pittsburgh. The March5-overexpression plasmid was transformed into XL1-Blue competent cells via heat shock (TIME) and plated onto ampicillin containing agar plates, while bacterial stab for eGFP was streaked onto agar plates. After picking colonies, 200 mL of LB media was inoculated and incubated at 37°C overnight at 200 RPM. Plasmids were purified using the Plasmid Maxi Kit (QIAGEN) and the resultant DNA was sent for Sanger Sequencing by Genewiz to confirm the sequence using the following primers in **Table 1**:

Table 1: Primers for Plasmid Sequencing

Description	5` (Forward) Primer (5`-3`)	3` (Reverse) Primer (5`-3`)
March5 plasmid insert	CACCATGCCGGACCAAGCCCTA	TGCTTCTTCTTGTTCTGGATAATTC
March5 plasmid vector	CGCAAATGGGCGGTAGGCGTG (CMV-Forward)	TAGAAGGCACAGTCGAGG (BGHR)

Sequencing confirmed the plasmid contained the correct sequence of human March5 in accordance with NCBI reference number NP_060294.1 followed by a V5-His tag. To transiently introduce DNA into RASMC, either plasmid was complexed with TransIT-X2 transfection reagent (Mirus MIR 6004) in serum-free Opti-MEM (Thermo Fisher 31985088) for 20-30 minutes at room

temperature. DNA-lipid complex was then added dropwise to RASMC cultured in normal growth media for 6 h before washing with PBS and replacing with fresh growth media before continuing any further experimental manipulation. As a positive control, confirmation of plasmid incorporation was confirmed via fluorescence microscopic imaging for fluorescence by eGFP.

2.2.6 Protein Extraction & Western Blot Analysis

For Western blot analysis, growth media from cell culture plates was aspirated and the cells were washed with cold PBS. Cells were then collected via scraping into ice cold PBS and centrifuged at 1200 x g at 4°C. Following removal of the supernatant, the cellular pellet was resuspended in cOmplete Lysis-M Buffer (Roche 471995601) containing protease and phosphatase inhibitors, vortexed briefly, and placed on ice for lysis for 30 minutes. Lysate was then centrifuged at 10,000 x g for 10 minutes at 4°C to remove cellular debris and subjected to Pierce BCA Protein assay (Thermo Fisher) to determine protein concentration. Equal amount of protein extracts were then loaded and separated on 8% acrylamide gels using a the Mini-PROTEAN Tetra System (Bio-Rad). After gel electrophoresis, the proteins were transferred to 0.45 µm nitrocellulose membranes overnight (16 h) at 75 mA at 4°C using a TE22 Might Small Transfer Unit (Hoefer) in 20% methanol containing buffer. The membranes were then blocked with Odyssey blocking buffer (LI-COR Biosciences) for 1 h and incubated with various primary antibodies (see **Table 2**) overnight at 4°C with gentle shaking.

Table 2: Antibodies used for Western blot analysis

Protein	Vendor	Catalog #	Species	Dilution
β -actin	Abcam	8226	Mouse	1:2000
Cyclin A	Santa Cruz	sc-271682	Mouse	1:250
Cyclin E	Santa Cruz	sc-481	Rabbit	1:500
p-Drp1 (Ser637)	Cell Signaling	4867	Rabbit	1:1000
Drp1	Cell Signaling	8570S	Rabbit	1:500
March5	Abcam	185054	Rabbit	1:250
Mfn1	Abcam	126575	Mouse	1:1000
Mfn2	Abcam	56889	Mouse	1:1000
Opa1	Abcam	42364	Rabbit	1:1000
p21 ^{Waf1/Cip1}	Cell Signaling	2947S	Rabbit	1:500
α -Tubulin	Calbiochem	CP06	Mouse	1:5000
Ubiquitin	Cytoskeleton	AUB01	Mouse	1:500
Secondary Antibodies				
Donkey anti-Rabbit (680 nm)	LI-COR	926-68073	Donkey	1:10.000
Goat anti-Mouse (800 nm)	LI-COR	926-32210	Goat	1:10.000

Afterward, membranes were washed with 0.1% TBST and incubated with appropriate fluorescently-labeled secondary antibody (see above) for 1 h at room temperature (1:10,000 dilution; LI-COR Biosciences). Membranes were washed again with TBST then scanned using an Odyssey Infrared Imaging System (LI-COR Biosciences).

2.2.7 Immunoprecipitation

RASMC were lysed with immunoprecipitation (IP) lysis buffer containing 25 mM Tris-HCl (pH 7.4), 150 mM NaCl, 1 mM EDTA, 1% NP-40 alternative, 3% glycerol, protease cocktail inhibitor (Roche) and placed on a tube rotator at 4°C for 1 h. Resultant lysate was spun at 10,000 x g and the supernatant placed into a new tube. After measuring protein concentration via BCA assay, 500-1000 µg of protein was incubated with 2 µg of antibody against Mfn1 (Abcam 104274) per 1 mg of protein on a tube rotator at 4°C overnight. Protein A/G magnetic beads (Pierce) were washed with Tris Buffered Saline (TBS) containing 20 mM Tris-HCl (pH 7.6) and 150 mM NaCl and added to the antigen/antibody mixture for 2 h at 4°C. The beads were collected on a magnetic stand and washed 3 times with IP lysis buffer. Glycine elution buffer containing 0.1 M glycine-HCl (pH 2.5) was added to the precipitate complex/bead mixture for 10 min at room temperature with constant agitation, after which the eluent was collected and neutralized with 1M Tris (pH 9.5). Laemmli buffer was added to the neutralized eluent after which samples were subjected to Western blot analysis.

2.2.8 RNA Isolation and Real-Time PCR with TaqMan Reagents

RNA was isolated with TRI reagent and cDNA was synthesized as described in **section 3.2.4**. Gene expression was measured using real-time PCR on the same Quantstudio 5 Real-Time PCR System (Thermo Fisher) with the following TaqMan primers (Thermo Fisher) for multiplexing:

Table 3: TaqMan Probes

Gene	TaqMan
Mfn1	Rn00685413_g1
Actb	Rn00667869_m1

2.2.9 Cell Cycle Analysis by Flow Cytometry

Where applicable, RASMC were transfected as described in **section 3.2.3**. RASMC were serum starved in basal RASMC media for 24 h, followed by stimulated proliferation with 10 ng/mL PDGF-BB in serum starve media. At various time periods, RASMC were collected via trypsinization and centrifugation. RASMC were then transferred to a clean centrifuge tube and resuspended to a concentration of 1×10^6 cells per mL. Cells were washed twice with PBS, after which they were fixed with the dropwise addition of cold 70% ethanol while under constant agitation to avoid cellular clumping. Following 30 min of fixation at 4°C, RASMC were

centrifuged and resuspended in 10 µg/mL RNase followed by dilution in 50 µg/mL propidium iodide (PI) in PBS. Cells were then stained by incubation in this resultant solution for 10 min at 37°C before proceeding immediately to flow cytometric analysis using an LSRFortessa cell analyzer (BD Biosciences). PI fluorescence was collected using an APC band pass filter (670/14). Intact RASMC were gated for based on size followed by doublet discrimination to select single cells only. Relative cell cycle subpopulations based on PI fluorescence were calculated in FlowJo using the Watson pragmatic algorithm.

2.2.10 Confocal Microscopy

RASMC were plated onto coverslips (Fisher Scientific) in 6 well plates. After undergoing experimental manipulation, coverslips were washed with cold PBS followed by fixation in 2% paraformaldehyde at room temperature. Coverslips were washed again and stored at 4°C until undergoing staining. Coverslips were first removed from plates and remaining PBS was aspirated. Cells were permeabilized with 0.1% Triton x-100 in PBS for 15 min and subsequently washed with PBS. Coverslips were blocked with 20% donkey serum for 1 h. Following washes with PBS containing 0.5% BSA (PBB), coverslips were incubated with the following primary antibodies overnight at 4°C:

Table 4: Antibodies for immunofluorescence microscopy

Protein	Vendor	Catalog #	Species	Dilution
Mfn1	Abcam	126575	Mouse	5 µg/mL
Tom20	Proteintech	11802-1-AP	Rabbit	5 µg/mL
Secondary Antibodies				
Donkey Anti-Mouse Cy5	Jackson ImmunoResearch	715-605-150	Donkey	1:1000
Donkey Anti-Rabbit Cy3	Jackson ImmunoResearch	711-165-152	Donkey	1:1000
Phalloidin Alexa Fluor 488	Thermo Fisher	A12379	-	1:500

After PBB wash, coverslips were then incubated with corresponding secondary antibody for 1 h. Finally, coverslips were washed with PBB, stained with 4',6-diamidino-2-phenylindole (DAPI) for 5 min, and subsequently washed with PBS. Remaining PBS was aspirated after which coverslips were adhered with gelvatol to Superfrost Plus Microscope Slides (Fischer Scientific). Finally, images were obtained using a Nikon A1 Confocal Microscope System (Nikon) with a 60x oil objective lens. Images were processed and analyzed using NIS-Elements Software (Nikon).

2.2.11 Statistics

Data are represented as mean \pm SEM. Analyses were performed with GraphPad Prism 8 (La Jolla, Calif). Continuous data were compared between groups with one-way or two-way ANOVA with posthoc Sidak test. Tukey test was used when only comparing main effect. If comparing between only two groups, a paired student t-test was used.

2.3 Results

2.3.1 Nitrite Inhibits RASMC PDGF-Induced Proliferation through Mfn1 Upregulation

As previously discussed, nitrite has been shown to inhibit neointimal hyperplasia *in vivo*. To determine whether nitrite inhibits RASMC proliferation *in vitro*, RASMC were treated with nitrite (0-25 μ M for 1 h) in serum starved media and afterwards were stimulated to proliferate by treatment with PDGF (10 ng/mL). Cellular proliferation was assessed 24 h later by measuring 3 H-thymidine incorporation (**Figure 6**). Consistent with prior studies, nitrite concentration-dependently decreased RASMC proliferation (Alef et al.).

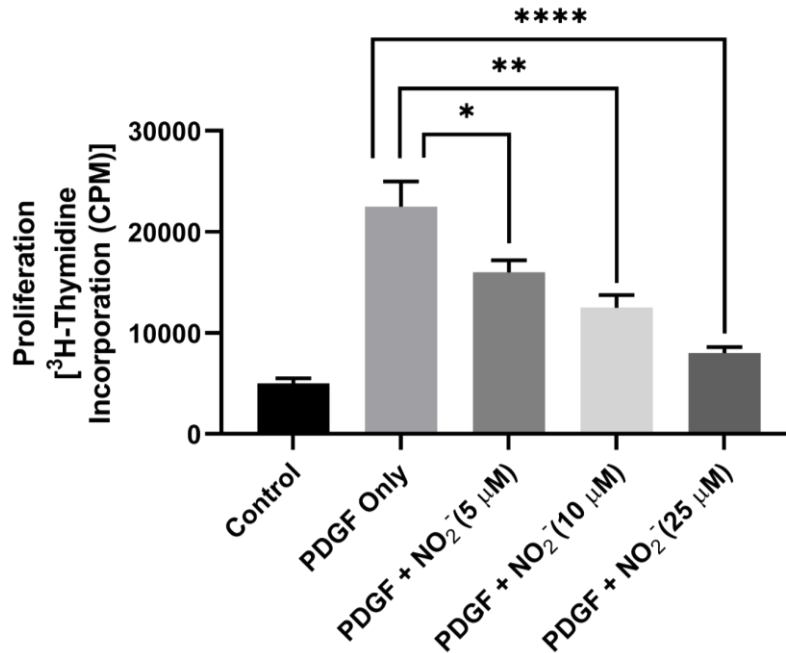


Figure 6: Nitrite inhibits PDGF-induced proliferation. ³H-thymidine incorporation measured by scintillation spectroscopy. RASMC were pretreated with nitrite (5, 10 or 20 μM; 30 min) followed by stimulation of proliferation with PDGF (10ng/mL), after which ³H-thymidine was added to media. Nitrite significantly inhibited RASMC proliferation in a concentration dependent manner (mean ± SEM, n=4; one way ANOVA with Tukey's multiple comparisons test; *P<0.05, **P<0.01, *P<0.0001).**

Mitochondrial dynamics have previously been shown to be a regulator of cell cycle (Mitra) and we have previously shown that nitrite stimulates mitochondrial fusion (Pride et al.; Khoo et al.). Therefore, we next assessed the effect of nitrite on mitochondrial dynamics in RASMC. RASMC were treated with nitrite and mitochondrial morphology and networks were visualized by staining with OMM protein Tom20 and imaging with confocal fluorescence microscopy (**Figure 7**). In accordance with previous findings, cellular mitochondrial networks were elongated after nitrite treatment compared to untreated control cells.

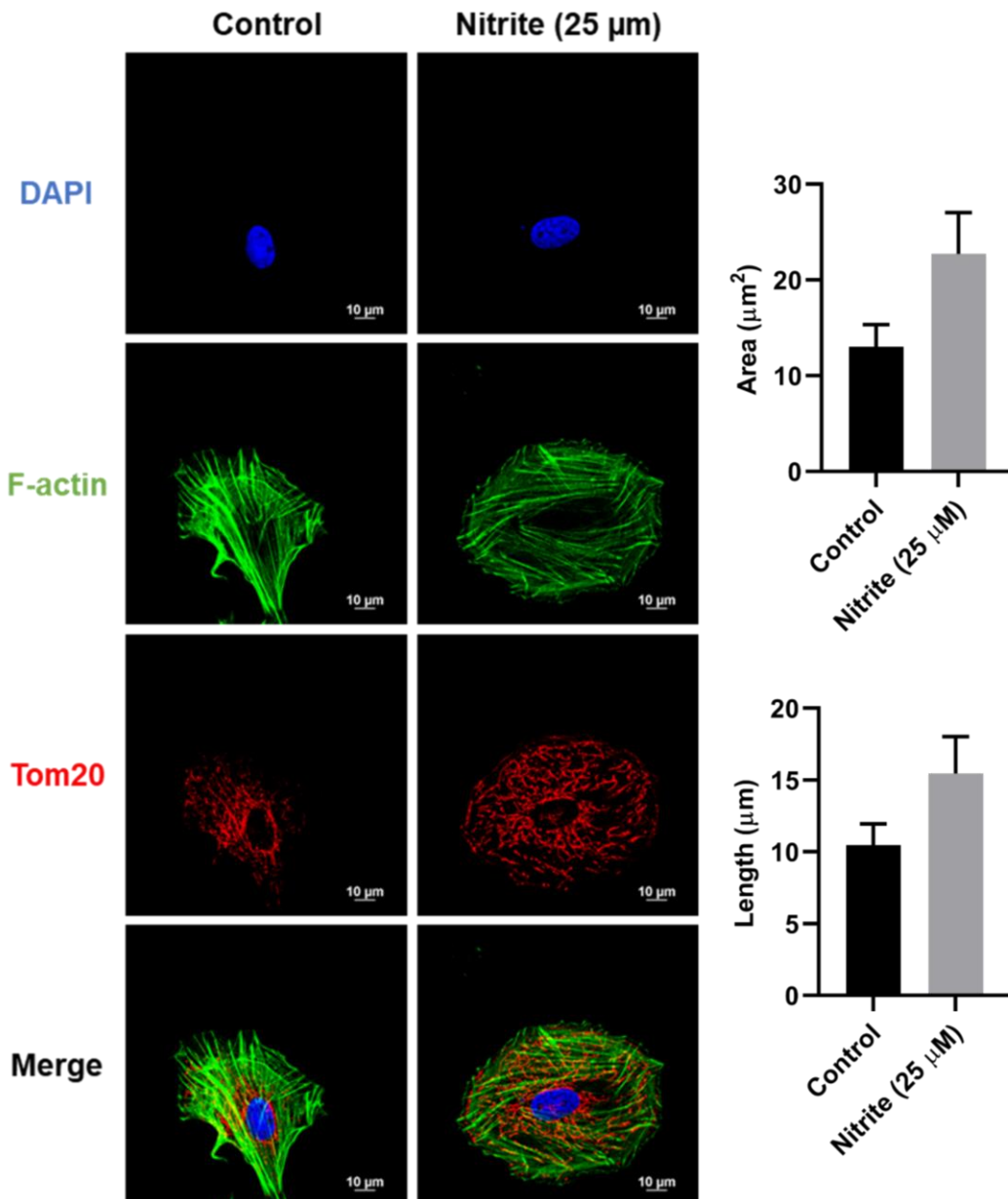


Figure 7: Nitrite stimulates mitochondrial fusion in RASMC. RASMC were seeded on coverslips in 6 well plates and cultured in normal 10% FBS growth media. Once 50% confluent, RASMC were treated with nitrite (25 μM) for 24 h, at which time coverslips were fixed with PFA, stained with DAPI to show nuclei, phalloidin to mark actin filaments and denote cell borders, and Tom20 to as a mitochondrial marker. Images were obtained using Nikon A1 Confocal Microscope System (Nikon) with a 60x oil objective lens. Images were processed and

analyzed using NIS-Elements Software (Nikon) to quantify mitochondrial area and length (mean \pm SEM, n=15; unpaired t-tests; P>0.05).

We next sought to determine which dynamics proteins were responsible for the nitrite-dependent increase in fusion. Using Western blot analysis, measurement of the predominant catalyst of fission, Drp1, and its inhibitory phosphorylation site (serine 637) showed no significant change with nitrite treatment (**Figure 8A-B**). In contrast, expression of the fusion protein Mfn1 showed a significant increase after nitrite treatment. Notably, nitrite did not significantly alter expression levels of Mfn2 or Opa1 (**Figure 8B**).

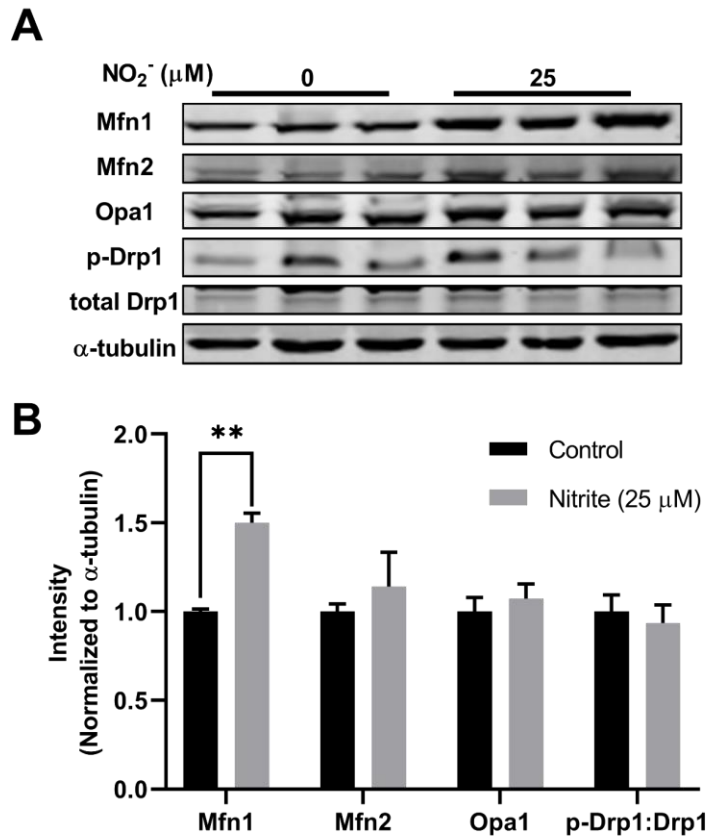


Figure 8: Nitrite upregulates Mfn1. (A) Representative Western blot showing RASMC treated with or without nitrite (25 μM). (B) Quantification of protein of interest band intensity normalized to α-tubulin shows that nitrite significantly increases Mfn1 expression while the levels of other mitochondrial dynamics proteins remain unchanged (mean ± SEM, n=3; two-way ANOVA with Sidak's multiple comparisons test; **P<0.01).

To determine whether nitrite-dependent upregulation of Mfn1 was required for the inhibition of RASMC proliferation observed, we next genetically silenced Mfn1 using siRNA in RASMC. Treatment with PDGF stimulated proliferation to similar levels in both RASMC transfected with non-targeting (control) or siRNA targeting to Mfn1. However, while nitrite inhibited proliferation in controls cells, this effect of nitrite on proliferation was significantly attenuated in RASMC lacking Mfn1 expression (**Figure 9**). These data demonstrate that Mfn1 upregulation is required for nitrite-mediated inhibition of proliferation induced by PDGF.

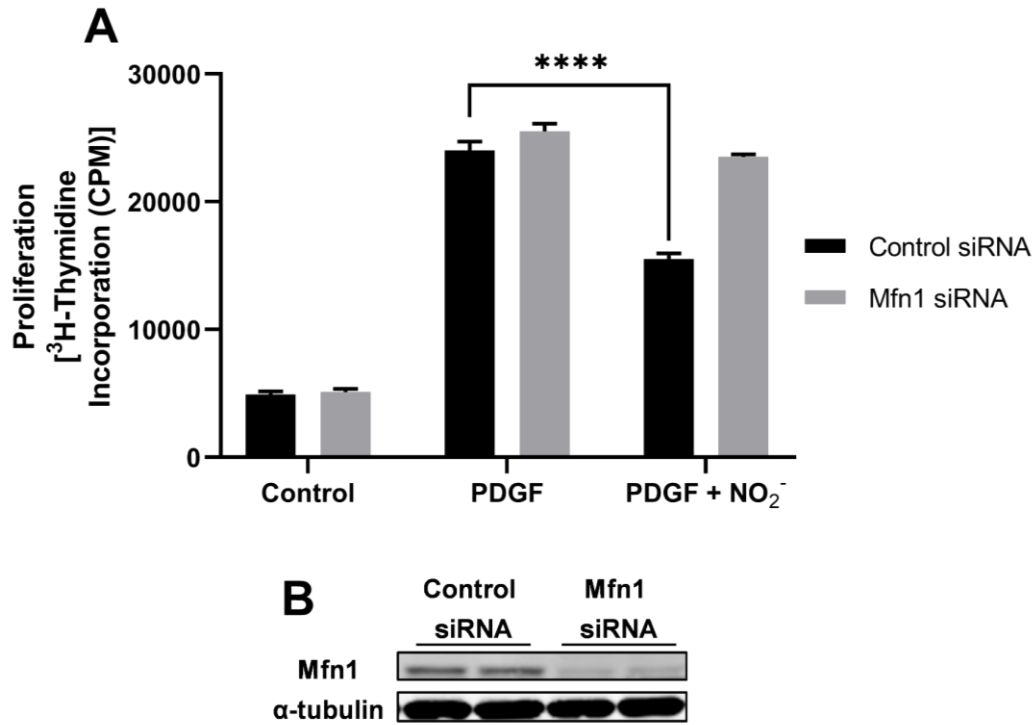


Figure 9: Nitrite-mediated upregulation of Mfn1 is required to inhibit proliferation. ³H-thymidine incorporation measured by scintillation spectroscopy (A). RASMC were transfected with either non-targeting (control) or Mfn1-targeting siRNA for 24 h followed by PDGF (10 ng/mL) stimulated proliferation in the presence or absence of nitrite (25 μ M) for another 24 h. Representative Western blot (B) depicting efficient knockdown of Mfn1 protein expression. Nitrite potently inhibited PDGF-induced proliferation in control cells, however had no effect in Mfn1 knockdown cells (mean \pm SEM, n=3; two-way ANOVA with Sidak's multiple comparisons test; ****P<0.0001).

Mitochondrial hyperfusion has been shown to stimulate cell cycle arrest (Mitra et al.). Thus, we next tested the effect of nitrite on cell cycle progression in RASMC. Cell cycle progression in RASMC treated with and without nitrite (25 μ M, 24 h) was analyzed via flow cytometry. Nitrite-treated RASMC showed a greater population in G₁ phase accompanied by a decreased population in S phase compared to untreated RASMC, suggesting nitrite treatment causes block in G₁-S phase progression (**Figure 10**).

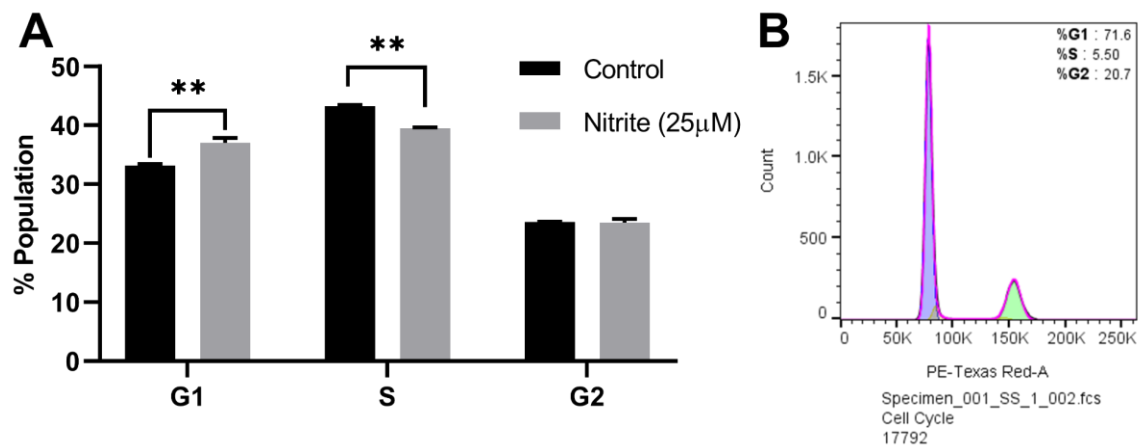


Figure 10: Nitrite treatment arrests RASMC in G₁-S phase progression. (A) Quantification of cell cycle analysis by flow cytometry showing representative PI fluorescence with algorithmic fit overlay (B). RASMC were treated with nitrite (25 μ M) in normal growth media for 24 h, after which cells were collected and DNA stained with PI. RASMC treated with nitrite showed a greater population in G₁ phase and less in S phase compared to untreated control cells (mean \pm SEM, n=3; two-way ANOVA with Sidak's multiple comparisons test; **P<0.01).

2.3.2 Nitrite Inhibits March5-Mediated Ubiquitination of Mfn1 to Upregulate its Protein Expression

We next sought to determine the mechanism by which nitrite increases Mfn1 levels. To determine whether nitrite increases Mfn1 protein synthesis, Mfn1 mRNA levels were measured in RASMC treated with or without nitrite (25 μ M; 24 h). Nitrite treatment had no significant effect on Mfn1 mRNA levels, suggesting protein synthesis was not increased by nitrite (**Figure 11A**). We next tested whether nitrite inhibited Mfn1 protein degradation by treating RASMC with or without nitrite in the presence of cycloheximide (5 μ g/mL) to inhibit translation of all mRNA. RASMC treated with cycloheximide alone expressed significantly lower levels of Mfn1 protein than untreated controls cells. However in nitrite-treated RASMC, cycloheximide treatment had little effect on Mfn1 protein levels, consistent with the concept of nitrite-dependent inhibition of Mfn1 protein degradation (**Figure 11B-C**).

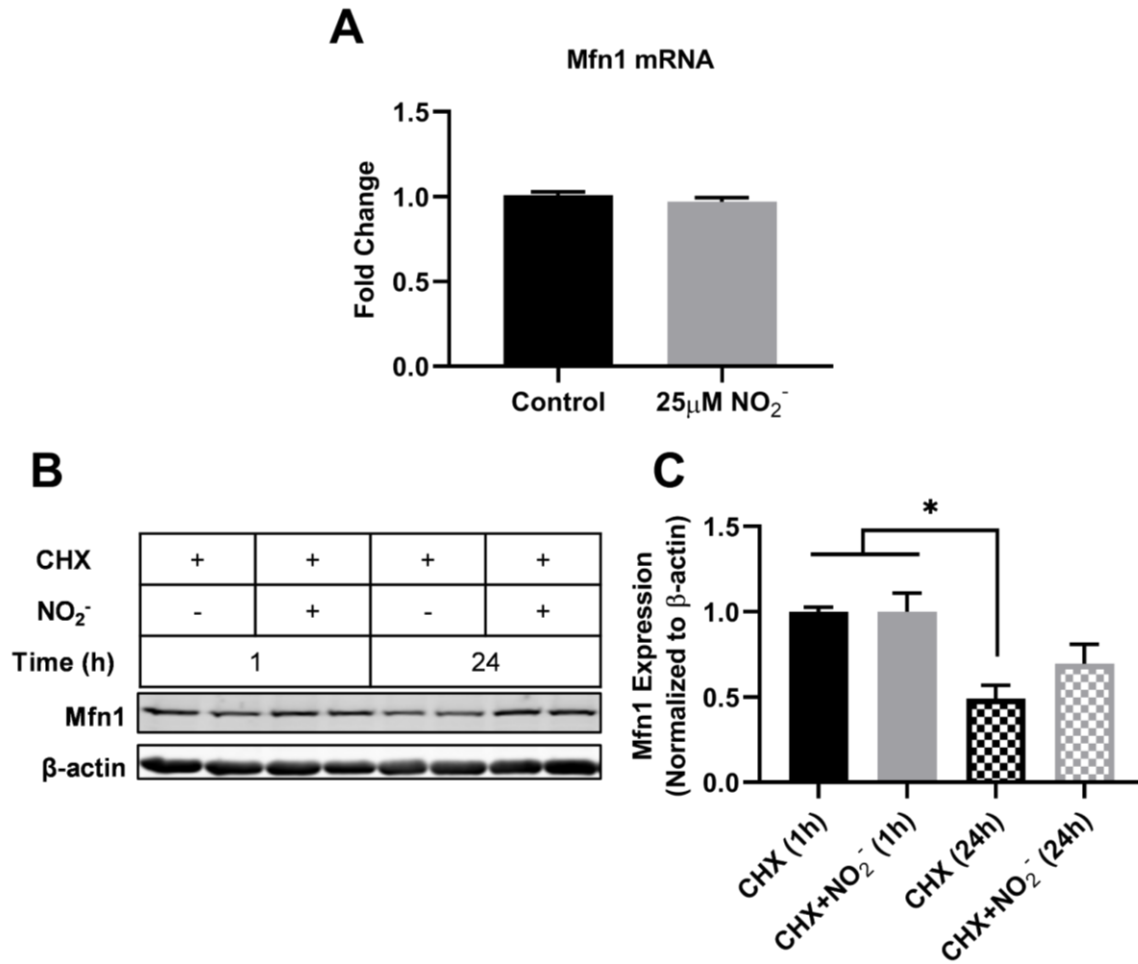


Figure 11: Nitrite upregulates Mfn1 by inhibiting its degradation. (A) Levels of Mfn1 mRNA measured by qPCR. Transcript levels reported as fold change relative to β-actin levels normalized to control untreated cells (mean ± SEM, n=6; unpaired t-test; P>0.05). (B) Representative Western blot analysis of RASMC treated with CHX with or without nitrite (25 μM) for 1 h or 24 h with quantification normalizing to β-actin (C) (mean ± SEM, n=3; one-way ANOVA with Tukey's multiple comparisons test; *P<0.05).

Mfn1 is primarily degraded by the ubiquitin-proteasome system, in which Mfn1 is first ubiquitinated by E3 ligases and then degraded by the 20S subunit of the proteasome. To determine whether nitrite inhibits Mfn1 degradation by inhibiting the UPS, activity of the 20S the proteasome was measured in RASMC treated with nitrite (**Figure 12A**). Nitrite treatment did not change the activity of the 20s proteasome compared to untreated cells, demonstrating that nitrite does not globally inhibit proteasome activity. We next tested whether nitrite inhibits ubiquitination of Mfn1 to prevent proteasomal degradation. RASMC were treated for 6 h with or without nitrite (25 μ M) in the presence of MG132 (50 μ M) to inhibit the 20S proteasome, allowing measurement of all ubiquitinated proteins prior to proteasomal degradation, after which Mfn1 was immunoprecipitated. Measurement of ubiquitinated Mfn1 after nitrite treatment was decreased compared to control (**Figure 12B-C**). In sum, these data demonstrate that nitrite inhibits Mfn1 degradation by inhibiting its ubiquitination, resulting in increased protein expression.

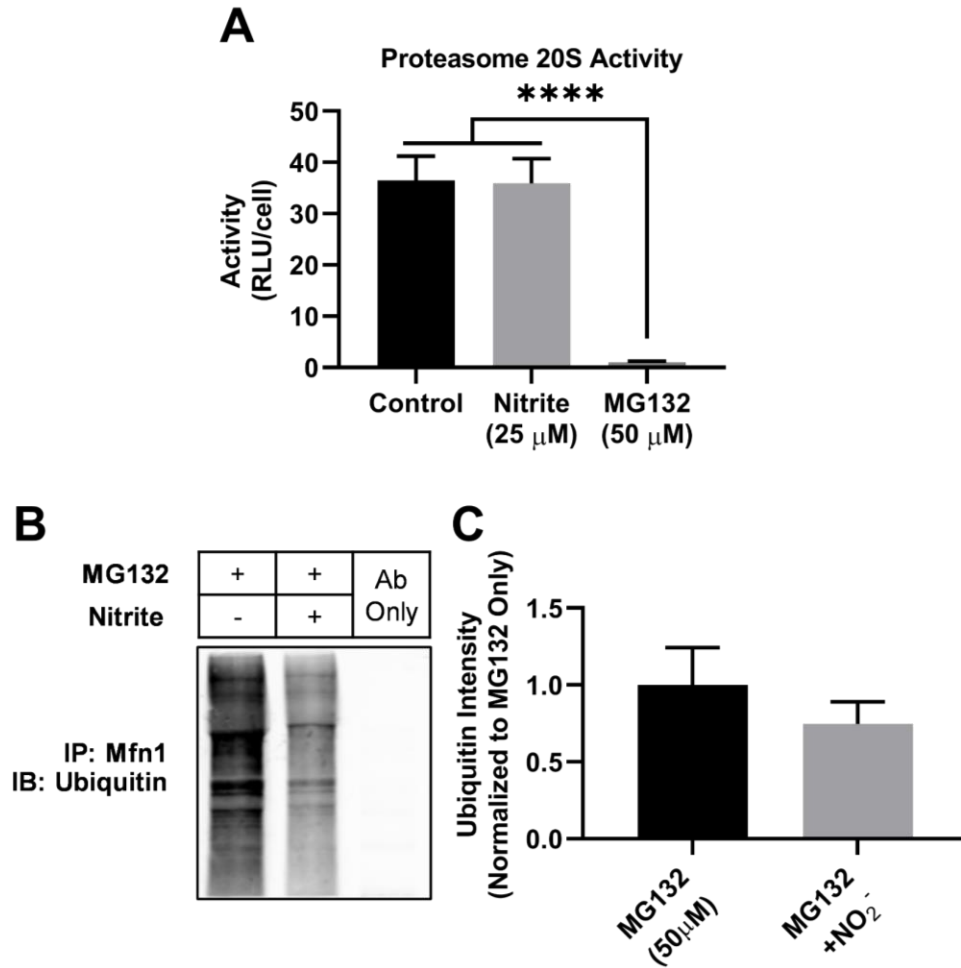


Figure 12: Nitrite inhibits ubiquitination of Mfn1. (A) Proteasomal activity assay. Activity expressed as relative luminescence units (RLU) normalized to crystal violet staining following assay. MG132 was used as a positive control for proteasomal inhibition (mean \pm SEM, $n=3$; one-way ANOVA with Dunnett's multiple comparisons test; **** $P<0.0001$). (B) Representative immunoblot of immunoprecipitated Mfn1 probing for ubiquitin. RASMC were treated for 6 h in the presence of MG132 (50 μ M) with or without nitrite (25 μ M), after which cells were lysed and Mfn1 was immunoprecipitated. Quantification (C) suggests nitrite decreases Mfn1 ubiquitination, although this result is not statistically significant (intensity \pm SEM, $n=6$; unpaired t-test; $P=0.3904$).

March5 is an OMM bound ring finger E3 ligase known to polyubiquitinate other OMM bound proteins and target their proteasomal degradation (Nakamura et al.). Additionally, March5 has been established as a regulator of mitochondrial dynamics which primarily promotes mitochondrial fission (Karbowski et al.). Specifically, it has been shown that Mfn1 is a primary target for March5-mediated polyubiquitination (Yong-Yea Park, Lee, et al.). To test whether nitrite alters March5 E3 ligase activity to increase Mfn1 levels, we transfected RASMC with siRNA to the March5 which was followed by nitrite treatment. As previously observed, nitrite increased Mfn1 protein levels in cells transfected with non-targeting siRNA (**Figure 13A-B**). In RASMC transfected with siRNA targeting March5, we saw a significant increase in Mfn1 protein levels, but nitrite did not increase these levels further. This suggests that March5 is likely the target for nitrite. Nitrite-dependent inhibition of March5 decreases ubiquitination and subsequent degradation of Mfn1 resulting in increased protein expression. To further test this hypothesis, we transiently overexpressed March5 using an expression vector (**Figure 13C-D**). In control, GFP-overexpressing cells, nitrite treated cells showed a trend to increased Mfn1 expression, although this result was not statistically significant. In March5-overexpressing cells, nitrite did not increase Mfn1 expression, suggesting that nitrite is unable to inhibit Mfn1 degradation with an overabundance of March5 present. These data provide are consistent with the idea that nitrite inhibits March5 to decrease Mfn1 ubiquitination resulting in increased Mfn1 protein levels.

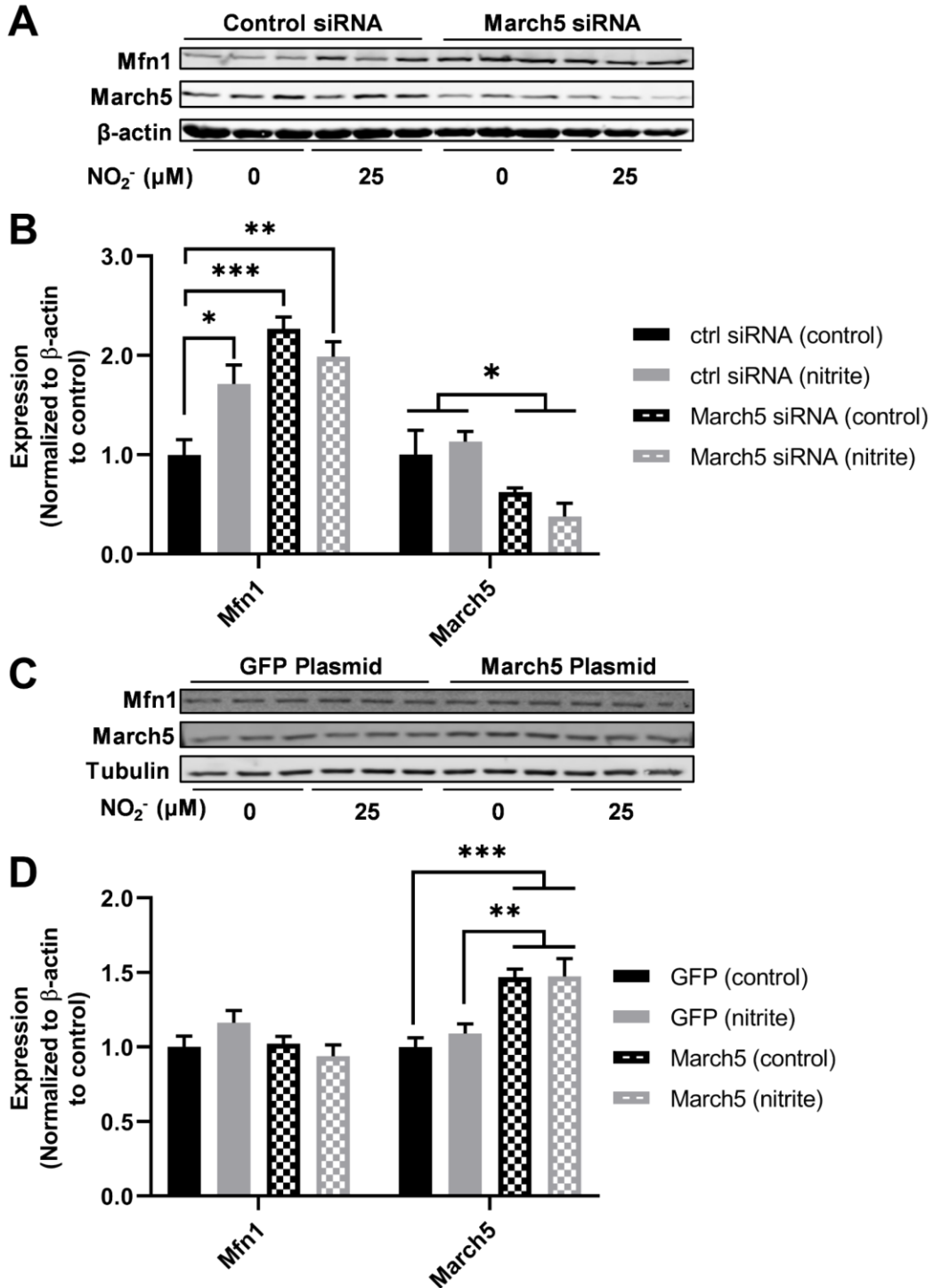


Figure 13: Nitrite inhibits March5 E3 activity to increase Mfn1 expression. (A) Representative Western blot analysis and quantification (B) with genetic silencing of March5. Nitrite significantly increased Mfn1 expression in control siRNA transfected cells. Transfection with siRNA to March5 significantly increased Mfn1 expression,

with nitrite having no additional effect (mean \pm SEM, n=3; two-way ANOVA with Tukey's multiple comparisons test; *P<0.05, **P<0.01, ***P<0.001). (C) Western blot analysis with quantification (D) following transient transfection with overexpression plasmids containing either eGFP or March5. Nitrite slightly increased Mfn1 expression in GFP-overexpressing cells compared to untreated control cells (P=0.4222), but had no effect in March5-overexpressing cells (mean \pm SEM, n=4; two-way ANOVA with Tukey's multiple comparisons test; **P<0.01; ***P<0.001).

2.4 Discussion

The major finding of this study is that nitrite inhibits VSMC proliferation *in vitro*. On a mechanistic level, this effect is due to a nitrite-dependent inhibition of March5, leading to the accumulation of Mfn1, which results in cell cycle arrest (**Figure 14**). These data add to the growing literature demonstrating that Mfn1 can regulate the cell cycle (Mitra). Moreover, they elucidate a novel mechanism by which nitrite modulates mitochondrial dynamics and cell cycle progression through the regulation of Mfn1 degradation. These results provide a mechanism that potentially underlies the therapeutic anti-proliferative actions of nitrite that attenuates neointimal hyperplasia in models of vascular injury (Alef et al.; Zuckerbraun et al.).

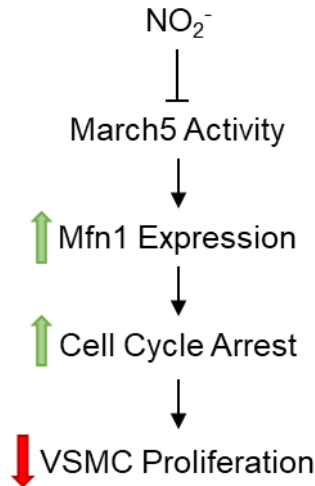


Figure 14: Mechanism by which nitrite inhibits VSMC proliferation. Nitrite inhibits polyubiquitination of Mfn1 by E3 ligase March5, thereby upregulating Mfn1 expression. Upregulation of Mfn1 is associated with mitochondrial fusion and cell cycle arrest; these effects ultimately inhibit stimulated VSMC proliferation to attenuate neointimal hyperplasia and restenosis.

While many studies have focused on the function of both Mfn1 and Mfn2 together, or Mfn2 alone, little is known about signaling mechanisms that are specific to Mfn1. With regards to the cell cycle, it is established that Mfn1, but not Mfn2, is degraded at the G₂/M phase by a mechanism stimulated by March5-mediated ubiquitination (Yong-Yea Park, Cho, et al.). This is consistent with the idea that regulation of March5 could specifically modulate Mfn1. While our data clearly show that nitrite inhibits March5, we have not explored the molecular mechanism of this inhibition. However, March5-mediated degradation of Mfn1 is known to be enhanced when Mfn1 is acetylated (Y-Y Park et al.; J.-Y. Lee et al.). Additionally, there is evidence that nitrite activates a number of deacetylases, including sirtuins 1 (SIRT1) and 3 (SIRT3), and thus could be

one potential mechanism by which nitrite decreases March5-mediated ubiquitination (Mo et al.; Lai et al.).

Notably our data show that nitrite inhibits March5 and decreases RASMC proliferation in normoxic oxygen tension. This is in contrast to the majority of prior studies that attribute the biologic effects of nitrite to its chemical reduction to bioavailable NO (Shiva; Castiglione et al.). The growing number of recent studies demonstrating normoxic effects of nitrite implicate oxidative mechanisms (Ling Wang et al.) and activation of protein kinases leading to downstream phosphorylative signaling events (Pride et al.; Mo et al.). Moreover, through peroxidase chemistry, nitrite is able to mediate protein nitration (Van Der Vliet et al.; Monzani et al.; Radi). Further study will determine whether these types of signaling may be operant in the nitrite-dependent inhibition of March5 we show here.

Importantly, NO has variable effects on VSMC proliferation *in vitro*. Low concentrations of NO promote VSMC proliferation, while higher concentrations inhibit proliferation (Hassid et al.; Komalavilas et al.; Kapadia et al.; Pearce et al.; del Soldato et al.). It is probable that in an *in vivo* model of vascular injury, a proportion of nitrite will be reduced to NO and possibly elicit similar mitogenic effects to NO. Thus, the characteristics of the local environment within the vasculature (such as oxygen tension and pH) will determine the signaling effects of nitrite. Understanding this balance between the oxidative and reductive chemical (and thus signaling) pathways of nitrite will be crucial to advancing its use as a therapeutic for vascular injury.

It is known that proliferative VSMC have decreased Mfn2 levels compared to quiescent VSMC, and that overexpression of Mfn2 in balloon angioplasty-injured rat carotid arteries prevents neointima formation (K.-H. Chen et al.; X. Guo et al.). Similarly, pulmonary artery smooth muscle cells (PASMC) from pulmonary arterial hypertension patients have decreased

Mfn2 levels compared to PASMC from healthy controls (Marsboom et al.). Even so, the role of Mfn1 has not been explored in hyperproliferative VSMC disorders, or whether nitrite alters mitochondrial dynamics or mitofusin expression *in vivo*. In nitrite treated animals, p21 expression is increased within the vessel wall compared to untreated animals, while in culture p21 expression is correlated to Mfn1 levels (Alef et al.; Son et al.). This suggests that Mfn1 expression might also be upregulated by nitrite *in vivo*. In this study, while we show that inhibition of RASMC proliferation by nitrite is dependent on Mfn1, the casual role for Mfn1 has not been addressed. Studies have shown that the mitofusins directly interact with a number of proteins involved in cell cycle progression and proliferation, such as p21 (K.-H. Chen et al.; K. H. Chen, Dasgupta, et al.; Pyakurel et al.). Metabolic reprogramming after mitofusin deletion has also been observed, leading to increased cell cycle progression and proliferation (Son et al.). Thus, additional work is required to determine how Mfn1 upregulation promotes cell cycle arrest such as through interactions with p21, and whether such a mechanism exists *in vivo*. The role of Mfn1 in VSMC proliferation may also differ in response to mitogenic stimuli other than PDGF, such as VEGF or IL-6 which are also upregulated after vascular injury and may also play a role during the pathogenesis of neointimal hyperplasia *in vivo* (Chaabane et al.). Moreover, to determine whether nitrite-mediated upregulation of Mfn1 similarly attenuates VSMC proliferation in neointimal *in vivo*, generation of smooth muscle specific Mfn1 KO mice would be required.

In conclusion, we have demonstrated that nitrite is a regulator of Mfn1 protein expression. The findings in this study also suggest that nitrite is a regulator of March5, however the mechanism by which nitrite alters enzymatic activity of E3 ligase activity remains to be explored. Compounds which inhibit March5 or other E3 ligases that promote mitochondrial fission could be potential therapeutic targets for the treatment of disorders involving hyperproliferative VSMC. Finally,

these data illustrate a nitrite-mediated mechanism which is presumably independent of reduction to NO, however further work is required to confirm these findings. Future studies may demonstrate alternative post-translational modifications or other means by which nitrite elicits biological effects.

3.0 Nitrite and Mitofusin-1 Regulate Smooth Muscle Cell Phenotype

3.1 Introduction

Vascular smooth muscle cell (VSMC) phenotypic switching is central to vascular remodeling and the pathogenesis of restenosis. During this process, VSMC switch from a contractile to “synthetic” phenotype, which is characterized by increased migration and proliferation. Proliferation and migration of these cells from the adventitia and media into the intimal layer propagates neointimal hyperplasia (Frismantiene et al.). Synthetic VSMC also contribute to neointimal formation through matrix remodeling by the production of matrix metalloproteinases (MMPs) and ECM proteins (Jukema et al.). In addition to increased migration and ECM protein secretion, phenotypic switching is characterized by loss of contractile gene expression in VSMC resulting in a “non-excitabile” smooth muscle cell which has lost its contractile function (House et al.). Many of the initial experiments providing evidence for phenotypic switching were conducted *in vitro*, through a protocol in which cultured VSMC are treated with growth factors such as PDGF or TGF- β to stimulate the switch from a contractile to this “synthetic” phenotype with signaling molecules (Owens et al.). Typically, one can assess VSMC phenotype *in vitro* by measuring migration or expression of contractile genes. Regularly measured genes involved in contractile function and cytoskeleton machinery include alpha smooth muscle actin (α -SMA), myosin heavy chain 11 (MYH11), calponin, and smooth muscle protein 22- α (SM22- α) which mark functionally differentiated VSMC (Gabbiani et al.; Miano et al.; Duband et al.). Additionally, myocardin and tet methylcytosine dioxygenase 2 (Tet2) are known master regulators of VSMC contractile machinery genes (Z. Xu et al.; R. Liu et al.). Krüppel-like

factor 4 (KLF4) is a zinc finger transcription of recent interest in the context of VSMC phenotypic switching; it has been shown that KLF4 expression inhibits VSMC proliferation while suppressing expression of VSMC differentiation markers (Zheng et al.; Deaton et al.; Sweet et al.). Simultaneous measurement of multiple genes is required to properly assess VSMC phenotypic modulation of VSMC, as members of the contractile machinery genes can be expressed by other cell lineages (Gomez and Owens). More recent evidence from murine models of vascular injury as well as atherosclerosis have now shown that VSMC phenotypic switching occurs *in vivo* and is central to disease development (Regan et al.; Gomez and Owens). By understanding the underlying mechanisms that promote VSMC phenotypic switching, new therapeutic strategies can be developed for treatment of vasculopathies and related disorders.

In the past decade, changes in mitochondrial dynamics and function have been associated with VSMC phenotypic switching (Perez et al.; Salabei and Hill; Boehme et al.; Wall et al.; Chiong et al.). For example, Salabei and Hill demonstrated that RASMC treated with PDGF to induce phenotypic switching had increased fatty acid oxidation (FAO) which was accompanied by mitochondrial fission, enhanced proliferation, and loss of contractile protein expression. Treatment with mitochondrial fission inhibitor Mdivi-1 prevented the increase in FAO and proliferation by PDGF, however loss of contractile protein expression was unaffected. Similar changes in metabolism have been observed in pulmonary smooth muscle cells which undergo a metabolic shift, becoming more reliant on glycolysis, and display mitochondrial fission when they are in synthetic phenotype in conditions such as pulmonary hypertension (Marsboom et al.). While these data suggest a link between VSMC phenotypic switching and mitochondrial dynamics, this relationship remains relatively unexplored (Vasquez-Trincado et al.).

In the previous chapter, we showed that nitrite inhibits proliferation in RASMC through a mechanism dependent on the upregulation of the mitochondrial fusion protein mitofusion-1 (Mfn1). Our lab has shown that nitrite treatment in normoxia promotes mitochondrial fusion while increasing ROS production (Pride et al.). Specifically in VSMC, we have also shown that nitrite increases ROS production, while others have shown that nitrite promotes migration in other various cell types through ROS-dependent signaling (Ling Wang et al.; Mo et al.). While the effects of nitrite on VSMC phenotypic switching have not been explored, ROS from various cellular sources have been shown to regulate VSMC phenotype in both development of contractile phenotype and in response to vascular injury during restenosis (Xiao et al.; Rodriguez et al.; Burtenshaw et al.). In this chapter, we test the hypothesis that nitrite modulates phenotypic switching through the upregulation of Mfn1. We specifically measure contractile gene expression and mitochondrial metabolic changes in response to nitrite treatment and silencing of Mfn1 in VSMC. We show that while both Mfn1 and nitrite regulate VSMC phenotypic switching, nitrite's effect are essentially independent of Mfn1 expression and instead reliant on ROS production.

3.2 Material & Methods

3.2.1 Reagents

Reagents were obtained from Sigma-Aldrich unless otherwise specified.

3.2.2 Cell Culture

Rat aortic smooth muscle cells (RASMC) were cultured as described in **section 2.2.2**.

3.2.3 Transfection

RASMC were transfected as described in **section 2.2.3**.

3.2.4 RNA Isolation and Real-Time PCR

RASMC were collected, centrifuged into pellets, and resuspended in TRI reagent (Sigma-Aldrich). Briefly, chloroform was added at 20% volume of TRI reagent and the subsequent mixture was subjected to centrifugation at 12,000 x g for 15 minutes at 4°C to separate RNA in the aqueous phase from protein and DNA. The RNA was precipitated with isopropanol, centrifuged, and washed with 75% ethanol. The RNA pellet was then dried at 55°C for 5 minutes and resuspended in RNase free H₂O. Concentration of RNA was measured by nanodrop. cDNA was prepared with iScript cDNA synthesis kit (Bio-Rad 1708890) using 500 ng of RNA in each reaction, incubating at 46°C for 20 minutes and 1 minute at 95°C for reverse transcriptase inactivation. cDNA reactions were stored at -20°C before proceeding to analysis by real-time PCR (qPCR). qPCR was performed using PowerUp SYBR Green Master Mix (Thermo Fisher) with fast chemistry (step 1: 95°C for 20 sec; step 2: 95°C for 3 sec; step 3: 60°C for 30 sec; step 4: repeat steps 2-3 for 40 cycles) on Quantstudio 5 Real-Time PCR System (Thermo Fisher). The following primers were designed for measurement of cDNA of glyceraldehyde 3-phosphate dehydrogenase (GAPDH), myosin heavy chain (MYH11), calponin, myocardin, smooth muscle protein 22- α (SM22- α), tet

methylcytosine dioxygenase 2 (TET2), and Kruppel-like factor 4 (KLF4) using NCBI primer-blast with a max PCR product of 200 base pairs having an intron inclusion between the target exons (see **Table 5**).. Once C_t values were obtained, expression of mRNA was expressed by calculating fold change as $2^{-\Delta\Delta C_t}$ relative to GAPDH expression relative to untreated control cells.

Table 5: Primers for Real-Time PCR

Gene	5` (Forward) Primer	3` (Reverse) Primer
GAPDH	5'-CAG TGC CAG CCt CGT CTC AT-3'	5'-CAA GAG AAG GCA GCC CTG GT-3'
MYH11	5'-CAG TTG GAC ACT ATG TCA GGG AAA-3'	5'-ATG GAG ACA AAT GCT AAT CAG CC-3'
Calponin	5'-TAC TAT AAC TCT GCC TAG GGG C-3'	5'-GCC TGA TCT CCC CAA ACT GT-3'
Myocardin	5'-CTC AGG CAT TAT CGG GAC ATA G-3'	5'-CAT AGG ATG GCT TCC GGA ATA-3'
SM22- α	5'-GCA TAA GAG GGA GTT CAC AGA CA-3'	5'-GCC TTC CCT TTC TAA CTG ATG ATC-3'
TET2	5'-AGG TTT GGA GAG AAG GGT AAA G-3'	5-'GAC CTC CGA TAC ACC CAT TTA G-3'
KLF4	5'-CTT TCC TGC CAG ACC AGA TG-3'	5'-GGT TTC TCG CCT GTG TGA GT-3'
α -SMA	5'-AGT CGC CAT CAG GAA CCT CGA G-3'	5'-ATC TTT TCG ATG TCG TCC CAG TTG-3'

3.2.5 Scratch Assay

RASMC were plated into 12 or 24 well tissue-culture treated plates (Corning). If undergoing transfection, cells were treated according to **section 2.2.3**. After 48 h, cells were scratched with a 10 uL pipette tip, washed with PBS, and the media was replaced with either normal media or media containing nitrite (25 μ M) with or without ROS scavengers TEMPOL (100 μ M) and MitoTEMPO (100 μ M). After 3, 6, 12, or 18 h, cells were stained with crystal violet and imaged with an Axiovert 40 CFL Trinocular Inverted Fluorescence Phase Contrast Microscope using a 4x objective lens (Zeiss). Images were acquired with an AxioCAM Mrc5 camera using Axiovision Rel. 4.8 software (Zeiss). Total wound area was then quantified using ImageJ.

3.2.6 Measurement of Cellular ROS

RASMC were seeded in black clear bottom tissue cultured treated 96 well plates for 24 h. Once 70% confluent, RASMC were treated with or without nitrite (20 μ M) in the presence of TEMPOL (100 μ M) and MitoTEMPO (100 μ M) for 12 h. Where specified, RASMC were pretreated 30 min prior to nitrite treatment with inhibitors of enzymatic ROS producers including allopurinol (50 μ M), apocyanin (20 μ M), and indomethacin (20 μ M). Following pharmacological treatment, the media was removed and either Amplex Red Reagent (Thermo Fisher, 5 μ M in PBS) or MitoSOX (Invitrogen, 5 μ M in PBS) was added to the plate. Fluorescence intensity was measured kinetically using a plate reader at ex/em 530/590 and 510/580 respectively.

3.2.7 Measurement of Cellular Energetics by XFe96 Extracellular Flux Bioanalyzer

RASMC were plated in 6 cm tissue culture treated dishes and transfected as described in **Section 2.2.3**. After 24 h, RASMC were trypsinized and 20,000 cells per well were plated into a Seahorse 96 well cell culture microplate (Agilent). After another 24 h, the media was aspirated and replaced with unbuffered Seahorse XF base DMEM containing 10 mM D-glucose, 1 mM sodium pyruvate, and 2 mM L-glutamine. Wells were also supplemented with 100 μ M L-carnitine and 100 μ M palmitate conjugated to bovine serum albumin (BSA) to measure fatty acid oxidation (FAO). The plate was then incubated for 1 h, after which it was placed into a Seahorse XFe96 Extracellular Flux Bioanalyzer (Agilent) and subjected to mitochondrial stress test according to **Figure 15**.

Following placement of the cell culture microplate into the Seahorse Bioanalyzer, basal respiration was measured, after which DMEM was first injected to assess cellular viability. Next, oligomycin (1.25 μ M) which inhibits Complex V of the ETC was injected, allowing measurement of ATP-linked respiration and proton leak. This was followed by injection of mitochondrial uncoupler carbonyl cyanide p-(trifluoro-methoxy) phenyl-hydrazine (FCCP; 1.0 μ M or 0.5 μ M for FAO wells), allowing measurement of maximal respiration by mitochondria. The difference between maximal and basal respiration, termed reserve capacity, could then be calculated. Finally, sources of non-mitochondrial oxygen consumption were measured after injection of rotenone (10 μ M), a Complex I inhibitor, and antimycin (1 μ M), a Complex III inhibitor. Where noted, cells were also treated with etomoxir to inhibit Carnitine palmitoyltransferase 1 (CPT1) dependent FAO. After the cell culture microplate was ejected from the bioanalyzer, cells were stained with crystal violet (CV), resuspended in 1% sodium dodecyl sulfate (SDS), and the absorbance at 550 nm was measured to calculate cell density in each well. Averaged oxygen consumption rate (OCR)

values across experiments were calculated by normalizing to CV absorbance (cell #) and subtracting the average non-mitochondrial respiration in each respective group.

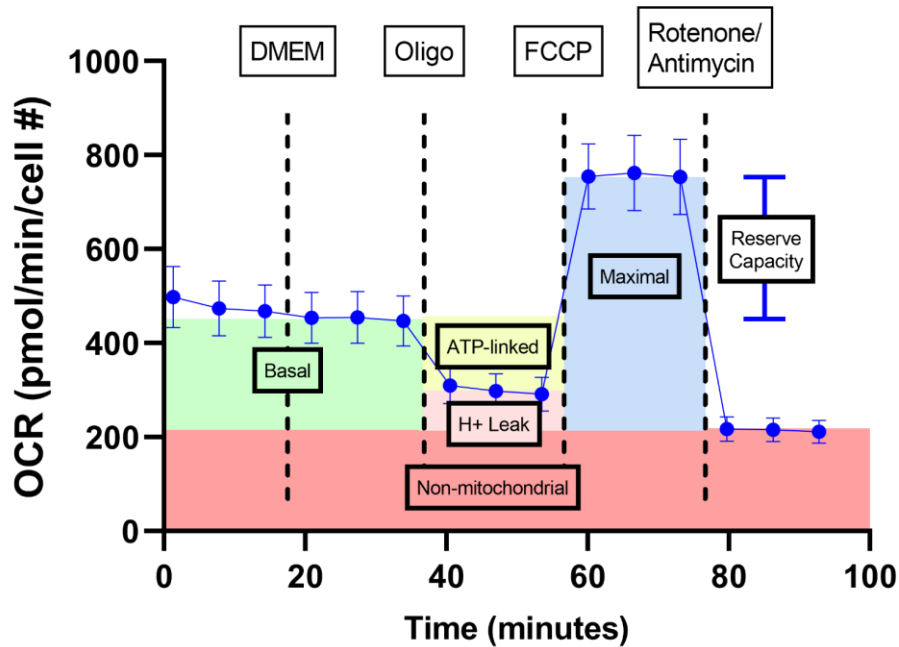


Figure 15: Measuring mitochondrial respiration. Cells are seeded in an even monolayer into the wells of a 96 well microplate. After the plate is placed into the Seahorse Bioanalyzer and allowed to equilibrate, baseline OCR measurements are recorded, which is the basal respiration by the cells. Afterward, oligomycin (oligo), a Complex V inhibitor, is injected into all wells within the plate. Any OCR signal measured at this point is from electron flux due to protons H^+ leak across the IMM, occurring through diffusion across the lipid membrane or inducible transport via adenine nucleotide translocase (ANT) or uncoupling proteins (UCPs). The difference between basal respiration and H^+ leak is the proportion of mitochondrial oxygen consumption linked to ATP production by Complex V (ATP-linked respiration). Injection with FCCP uncouples mitochondria, i.e. dissipates the mitochondrial membrane potential. Therefore, one can infer that this stage is the maximum rate at which the cells can consume oxygen, thus termed maximal respiration. By subtracting maximal from basal respiration, the reserve capacity can be calculated. This represents the potential of the cellular mitochondria to increase OCR, such as performing energy demanding tasks such as proliferation. Finally, rotenone, a Complex I inhibitor, and antimycin, a Complex III, are injected. Any measurable OCR is likely due to non-mitochondrial utilization, such as consumption of oxygen by cellular enzymes.

3.2.8 Statistics

Data are represented as mean \pm SEM. Analyses were performed with GraphPad Prism 8 (La Jolla, Calif). Continuous data were compared between groups with one-way or two-way ANOVA with posthoc Sidak test. Tukey test was used when only comparing main effect. If comparing between only two groups, a paired student t-test for variables that are normally distributed was used.

3.3 Results

3.3.1 Nitrite Promotes RASMC Phenotypic Switching

In the last chapter, we showed that nitrite inhibits PDGF-induced proliferation of rat aortic smooth muscle cells (RASMC) in normoxic conditions, but the effect of this anion on phenotypic switching remains unknown. During phenotypic switching, VSMC often become migratory in addition to decreasing contractile expression and increasing expression of MMPs (Frismantiene et al.). In the context of restenosis, this allows VSMC migration from the vessel medial to intimal layer, where these VSMC can proliferate and contribute to neointima formation. To determine whether nitrite modulates VSMC migration of cultured RASMC, we first performed scratch assays in the absence or presence of nitrite (25 μ M). Measurement of the scratch 12 hours after injury and treatment showed significantly greater scratch closure (smaller wound area) in nitrite-treated RASMC than untreated cells, suggesting, surprisingly that nitrite increases migration of RASMC (**Figure 16**).

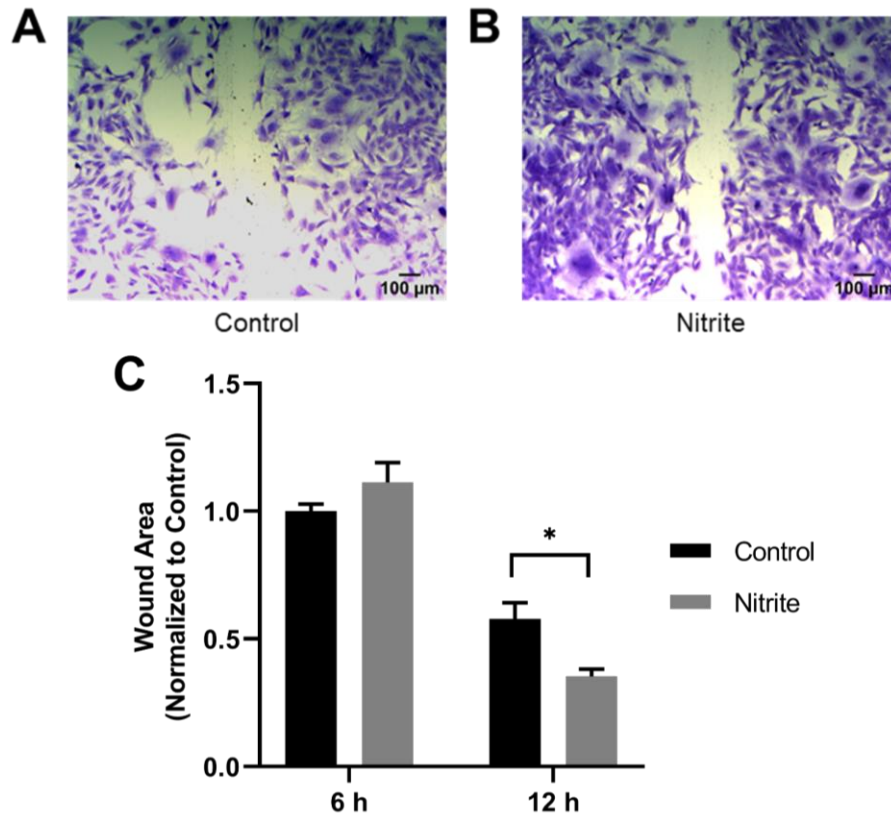


Figure 16: Nitrite promotes RASMC migration. RASMC were grown in cell culture plates until 90% confluency, at which time the cell monolayer was scratched with a pipette tip. Media was replaced with either normal or nitrite supplemented (25 μM) growth media. Cells were stained and fixed with crystal violet at the specified time points for visualization using an inverted microscope using a 10x objective lens (A-B). Wound area was quantified in ImageJ and normalized to 6 hour control cells (C) (mean ± SEM, n=12 images per group; two-way ANOVA with Tukey's multiple comparisons test; *P<0.05).

Increased migration is characteristic of synthetic VSMC phenotype. To assess whether the nitrite induced increase in migration was associated with phenotypic switching, we next measured VSMC contractile gene expression after nitrite treatment. RASMC cultured in normal growth media were treated with or without nitrite (25 μ M) and 24 hours later mRNA expression of key contractile genes, including Myh11, calponin, α -SMA, SM22- α , KLF4, myocardin, and Tet2, was measured by RT-PCR (**Figure 17**). We observed that nitrite treatment significantly decreased the mRNA levels of Myh11, α -SMA, and myocardin, and while it did not reach statistical significance, we also saw a trend to decreased expression of calponin, SM22- α , KLF4, and Tet2 (**Figure 17**). Contrary to our hypothesis that nitrite prevents the switch from contractile to synthetic phenotype, this data suggests that nitrite promotes RASMC switching from contractile to synthetic phenotype under these conditions.

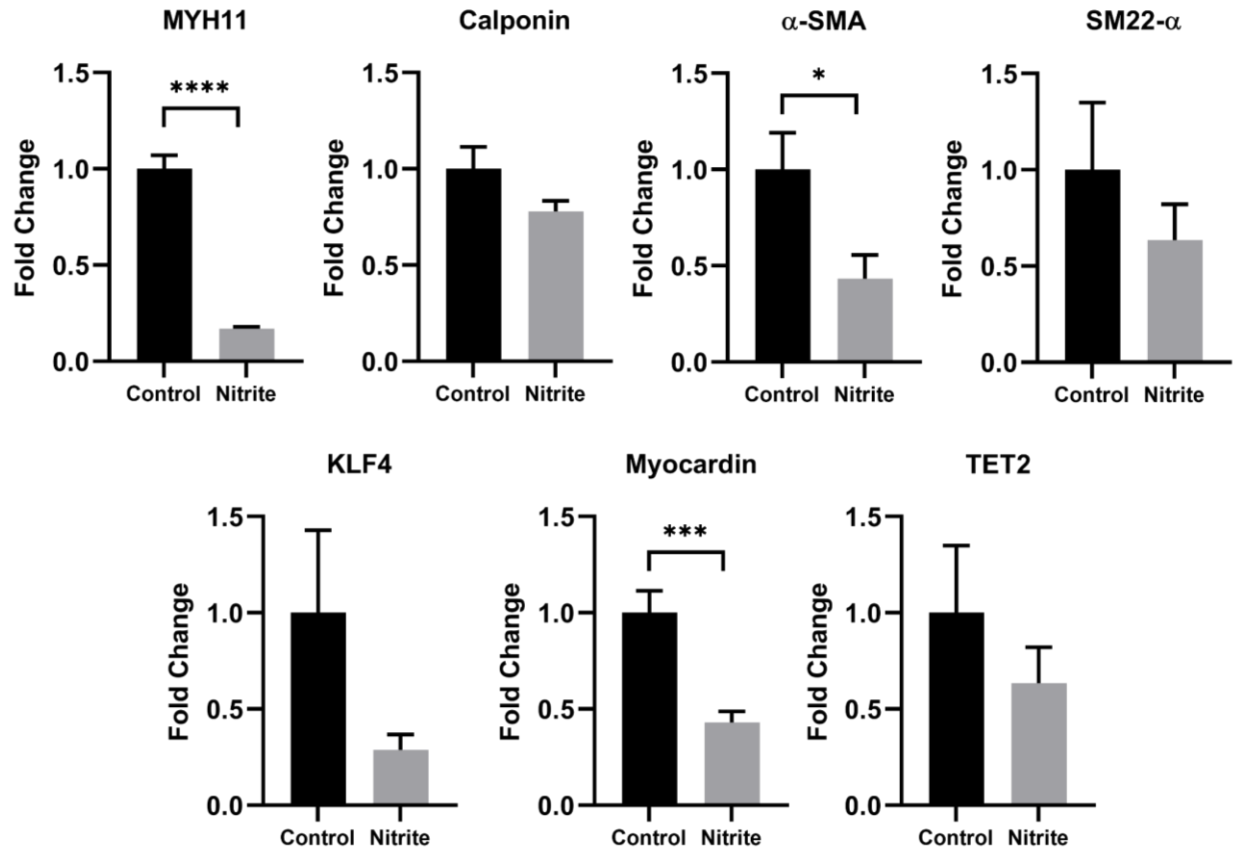


Figure 17: Nitrite decreases markers of contractile phenotype in RASMC. Cultured RASMC were washed with PBS and the media was replaced with normal or nitrite supplemented (25 μ M) growth media. After 24 h, cells were collected and the mRNA was extracted. Next, cDNA was synthesized and subjected to qPCR with primer pairs targeting various contractile genes. Levels of mRNA are expressed as fold change compared to untreated control siRNA transfected cells (mean \pm SEM, n=3; unpaired t-tests; *P<0.05; ***P<0.001; ****P<0.0001).

3.3.2 Nitrite-mediated VSMC Migration and Phenotypic Switching is Not Dependent on Mfn1

We previously showed that nitrite upregulates Mfn1 to inhibit RASMC proliferation. Thus, we next tested whether nitrite promotes migration and phenotypic switching through Mfn1. To test this, we genetically silenced Mfn1 in RASMC and performed scratch assays (**Figure 18**). RASMC were transfected with either control siRNA or siRNA targeted to Mfn1 and then subjected to scratch injury in the presence or absence of nitrite (25 μ M). Importantly, untreated RASMC in which Mfn1 was silenced showed a trend to increased migration compared to untreated control siRNA transfected cells at 12 h, although this result was not statistically significant (**Figure 18**). This is consistent with prior studies demonstrating that mitochondrial fission promotes VSMC migration and that Mfn1 expression inhibits migration (Chalmers et al.; Nguyen et al.; Li Wang et al.). Notably, treatment of RASMC lacking Mfn1 with nitrite showed significantly more migration than wildtype untreated cells, suggesting that nitrite does not require Mfn1 upregulation to promote migration (**Figure 18**).

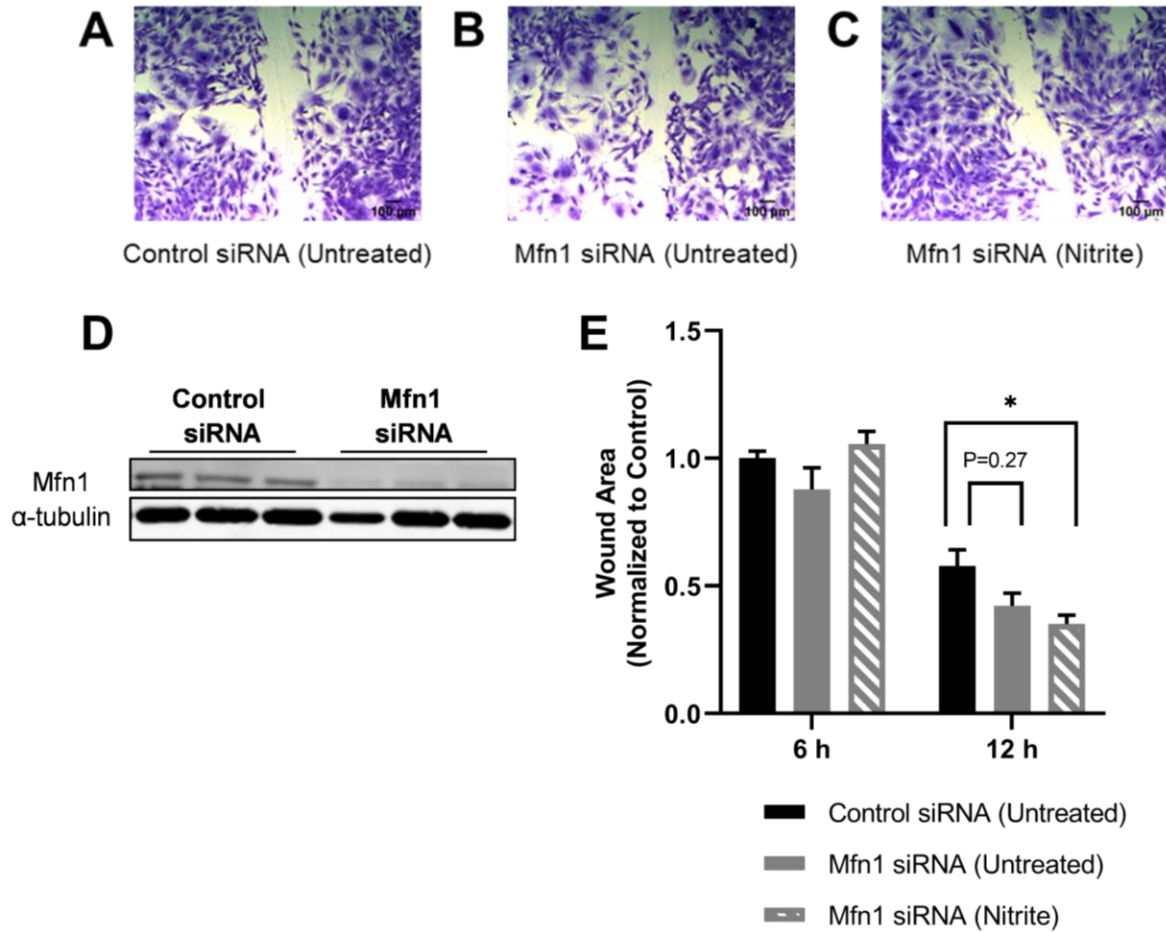


Figure 18: Nitrite promotes RASM C migration independent of Mfn1. RASM C were cultured in 12 well plates and transfected with either non-targeting control siRNA or Mfn1 targeting siRNA. After 48 h, the cell monolayer was scratched with a pipette tip and the cell media was replaced with either normal or nitrite supplemented (25 μ M) growth media. Cells were stained and fixed with crystal violet at the specified time points for visualization using an inverted microscope using a 10x objective lens (A-C). Wesern blot analysis was performed on lysates of separately transfected RASM C to confirm Mfn1 knockdown (D). Wound area was quantified in ImageJ and normalized to 6 hour control siRNA cells (E) (mean \pm SEM, n=12 images per group; two-way ANOVA with Tukey's multiple comparisons test; *P<0.05).

To test whether the nitrite-dependent loss of contractile genes was also independent of Mfn1, RASMC were transfected with either control siRNA or siRNA targeted to Mfn1. After 48 h the culture media was replaced with control or nitrite supplemented (25 μ M) growth media and gene expression of contractile genes was measured 24 h later. Compared to control siRNA transfected cells, Mfn1 knockdown cells had significantly decreased expression of Myh11 (**Figure 19**). Expression of calponin, α -SMA, SM22- α , KLF4, myocardin, and Tet2 were unaffected by Mfn1 silencing. With the addition of nitrite in Mfn1 knockdown cells, expression of Tet2 expression was significantly reduced while Myh11 expression was unchanged compared to untreated knockdown cells. Although only trending towards be statistically significant, expression of α -SMA, SM22- α , and myocardin in these cells were all decreased with nitrite treatment compared to untreated Mfn1 knockdown cells, suggesting Mfn1 is not required for nitrite's effects on the expression of these genes. In sum, these data demonstrate that nitrite-mediated decrease in contractile proteins is independent of Mfn1 and that Mfn1 expression (independent of nitrite) is required to at least partially maintain VSMC contractile phenotype.

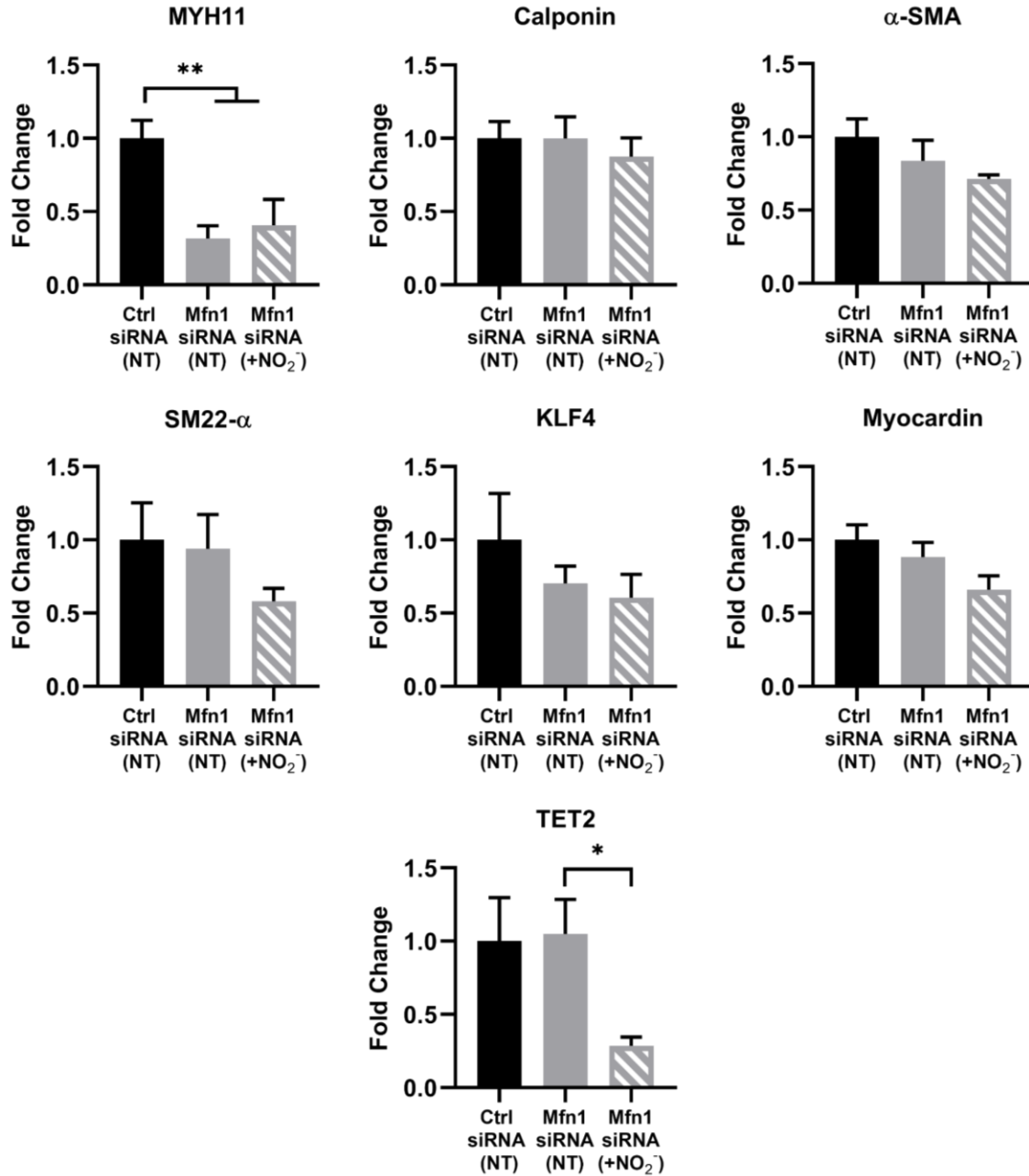


Figure 19: Nitrite regulates contractile gene expression in RASMC independent of Mfn1. RASMC were transfected with either non-targeting siRNA (control) or Mfn1 targeting siRNA for 24 h after which the media was replaced with either normal (NT) or nitrite supplemented (25 μ M) growth media (NO₂⁻). After an additional 24 h, cells were collected and the mRNA was extracted. Next, cDNA was synthesized and subjected to qPCR with primer pairs targeting various contractile genes. Levels of mRNA are expressed as fold change

compared to untreated control siRNA transfected cells (mean \pm SEM, n=3; one-way ANOVAs; *P<0.05; **P<0.01).

3.3.3 Nitrite and Mfn1 Alter RASMC Bioenergetics

VSMC phenotypic switching has been associated with changes in mitochondrial bioenergetics (Uebelhoer and Iruela-Arispe; Vallée et al.; Ryan et al.). Thus, we next investigated whether nitrite-mediated phenotypic switching is similarly associated with altered RASMC bioenergetics. To test this, we treated RASMC with nitrite (25 μ M) for 30 min which was followed by mitochondrial stress test using the Seahorse Bioanalyzer. Nitrite had no effect on resting cellular oxygen consumption (OCR), or basal respiration (**Figure 20A**). Additionally, nitrite had no effect on OCR after oligomycin treatment, affecting neither OCR due to proton leak or ATP-linked respiration. However, nitrite treatment significantly increased maximal respiration following injection of mitochondrial uncoupler FCCP (**Figure 20A**). As expected, this was associated with a significantly increased reserve capacity which is the difference between maximal and basal respiration. As we have shown that nitrite stimulates mitochondrial fusion (**Figure 7**), this could be due to increased membrane potential which is typically associated with more fused mitochondria.

Recent evidence highlights the regulation of mitochondrial metabolism by mitochondrial dynamics in VSMC (Salabei and Hill; Hong et al.; Ryan et al.). As the data above indicate that knockdown of Mfn1 promotes RASMC phenotypic switching, we wanted to determine whether loss of Mfn1 results in concomitant changes in cellular bioenergetics. RASMC were transfected with either nontargeting or Mfn1 siRNA and subjected to mitochondrial stress test. No changes were observed in basal or ATP-linked respiration. Additionally, there was no change in proton

leak between groups. Although not statistically significant, Mfn1 knockdown resulted in a decrease in maximal respiration under these conditions, which corresponded to a decrease in reserve capacity in these cells compared to control (**Figure 20B-C**).

It has been shown that compared to contractile phenotype, synthetic VSMC have increased reliance on FAO which is dependent on mitochondrial fission (Salabei and Hill). Additionally, metabolic switch to FAO has been associated in VSMC during pulmonary hypertension and metabolic reprogramming in various types of cancer (Sutendra et al.; Ma et al.). As we have demonstrated that Mfn1 partially regulates expression of contractile genes and migration in RASMC, we wanted to determine whether Mfn1 is also required for preventing this metabolic shift to FAO. RASMC were transfected with either control or Mfn1 siRNA followed by mitochondrial stress test in the presence of the fatty acids (FA) palmitate and L-carnitine. Similar to in the absence of fatty acids, Mfn1 knockdown had no effect on basal respiration, proton leak, or ATP-linked respiration. However, silencing of Mfn1 resulted in a significant increase in maximal respiration in the presence of FA compared to control siRNA transfected cells (**Figure 20D-E**). This effect was abolished with the addition of etomoxir (eto), which inhibits FA transport into the mitochondria by carnitine palmitoyltransferase I to prevent FAO. This suggests that although RASMC lacking Mfn1 can consume oxygen more readily in the presence of FA, they do not rely more on FAO compared to wildtype cells under basal conditions.

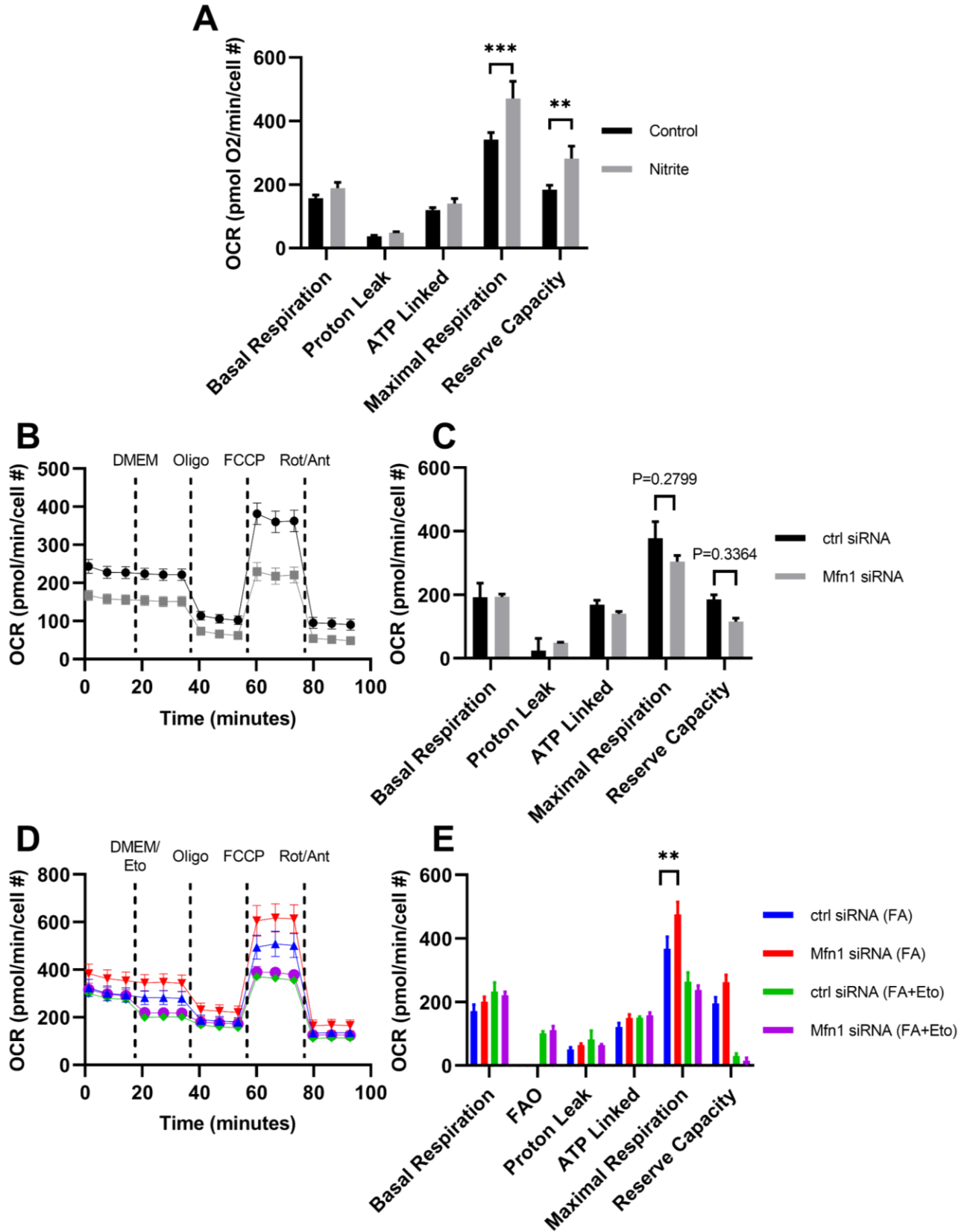


Figure 20: Nitrite and Mfn1 alter RASMC bioenergetics. RASMC were plated until a microplate until >90% confluency, at which time cells were treated with or without nitrite (25 μ M) in unbuffered basal DMEM for 30 min followed after which cells were subjected to mitochondrial stress test using Seahorse XFe96 Extracellular Flux Bioanalyzer as described in section 3.2.7. OCR is expressed as pmol/min normalized to CV absorbance and averaged between experiments (A) (mean \pm SEM, n=3; two-way ANOVA with Sidak's multiple comparisons test; **P<0.01 *P<0.001). Representative trace from mitochondrial stress test using Seahorse XFe96 Extracellular Flux Bioanalyzer (B) with average of experimental replicates (C). RASMC were transfected with either control (ctrl) or Mfn1 targeting siRNA, after which cells were subjected to mitochondrial stress test. RASMC then underwent stress test either under basal conditions. OCR is expressed as pmol/min normalized to CV absorbance and averaged between experiments (mean \pm SEM, n=3; two-way ANOVA with Sidak's multiple comparisons; P>0.05). Transfected RASMC also underwent stress test in the presence of fatty acid (FA) with or without receiving a first injection of etomoxir (FA+Eto). Representative trace from mitochondrial stress test using Seahorse XFe96 Extracellular Flux Bioanalyzer (D) with average of experimental replicates (E). OCR is expressed as pmol/min normalized to CV absorbance and averaged between experiments (mean \pm SEM, n=3; two-way ANOVA with Sidak's multiple comparisons; **P<0.01).**

3.3.4 Nitrite Promotes RASMC Phenotypic Switching by Increasing ROS Production

Nitrite has been shown to increase mitochondrial and cellular ROS production in epithelial cells and cardiomyocytes independent of Mfn1 expression (Pride et al.; Ling Wang et al.). Therefore, we next tested whether nitrite treatment stimulates ROS production in VSMC. Both total cellular and mitochondrial ROS production was measured in RASMC treated with nitrite (20 μ M). Compared to untreated cells, nitrite increased cellular H₂O₂ production in RASMC which was attenuated by both TEMPOL(100 μ M) or MitoTEMPO (100 μ M) (**Figure 21**). Altogether, total cellular ROS as measured by Amplex Red was increased by nitrite and only partially inhibited by MitoTEMPO treatment, and MitoSOX signal was only slightly increased by nitrite. These data suggest the majority of ROS is most likely not produced in mitochondria but is of cytosolic origin.

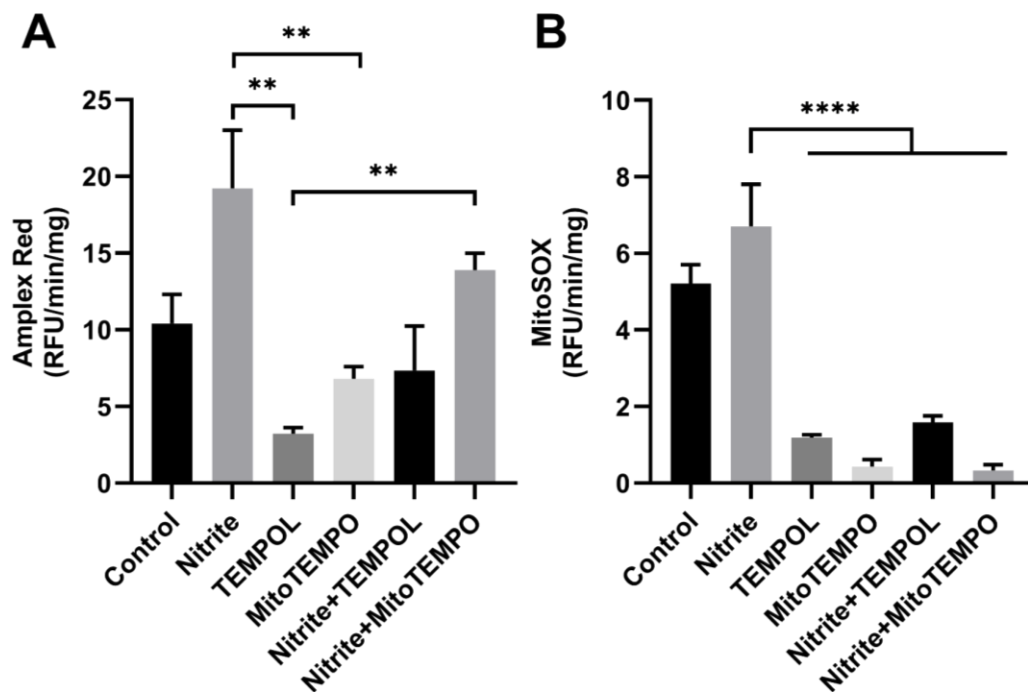


Figure 21: Nitrite increases cellular ROS production. RASMC were seeded into black clear bottom 96 well plates and treated with nitrite (20 μ M) with or without TEMPOL (100 μ M) or MitoTEMPO (100 μ M) for 12 h. After, extracellular H₂O₂ production was measured kinetically using Amplex Red (ex/em 530/590) and normalized to protein concentration (A) (mean RFU/min/mg \pm SEM, n=5; two-way ANOVA with Tukey's multiple comparisons test; *P<0.05). Similarly, mitochondrial superoxide production was measured kinetically using MitoSOX (ex/em 510/580) and normalized to protein concentration (B) (mean RFU/min/mg \pm SEM, n=5; two-way ANOVA with Tukey's multiple comparisons test; ****P<0.0001).

To determine the source of cytosolic ROS in nitrite treated cells, RASMC were pretreated with pharmacologic inhibitors of ROS producing proteins, including the xanthine oxidoreductase (XOR) inhibitor allopurinol, NAPDH oxidase (NOX) inhibitor apocynin, and cyclooxygenase (COX) inhibitor indomethacin, which was followed by treatment with nitrite (20 μ M). Compared to untreated cells, nitrite increased H₂O₂ production, and this increase was significantly attenuated by all inhibitors (**Figure 22**). These data suggest that nitrite-induced ROS production is dependent on the activity of a number of cytosolic enzymes in VSMC.

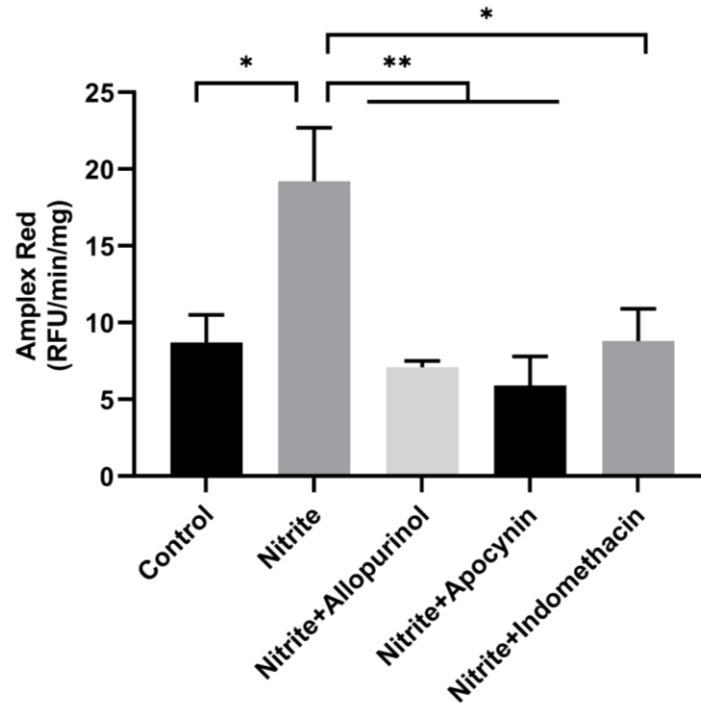


Figure 22: Nitrite requires oxidative enzyme activity to stimulate ROS production. RASMC were seeded into black clear bottom 96 well plates. Once confluent, RASMC were pretreated with allopurinol (50 μ M), apocynin (20 μ M), or indomethacin (20 μ M) for 30 min which was followed by nitrite treatment for 12 h. After, extracellular H_2O_2 production was measured kinetically using Amplex Red (ex/em 530/590) and normalized to protein concentration (A) (mean RFU/min/mg \pm SEM, n=5; two-way ANOVA with Tukey's multiple comparisons test; *P<0.05).

We next tested whether nitrite-dependent phenotypic switching was reliant on ROS production. RASMC were treated with nitrite (20 μ M) in the presence of TEMPOL (100 μ M) to scavenge cellular ROS. At 18 h, nitrite significantly increased wound closure compared to untreated cells, indicative of increased migration (**Figure 23A**). Treatment with TEMPOL attenuated this nitrite-mediated increase in migration, suggesting that ROS is required for nitrite's effects. To further investigate the role of ROS in nitrite-mediated phenotypic switching, RASMC were treated with nitrite for 12 h in the presence or absence of TEMPOL and expression of contractile genes MYH11 and α -SMA were measured by qPCR. Compared to control, nitrite treatment significantly decreased expression of both MYH11 and α -SMA (**Figure 23B**). Treatment with TEMPOL attenuated this significant decrease in expression of both genes. These data suggest that the decrease in contractile gene expression by nitrite is due to cellular ROS.

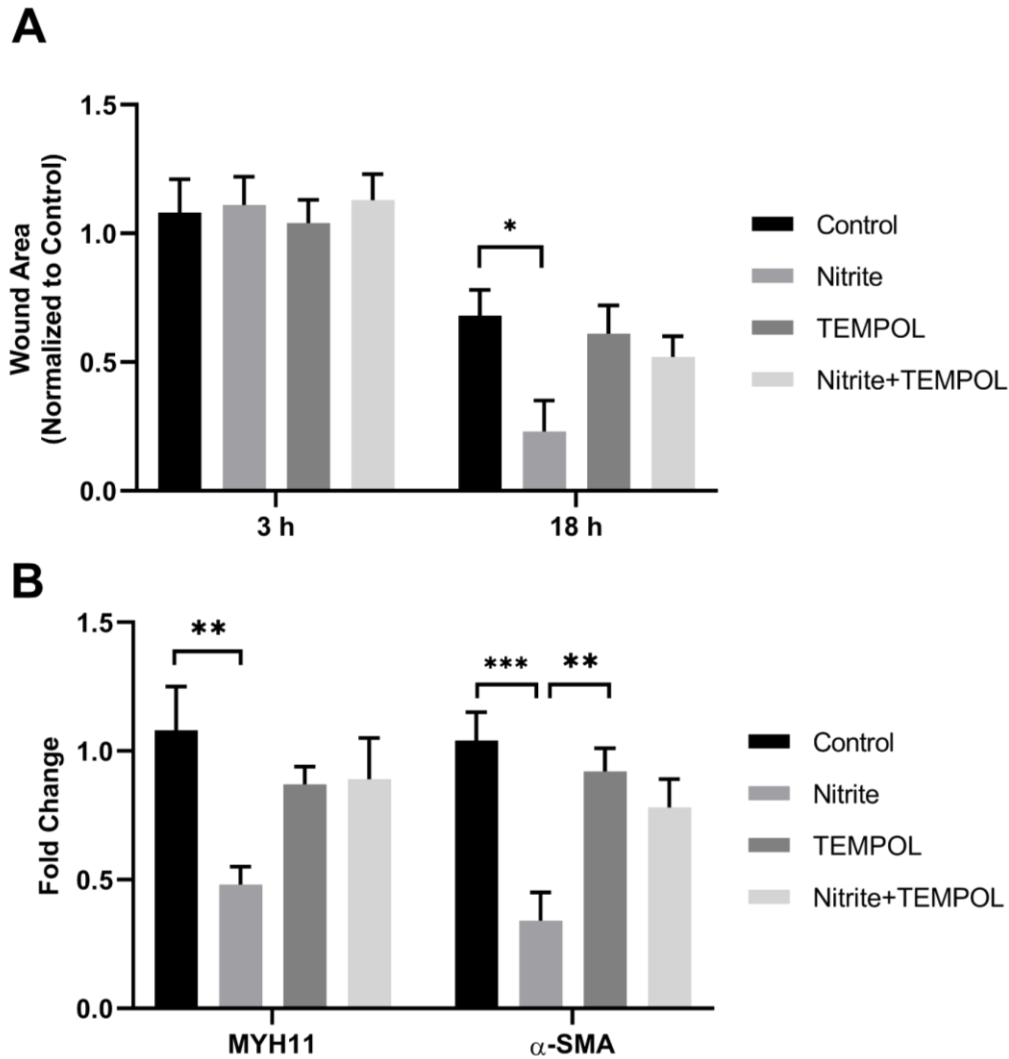


Figure 23: Nitrite is dependent on ROS production to promote RASMC phenotypic switching. RASMC were seeded in 12 well plates and once a confluent monolayer, were scratched with a pipette tip. The cell media was then replaced with either normal or nitrite supplemented (20 μ M) growth media with or without TEMPOL (100 μ M). Cells were stained and fixed with crystal violet at the specified time points for visualization using an inverted microscope using a 10x objective lens. Wound area was quantified in ImageJ and normalized to control untreated cells (A) (mean \pm SEM, n=5; two-way ANOVA with Tukey's multiple comparisons test; *P<0.05). Cultured RASMC were washed with PBS and the media was replaced with normal or nitrite supplemented (20 μ M) growth media with or without TEMPOL (100 μ M). After 12 h, cells were collected and the mRNA was extracted. Next, cDNA was synthesized and subjected to qPCR with primer pairs targeting

various contractile genes. Levels of mRNA are expressed as fold change compared to untreated control siRNA transfected cells (mean \pm SEM, n=5; two-way ANOVA with Tukey's multiple comparisons test; **P<0.01; ***P<0.001).

3.4 Discussion

This study demonstrates that nitrite regulates VSMC phenotypic switching *in vitro*, promoting transition from contractile to synthetic phenotype in RASMC as measured by migration and the loss of contractile gene expression (**Figure 16-Figure 17**). We found that this nitrite-dependent promotion of phenotypic switching was independent of the upregulation of Mfn1 and instead dependent on the stimulation of cytosolic ROS production (**Figure 24**).

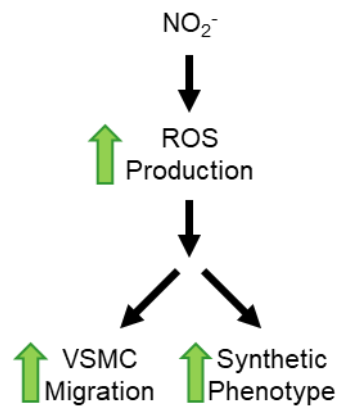


Figure 24: Nitrite promotes phenotypic switching by stimulating ROS production. Nitrite, independent of upregulating Mitofusin-1 (Mfn1), was found to increase migration and decrease contractile gene expression in cultured RASMC. These effects were dependent on a nitrite-mediated increase in ROS production primarily in the cytosol.

Most prior studies have explored the effects of NO and downstream cGMP on VSMC phenotype (Lincoln, Thomas; Lehnert et al.). This is the first study to directly measure the effects of nitrite on VSMC phenotype under normoxia, presumably in conditions where nitrite reduction to NO is energetically unfavorable. One previous study showed that nitrite promotes wound healing in airway epithelium in normoxia independent of cGMP production (Ling Wang et al.). Interestingly in that study, nitrite treatment was associated with increased superoxide production and required hydrogen peroxide (H₂O₂). Consistent with this mechanism, here we showed that nitrite primarily increased non-mitochondrial ROS production in RASMC, and that ROS production was required to promote migration and loss of contractile gene expression (**Figure 23**). While the exact origin of nitrite-induced ROS remains unclear, inhibition of XOR, NOX, or COX significantly attenuated nitrite-mediated ROS production suggesting that some general mechanism of increased pro-oxidant activity is involved. ROS such as H₂O₂ are known to perform physiological signaling through direct oxidation of proteins (Finkel). Additionally, ROS have been shown to promote migration by oxidizing and thereby regulating proteins involved in cellular motility, including cytoskeletal machinery like actin and myosin motor proteins (Rudzka et al.; J.-S. Kim et al.; Q. Xu et al.). More specifically, it has been shown that oxidation of cysteine residues of actin binding protein cofilin can promote cellular migration (Cameron et al.). Thus, nitrite could promote migration after scratch assay in RASMC through any of these pathways.

More specifically to VSMC, ROS species have been established as direct regulators of VSMC phenotypic switching, including H₂O₂ which is known to promote VSMC migration (San Martín and Griendling; Galley and Straub). Additionally, ROS-mediated signaling has been shown to regulate VSMC contractile gene expression (Byon et al.). For example, ROS is known to promote expression of calponin and myocardin in VSMC *in vivo* (Chettimada et al.). Additionally

Nox4, a major producer of superoxide, is critical for embryonic development of VSMC and can stimulate production of SRF and myocardin leading to downstream expression of Myh11 and α -SMA (Xiao et al.). These mechanisms could be mediated by reactive species through redox-regulated transcription factors such as CREB or Nrf2 which are known to modulate VSMC phenotype (Hudson et al.; Klemm et al.; Byon et al.). While physiological levels of cellular ROS can mediate these signaling processes, overproduction of ROS could lead to dysregulation resulting in switching to VSMC synthetic phenotype and alterations in gene expression. Further study is required to determine the downstream mediators of nitrite-induced ROS. In addition to promoting ROS production, nitrite itself could undergo oxidation to form reactive nitrogen species (RNS) which could also post-translationally modify and thus regulate cellular proteins. Nitrite can be oxidized by peroxidases or enzymes containing a ferryl heme center in the presence of H_2O_2 to nitrogen dioxide or peroxynitrite, which can mediate protein tyrosine nitration (Bian et al.; Brennan et al.). Recent work has shown that Myocardin itself can undergo *S*-nitrosation which decreases its transcriptional activity, which might occur with nitrite treatment in cellular compartments with low oxygen tension to favor reduction to NO (Liao et al.). Modification of cytoskeletal proteins involved in cellular migration or proteins which regulate XOR, NOX, and COX either through tyrosine nitration or *S*-nitrosation could lead to their activation and increased H_2O_2 production. It is also possible that nitrite could increase ROS production in other cellular compartments such as the mitochondria or peroxisome which would lead to intracellular crosstalk via ROS signaling to activate these cytosolic oxidative enzymes (Di Meo et al.).

Surely, the molecular species which are primarily responsible for promoting this phenotypic switch in response to nitrite are currently unknown and require further investigation. Even so, understanding the order of these nitrite-mediated signaling events may shed light on

potential targets for either epigenetic or post-translational modification. For example, in many of our experiments, we observed a decrease in Myocardin expression with nitrite treatment which could account for the decreased expression of contractile machinery like Myh11, α -SMA, and Calponin which are transcriptionally regulated by Myocardin-SRF complexes (Miano; Long et al.; Z. Xu et al.). However, the activity of Myocardin at these CArG elements upstream of these genes should be measured to confirm this notion. Tet2, which was also decreased with nitrite in the absence of presence of Mfn1, regulates Myocardin-dependent transcription through DNA hydroxylation of 5-methylcytosine to promote demethylation of DNA and chromatin remodeling (R. Liu et al.). Also involved in the transcriptional regulation of VSMC phenotypic switching is KLF4, which is a known repressor of Myocardin-mediated transcription that is under tight temporal regulation (Y. Liu et al.; Zheng et al.). Although KLF4 was decreased at the time of RNA extraction, it is possible that at earlier timepoints, KLF4 levels or activity may be increased with nitrite treatment, resulting in suppression of Myocardin-mediated transcription. Thus, careful investigation into the temporal and compartmental basis of these signaling events is required to understand the effects of nitrite on contractile gene expression.

Importantly, the finding that nitrite potentiates VSMC migration and switching to a synthetic phenotype is contrary to our original hypothesis that nitrite would promote contractile phenotype through upregulation of Mfn1. Interestingly, knockdown of Mfn1 (independent of nitrite) slightly increased VSMC migration and promoted the switch to a synthetic phenotype. Mitochondrial dynamics have been linked to changes in VSMC phenotype, with mitochondrial fission promoting VSMC migration (Chalmers et al.; Li Wang et al.; Lim et al.; Nguyen et al.). Our finding is consistent with this prior literature. However, less is known about the role Mfn1 and Mfn2 play in regulating VSMC gene expression. We showed that silencing of Mfn1 RASMC

promoted significantly decreased expression of Myh11 (**Figure 19**). As mitochondria travel along the cytoskeleton, expression of cytoskeletal genes like Myh11 could be regulated through interactions with mitochondria and outer membrane proteins (Bartolák-Suki et al.). Additionally, as mitochondrial fission has been linked to mitochondrial ROS production, localized mitochondrial ROS could oxidize these proteins leading to cytoskeletal protein degradation leading to feedback signaling mechanism. For example, Myocardin is known to interact and be sequestered in the cytosol by the cytoskeleton and upon actin polymerization, translocates to the nucleus to promote transcription of downstream cytoskeleton genes (Pipes et al.). This results in a feedback mechanism inhibiting SRF-mediated transcription of CArG-dependent genes including Myh11 and α -SMA (Gomez, Swiatlowska, et al.).

Taking together, the results from chapter 2 and 3 show that nitrite inhibits RASMC proliferation while promoting migration and phenotypic switching to a synthetic phenotype. Additionally, while Mfn1 is required for nitrite to inhibit RASMC proliferation, nitrite promoted synthetic phenotype is mostly independent of Mfn1 expression. In addition to measuring VSMC migration and contractile gene expression, we also measured mitochondrial respiration after nitrite treatment and Mfn1 knockdown. In agreement with previously published data, normoxic nitrite treatment increased maximal respiration and reserve capacity (**Figure 20A**) (Pride et al.). In Mfn1 knockdown RASMC, maximal respiration and reserve capacity were decreased (**Figure 20B-C**) which were increased in the presence of FA (**Figure 20D-E**). It is interesting that although nitrite treatment promotes VSMC synthetic phenotype, and separately Mfn1 knockdown alone promotes VSMC synthetic phenotype, these perturbations result in different bioenergetic profiles. Previously, it has been reported that RASMC treated with PDGF in complete serum have increased maximal respiration and reserve capacity due to increased glycolytic flux (Perez et al.).

Additionally, RASMC which were induced into contractile phenotype with serum starvation then stimulated with PDGF to induce synthetic phenotype had an increased reliance on FAO (Salabei and Hill). Increased reserve capacity could allow increased ATP production to meet the bioenergetics demands such as to promote phenotypic switching and migration or cellular proliferation after vascular injury. *In vivo* experiments would be required to determine the changes in metabolism due to Mfn1 deletion as the available nutrients could be critical in determining the VSMC phenotype and proliferation. This is due the differences in reserve capacity we observed in Mfn1 knockdown RASMC with or without FA present. Additionally, the changes in mitochondrial respiration with nitrite could also play a role in promoting VSMC synthetic phenotype while inhibiting proliferation, however more experiments would be required to investigate this crosstalk.

4.0 Mitofusin-1 Regulates Smooth Muscle Cell Vasoreactivity and Proliferation *In Vivo*

4.1 Introduction

Physiologically, blood vessel tone is maintained by vascular smooth muscle cells (VSMC), which, in their highly differentiated contractile phenotype, react to the biomechanical cues of the vessel wall to regulate blood flow. VSMC facilitate blood flow at every step of the arterial tree, beginning at the aortic root which buffers pulsatile blood flow from the left ventricle of the heart (Safar et al.). Conductive arteries such as the aorta and carotids are made up of many layers of VSMC which alternate with elastin and collagen fibers, thus primarily serving as an elastic reservoir or conduit. Although these arteries modulate flow through constriction and dilation, it is the smaller muscular and resistance arteries further down the vascular tree, such as the femoral and mesenteric arteries, which are primarily responsible for maintaining systemic blood pressure. This is due to their increased percentage of VSMC per area within the vessel wall allowing for higher contractility (Mulvany). In addition to these structural and functional differences, the arteries of the vascular tree differ in VSMC remodeling during disease. Conduit arteries typically undergo hypertrophic modeling such as during neointimal hyperplasia, while eutrophic modeling is typically observed in resistance arteries and associated with development of systemic hypertension (Brown et al.). During hypertrophic remodeling in neointimal hyperplasia, VSMC de-differentiate to their synthetic phenotype and propagate pathogenesis of restenosis through increased rates of migration and proliferation (Halayko and Solway).

Alterations in mitochondrial dynamics have previously been associated with the propagation of pathogenesis after vascular injury. For example, primary mitochondrial fission

protein dynamin related protein-1 (Drp1) has been shown to promote proliferation of pulmonary artery smooth muscle cell (PASMC) from patients with pulmonary hypertension compared to healthy controls by increasing mitochondrial fission (Marsboom et al.). PASMC from pulmonary hypertension patients also have lower expression levels of Mfn2 compared to controls (Marsboom et al.). Furthermore, overexpression of Mfn2 in the vessel wall has been shown to decrease neointima formation in balloon injured rat carotid arteries and decrease atherosclerotic lesion size in rabbits (K.-H. Chen et al.; Y. hong Guo et al.). These data suggest that fission events propagate pathogenic VSMC proliferation *in vivo*. However, these studies do not investigate the role of dynamics in maintaining physiological vessel function.

Prior studies of mitochondrial dynamics and vascular injury predominantly focus on the fusion protein Mfn2. However, Mfn1 and Mfn2 are differentially regulated and play distinct roles in fission events. Mfn2 is highly involved in regulating ER-mitochondrial contacts which can promote mitochondrial fission (Filadi et al.). Mfn1, while not involved in mediating ER-mitochondrial contacts, has been shown to be the primary outer membrane fusion protein (Ishihara). Additionally, Mfn1 and Mfn2 are distinctly regulated via post-translational modifications, such as ubiquitination by E3 ligase March5 which targets Mfn1 but not Mfn2 for proteasomal degradation (Y-Y Park et al.; Sugiura et al.). Transgenic mice with global silencing of Mfn1 and Mfn2 have been made which results in embryonic lethality when both paralogs are absent (H. Chen, Detmer, et al.). Additionally, global single homozygous deletion of either Mfn1 or Mfn2 has been performed which results in neurological degeneration in Mfn2 but not Mfn1 knockout mice (H. Chen, McCaffery, et al.). Others have also investigated the effects of double deletion of Mfn1/2 in the heart which results in cardiomyocyte necrosis and cardiac remodeling

(Song et al.). However, the role of smooth muscle-specific Mfn1 deletion and its function in physiological and pathological vascular function has not been tested.

In the previous chapters, we showed that nitrite specifically upregulates Mfn1 (but not Mfn2) to inhibit RASMC proliferation *in vitro*. In contrast, we showed that nitrite promotes RASMC migration and loss of contractile gene expression, consistent with phenotypic switching in a manner independent of Mfn1. Further, genetic silencing of Mfn1 alone partially promoted phenotypic switching in RASMC. To test the physiological role of Mfn1 in vascular function, we developed a novel smooth muscle-specific Mfn1 knockout mouse (SMC-Mfn1^{-/-}). Herein, we characterized vascular function in SMC-Mfn1^{-/-} mice by performing *ex vivo* wire myography experiments and measuring blood pressure *in vivo* through radio telemetry. We then tested the role of Mfn1 and the interplay between Mfn1 and nitrite in pathology by subjecting wildtype (WT) and SMC-Mfn1^{-/-} mice to vascular injury. Herein, we demonstrate that Mfn1 regulates physiological vessel tone to different levels in large versus small vessels. Additionally, we show that SMC-Mfn1^{-/-} mice are more sensitive to models of vascular injury and that the absence of Mfn1 in smooth muscle alters the nitrite-mediated response to injury.

4.2 Materials & Methods

4.2.1 Reagents

Reagents were obtained from Sigma-Aldrich unless otherwise specified.

4.2.2 Cell Culture

Rat aortic smooth muscle cells (RASMC) were cultured as described in **section 2.2.2**.

4.2.3 Transfection

RASMC were transfected as described in **section 2.2.3**.

4.2.4 Murine Model Generation

Female B6.129(Cg)-Mfn1^{tm2Dcc}/J mice which contain homozygous loxP flanked Mfn1 alleles (Mfn1^{fl/fl}) were obtained from Jackson Laboratories and were first described in Chen, McCaffery, & Chan, 2007. Male B6.FVB-Tg(Myh11-cre/ERT2)1Soff/J mice (MYH11-Cre^{ERT2}) which contain a tamoxifen-inducible Cre recombinase under the MYH11 promoter were received as a kind gift from Dr. Adam Straub. Male MYH11-Cre^{ERT2} mice were crossed with female Mfn1^{fl/fl} mice according to the following breeding scheme:

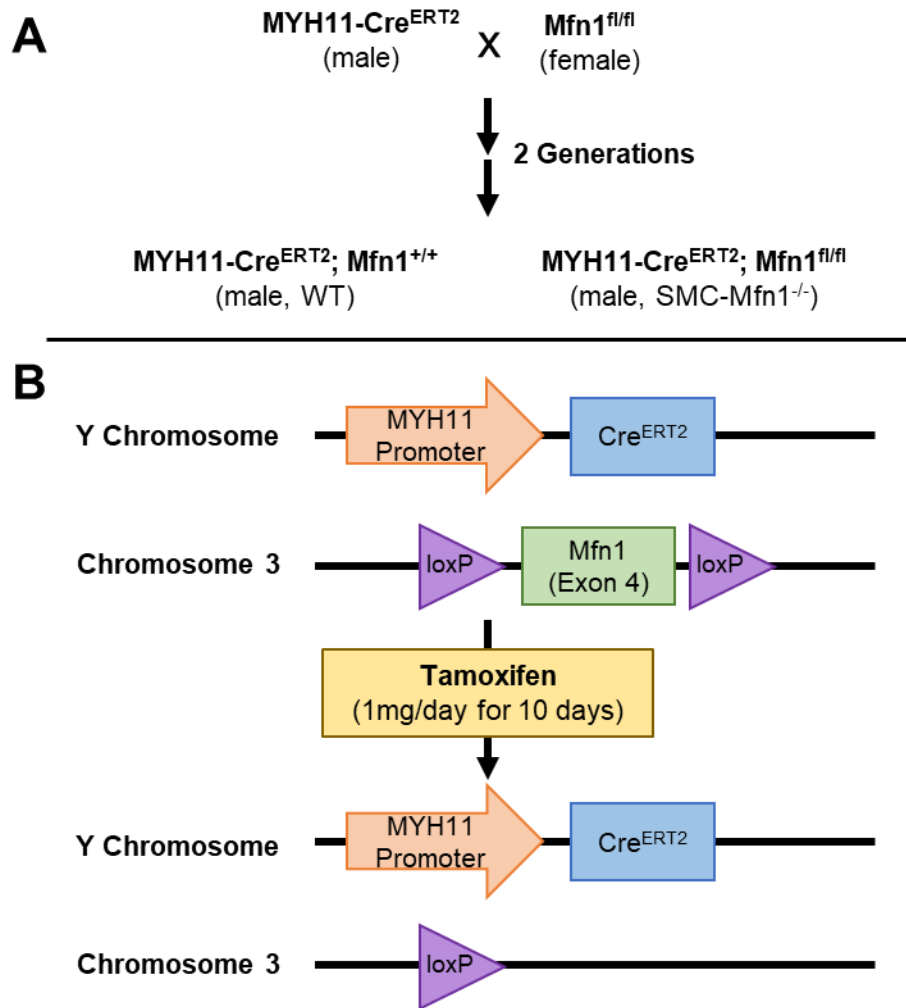


Figure 25: Generation of smooth muscle-specific Mfn1 knockout mouse. Male MYH11-Cre^{ERT2} were crossed with female Mfn1^{fl/fl} mice. After two generations of breeding (A), we obtained male MYH11-Cre^{ERT2} mice homozygous for either the wildtype (WT) Mfn1 gene and or the floxed Mfn1 gene (Mfn1^{fl/fl}). Induction of cre-recombinase expression was induced with tamoxifen administration (B). Cre-Lox recombination results in the excision of the G1-GTPase domain on exon 4 of the Mfn1 gene and causes a frameshift, preventing formation of any functional Mfn1 protein (H. Chen, McCaffery, et al.).

Confirmation of genotype was performed by PCR of DNA obtained from mouse ear snips. Briefly, tissue was boiled at 95°C in a solution containing 20 mM NaOH and 0.2 M EDTA for 1 h followed by neutralization with 40 mM Tris-HCl pH 5. This was followed by PCR (step 1: 95°C for 2 min; step 2: 95°C for 30 sec; step 3: 60°C for 30 sec; step 4: 72 °C for 30 min; step 5: repeat steps 1-4 for 35 cycles; step 6: 72 °C for 2 min) using the following sets of primers:

Table 6: Genotyping Primers

Description	5` (Forward) Primer (5`-3`)	3` (Reverse) Primer (5`-3`)
Mfn1 ^{fl/fl}	TGGTAATCTTTAGCGGTGCTC	GGAGGACTTTATCCCACAGC
MYH11-Cre ^{ERT2}	TGACCCCATCTCTTCACTCC	AGTCCCTCACATCCTCAGGTT

Mice containing the MYH11-Cre^{ERT2} transgene homozygous for wildtype Mfn1 (WT) were used as control mice. Mice containing the MYH11-Cre^{ERT2} transgene homozygous for the floxed Mfn1 allele were termed Mfn1^{-/-}. To induce Cre-Lox recombination in mice age 8-12 weeks, tamoxifen (Sigma Aldrich T5648-1G) was first dissolved in 100% ethanol with occasional vortexing. Once fully dissolved, tamoxifen solution was then dissolved into warm corn oil at a final concentration of 10 mg/mL and administered via intraperitoneal injection at a dose of 1 mg per day over a total of 10 days with two days break after the first 5 injections.

Confirmation of knockout was performed by Western blot analysis of isolated thoracic aortas. Briefly, the aorta was removed from the thoracic cavity after mouse sacrifice. Following washing in PBS, the aorta was cleaned of adventitial tissue and then cut open to expose the lumen. The endothelium was then denuded using a cotton swag. Cleaned tissue was homogenized with a

dounce tissue grinder, resuspended in Roche lysis buffer, and subjected to Western blot analysis as described in **section 2.2.6**.

4.2.5 Cryosectioning and Tissue Preparation for IHC of OCT Embedded Tissue

Carotid arteries from WT and *Mfn1*^{-/-} mice which had received tamoxifen injection were isolated, washed with PBS, and fixed in 2% paraformaldehyde for 1 h. Arteries were then placed in 30% sucrose for 24 h, replacing the sucrose solution every 8 h. Afterward, arteries were removed and flash frozen using liquid N₂-cooled 2-methylbutane (Fisher Cat No. O3551-4) and embedded into OCT compound in a small cassette by freezing. Arteries were sectioned using a cryostat into 8 μm slices which were placed onto Superfrost Plus Microscope Slides (Fischer Scientific). Once ready for imaging, frozen sections were thawed for 10 min and rehydrated in PBS for 5 min. Following permeabilization for 10 min with 0.1% Triton X-100, sections were blocked in PBS contained 5% BSA (PBB) with the addition of 20% donkey serum. After washing with PBB 5 times, sections were incubated with the following primary antibodies for 24 h at 4°C:

Table 7: Primary Antibodies for IHC of OCT Embedded Tissue

Protein	Vendor	Catalog #	Species	Dilution
Mfn1	Abcam	126575	Chicken	5 μg/mL
α-SMA	Abcam	5694	Rabbit	5 μg/mL

Sections were then washed with PBB 5 times and incubated with the following secondary antibodies for 1 h:

Table 8: Secondary Antibodies for IHC of OCT Embedded Tissue

Protein	Vendor	Catalog #	Species	Dilution
Anti-Chicken Cy3	Sigma Aldrich	AP194C	Donkey	1:500
Anti-Rabbit Cy5	Jackson ImmunoResearch	715-605- 150	Donkey	1:500

Afterward, tissue was stained with DAPI for 5 min, washed, and a coverslip was placed over the slide using gelvatol.

4.2.6 Wire Myography

Thoracic aorta, carotid, and third order mesenteric arteries were rapidly excised placed in room temperature physiological salt solution (PSS) (containing (in mM): NaCl 119, KCl 4.7, MgSO₄ 1.17, KH₂PO₄ 1.18, D-glucose 5.5, NaHCO₃ 25, EDTA 0.027, CaCl₂ 2.5, pH 7.4) cleaned of fat, and cut into 2mm rings. Artery segments were placed on a 2pin (aorta)/wire (carotid & mesenteric) myograph (DMT 620M) filled with PSS and bubbled with 95% O₂ 5% CO₂ at 37°C. Following a 30 min rest, aortas were incrementally stretched to 500 mg initial tension while carotid and mesenteric arteries were gradually stretched to a tension corresponding to a transmural pressure of 80 mmHg. Next, arteries were constricted with 60 mM KCl for 5 min to test viability and used as maximum constriction. Arteries were then washed 3 times with PSS and allowed to

rest for 30 min or incubated with MitoTEMPOL (Cayman) if undergoing pretreatment. A final wash was performed and vessels rested for an additional 10 min.

Following the final 10 min rest period, vessels were constricted with a dose response of prostaglandin f2 α (100 nM-10 μ M) for aorta, PE (500 nM-10 μ M) for carotid, and U46619 (100 nM-500 nM) for mesenterics. After reaching plateau, a cumulative dose response curve of Ach (10 nM-100 μ M), SNP (1 nM-100 μ M), or Bay 58-2667 (Cayman, 1 pM-1 μ M) was performed to assess endothelial-dependent and independent relaxation, respectively. Ca⁺ free PSS containing 100 μ M sodium nitroprusside was added to determine maximal dilation.

4.2.7 Radio Telemetry

Continuous blood pressure readings were collected using a pressure catheter (HD-X10, Data Sciences International (DSI)). Briefly, mice were anesthetized with isoflurane and the catheter was implanted in the left carotid artery, which was connected to a radiotransmitter placed subcutaneously along the flank. Mice were allowed to recover 14 days after implantation, after which baseline measurements were recorded continuously for 5 h using Dataquest A.R.T. 20 software (DSI). Mice were then administered either vehicle (0.9% NaCl) or nitrite (25 mg/kg) via intraperitoneal injection. Following 1 h after injection, blood pressure was recorded for 2 h and compared to baseline recordings.

4.2.8 Carotid Ligation Model

Wildtype and SMC-Mfn1^{-/-} mice were subjected to partial carotid ligation as described previously (Korshunov and Berk). First, mice were anesthetized with isoflurane (2%). Following

incision above the ribcage and blunt dissection to reveal the underlying vasculature, a suture was looped circumferentially around the right common artery just below the carotid bifurcation to achieve partial ligation. Mice were placed under a heat lamp following surgery until recovered, after which they were placed into separate cages containing either normal drinking or drinking water supplemented with nitrite (1.5 g/L). After 3 weeks, mice were euthanized with CO₂ and perfused with PBS followed by 4% PFA. Carotid arteries were isolated, fixed overnight in 4% PFA, and embedded into paraffin blocks. After, 10 µm sections obtained using a microtome (Leica) were placed onto a Superfrost Plus Microscope Slides (Fischer Scientific).

4.2.9 Deparaffinization and Immunofluorescence Staining

Sections mounted on microscope slides were deparaffinized by rehydrating in xylene followed by washing in ethanol gradients. Sections then underwent antigen retrieval in unmasking solution (Vector Labs H-3300) and microwaved for 20 min. Once cooled, sections were washed with PBS and then blocked in blocking buffer (0.6% fish skin gelatin, 1% horse serum). Sections were incubated with the following primary antibodies in blocking buffer overnight at 4°C:

Table 9: Primary Antibodies for IHC

Protein	Vendor	Catalog #	Species	Dilution
Mfn1	Abcam	126575	Mouse	4 µg/mL
Ki67	Abcam	15580	Rabbit	1 µg/mL
Acta2-FITC	Sigma Aldrich	F3777	Mouse	1:500

Afterward, sections were washed and then incubated in the following secondary antibodies:

Table 10: Secondary Antibodies for IHC

Protein	Vendor	Catalog #	Species	Dilution
Anti-Mouse AlexFluor-555	Thermo Fisher	A31573	Donkey	1:250
Anti-Rabbit AlexFluor-647	Thermo Fisher	A31570	Donkey	1:250
*Acta2-FITC	Sigma Aldrich	F3777	Mouse	1:500

Sections were then stained with Acta2-FITC (see **Table 10**) and DAPI (Thermo, D1306; 1:1000 dilution) for 1 h followed by washing. Prolong Gold mounting solution (Invitrogen P36930) was placed over the sections and a coverslip was applied to cover the microscope slide.

4.2.10 Confocal Microscopy

Images were obtained using a Nikon A1 Confocal Microscope System (Nikon) with a 20x objective lens. Images were processed and analyzed using NIS-Elements Software (Nikon).

4.2.11 Masson's Trichrome Staining

Following deparaffinization, sections were submerged in Bouin's solution for 1 h at 60°C followed by washing with water for 5 min. This was followed by staining of nuclei with Weigart's iron hemaotylin working solution and another 5 min wash. Tissue sections was then stained in succession with Biebrich scarlet-acid fuschin solution, phosphotungstic/phosphomolybdic acid,

and aniline blue with washing with water in between, after which sections were cleared with xylene and a coverslip was applied with xylene mounting medium.

4.2.12 Light Microscopy

Images of Masson Trichrome stained tissue were obtained using Trinocular Inverted Fluorescence Phase Contrast Microscope using a 20x objective lens (Zeiss). Images were acquired with an AxioCAM Mrc5 camera using Axiovision Rel. 4.8 software (Zeiss). Intimal and medial areas were then quantified using ImageJ.

4.2.13 Nitrite Measurement

Levels of nitrite in plasma, heart, and skeletal muscle (quadriceps) nitrite were measured using reductive chemiluminescence using tri-iodine in a Sievers 280i Nitric Oxide Analyzer as previously described (MacArthur et al.).

4.2.14 Protein Extraction & Western Blot Analysis

See **section 2.2.6** for detailed methodology. The following antibodies were used for Western blot analysis in this chapter:

Table 11: Antibodies used for Western blot analysis

Protein	Vendor	Catalog #	Species	Dilution
Mfn1	Abcam	126575	Mouse	1:1000
α -smooth muscle actin (SMA)	Abcam	5694	Rabbit	1:1000
sGC β 1	Cayman	160897	Rabbit	1:1000
α -Tubulin	Calbiochem	CP06	Mouse	1:5000
Donkey anti-Rabbit (680 nm)	LI-COR	926-68073	Donkey	1:10.000
Goat anti-Mouse (800 nm)	LI-COR	926-32210	Goat	1:10.000

4.2.15 Measurement of cGMP

Cellular cGMP levels were measured using a cGMP ELISA kit (Cayman 581021). Briefly, cells were treated at various concentrations with DEA NONOate (Cayman), Bay 41-2272 (Cayman), and Bay 58-2667 (Cayman). After 20-30 minutes, cells were lysed on ice with 0.1 M HCl for 10 minutes. Afterwards, cell debris was pelleted via centrifugation and the resulting supernatant was collected and neutralized with ELISA kit buffer. Cellular cGMP levels were quantified by fitting the standard curve with a 4 parameter logistic regression which was normalized to protein concentration as measured by absorbance at 280 nm and calculated using the Warburg-Christian method.

Tissue cGMP levels were measured using cGMP Chemiluminescent Assay Kit (Cell Signaling) according to manufacturer's instructions. Briefly, multiple third order mesenteric arteries were isolated from WT or Mfn1^{-/-} mice and homogenized in provided lysis buffer with a Dounce homogenizer on ice. Homogenates were centrifuged at 1200xg to collect cellular debris,

after which the supernatant was subjected to cGMP measurement by competitive ELISA comparing to a standard of known cGMP concentrations. Levels of cGMP were normalized to protein concentration which was quantified using Pierce BCA Protein Assay Kit (Thermo Fisher).

4.2.16 Measurement of Cellular ROS

Mesenteric arteries were isolated from WT and SMC-Mfn1^{-/-} mice and placed into a black 96 well plate in PBS. Amplex Red Reagent (Thermo Fisher, 5 μ M in PBS) was then added to each well and fluorescence intensity was measured kinetically using a plate reader at ex/em 530/590. Amplex Red signal was normalized to protein concentration which was quantified using Pierce BCA Protein Assay Kit (Thermo Fisher).

4.2.17 Statistics

Data are represented as mean \pm SEM. Analyses were performed with GraphPad Prism 8 (La Jolla, Calif). Continuous data were compared between groups with one-way or two-way ANOVA with posthoc Sidak test. Tukey test was used when only comparing main effect. If comparing between only two groups, a paired student t-test for variables that are normally distributed was used. For telemetry experiments, repeated measures one-way ANOVA was used to compare blood pressure before and after nitrite administration.

4.3 Results

4.3.1 Verifying Smooth Muscle Cell-specific KO of Mfn1

To generate smooth muscle cell (SMC)-specific Mfn1 knockout mice (Mfn1^{-/-}), female C57BL/6 mice containing a floxed Mfn1 allele were crossed with male mice containing a Cre recombinase transgene under the MYH11 promoter (MYH11-CreER^{T2}). After two generations, male mice containing the MYH11-CreER^{T2} transgene homozygous for either wildtype Mfn1 (WT) or floxed Mfn1 allele (Mfn1^{-/-}) were obtained. PCR of genomic DNA from ear snips using primers for Mfn1 and MYH11-CreER^{T2} confirmed correct genotypes (**Figure 26A**). From age 8-12 weeks, mice were then administered tamoxifen via intraperitoneal injection to induce Cre nuclear translocation and DNA excision. To verify that Mfn1 knockout was specific to smooth muscle, aortas denuded of endothelium and stripped of adventitia as well as hearts were isolated and homogenized. Western blot analysis from these lysates shows that Mfn1 protein expression is absent in aortic but not heart lysates (**Figure 26B**) suggesting genetic knockout is specific to smooth muscle in these mice. To verify these findings, confocal fluorescence microscopy was also performed on carotid arteries isolated from these mice, staining for α -SMA to identify VSMC and Mfn1. Immunofluorescence imaging showed little to no Mfn1 fluorescence within the smooth muscle layer of Mfn1^{-/-} mice compared to WT animals, thus confirming SMC-specific knockout (**Figure 26C**).

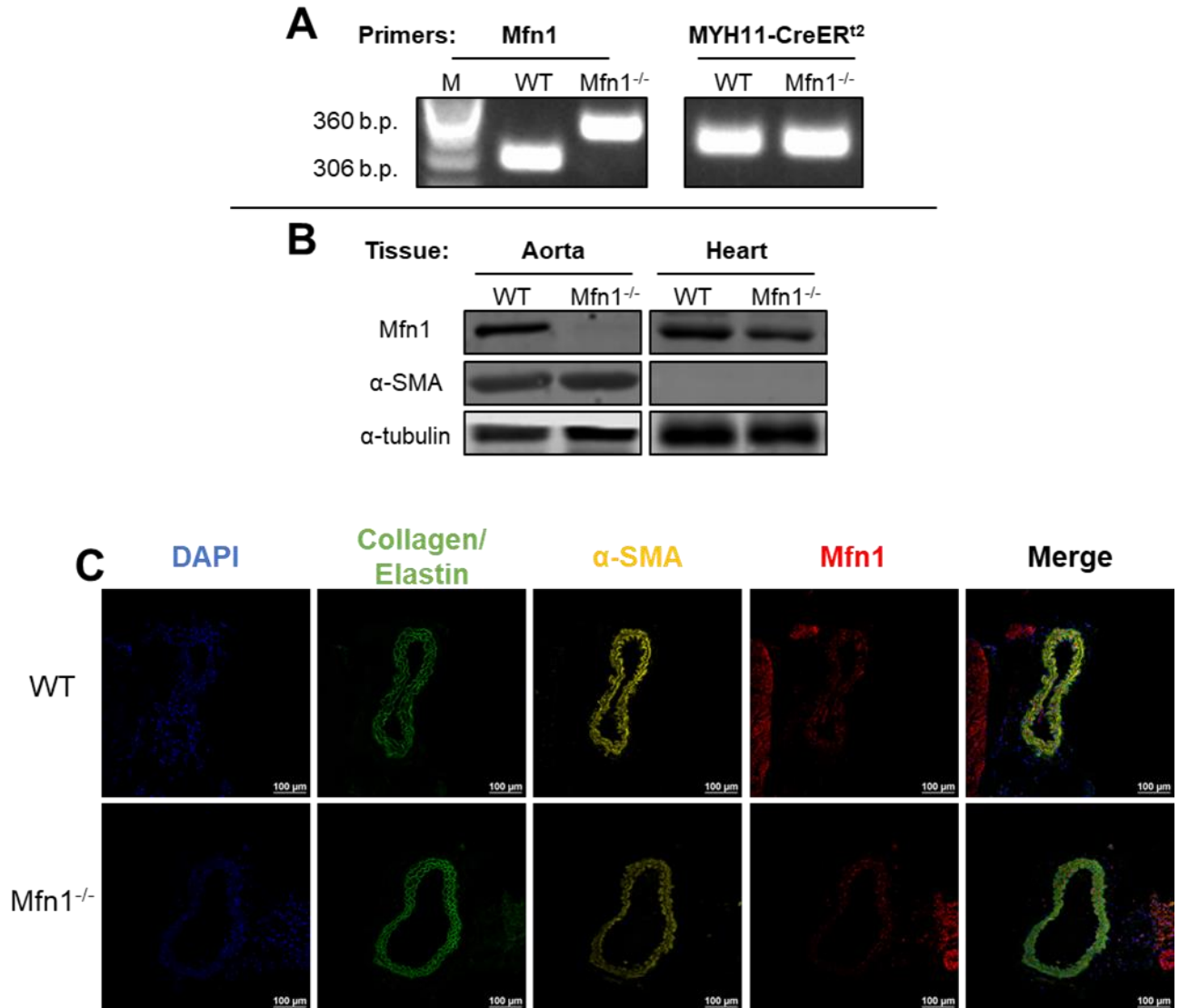


Figure 26: Verification of efficient deletion of Mfn1 in SMC. Mice were bred to generate MYH11-CreER^{T2} expressing mice containing either the wildtype (WT) or floxed Mfn1 gene (Mfn1^{-/-}). PCR of DNA from ear snips (A) verifies correct base pair (b.p) length for both genotypes as well as presence of MYH11-CreER^{T2} transgene. At ages 8-12 weeks, mice were administered tamoxifen via intraperitoneal injection. After euthanasia following experimental procedures, protein lysates from aortas and hearts were subjected to Western blot analysis which shows smooth muscle-specific knockout of Mfn1 (B). Confocal fluorescence microscopy of carotid arteries from WT and Mfn1^{-/-} mice staining for DAPI to mark nuclei, autofluorescence in the GFP channel identifying

collagen and elastin, α -SMA to identify VSMC, and Mfn1 (C). Qualitative analysis confirms deletion of Mfn1 within the VSMC layer.

4.3.2 The Effects of SMC-specific Deletion of Mfn1 on Systemic Blood Pressure

To determine the effects of SMC Mfn1 deletion on systemic blood pressure, pressure catheters connected to radiotransmitters were placed intraluminally within the left carotid artery of WT and SMC-Mfn1^{-/-} mice. Following recovery from device placement, baseline blood pressure measurements were recorded. Compared to WT, SMC-Mfn1^{-/-} mice had slightly lower systolic blood pressure which was not statistically significant (**Figure 27A**). Additionally, diastolic blood pressure in WT mice was similar to SMC-Mfn1^{-/-} mice levels (**Figure 27B**).

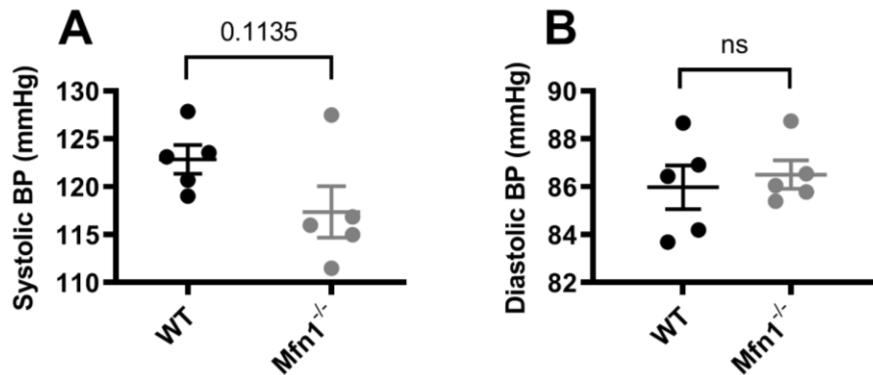


Figure 27: Deletion of Mfn1 does not alter blood pressure. Wildtype (WT) and smooth muscle specific Mfn1 knockout mice (SMC-Mfn1^{-/-}) were subjected to radio telemetry for blood pressure measurement. Following recovery after radiotransmitter implantation, baseline blood pressure (BP) measurements were recorded. Baseline systolic (A) and diastolic (B) blood pressure in SMC-Mfn1^{-/-} mice were not significantly different when compared to WT (mean BP \pm SEM, n=5; unpaired t-tests; P>0.05).

We next tested whether these mice were differentially responsive to blood pressure modulators. Nitrite administration, through its conversion to nitric oxide, mediates vasodilation and decreases systemic blood pressure in rodents and humans (Larsen et al.; Ghosh et al.; Feelisch, Akaike, et al.; Cosby et al.). WT and SMC-Mfn1^{-/-} were administered nitrite (25 mg/kg) via intraperitoneal injection. Systolic blood pressure decreased significantly and to an equal extent in both WT and SMC-Mfn1^{-/-} mice, suggesting that Mfn1 deletion does not alter nitrite-mediated vasodilation and lowering of systemic blood pressure (**Figure 28A,C**). Diastolic blood pressure was unaltered by nitrite administration in both groups (**Figure 28B,D**)

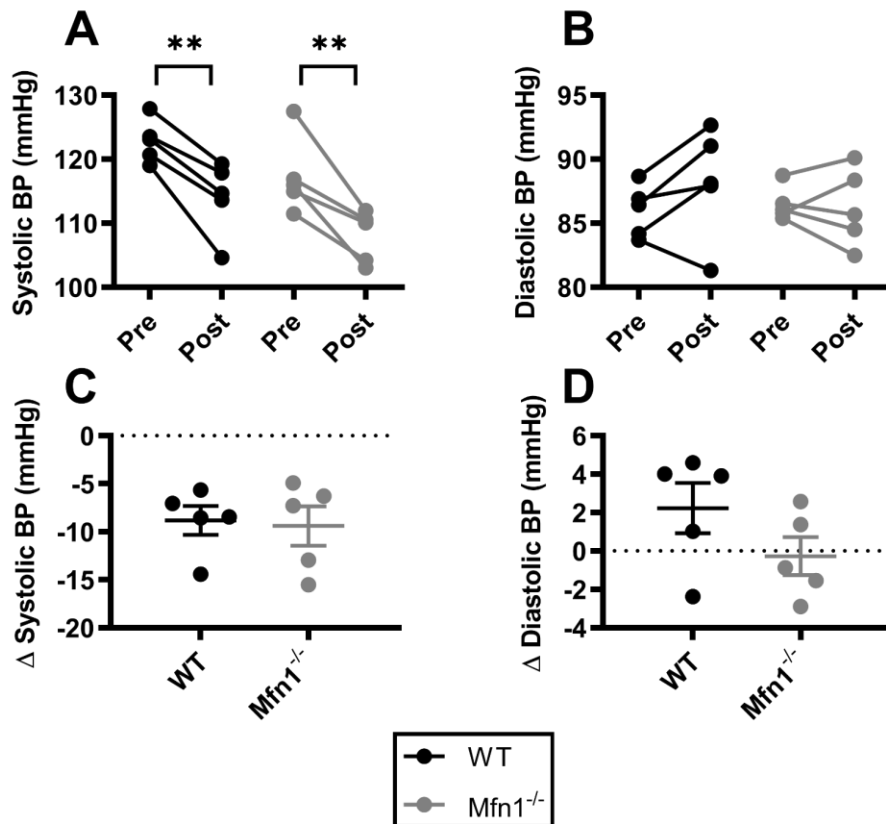


Figure 28: Blood pressure lowering effects of nitrite are unaffected by Mfn1 deletion. Following recovery after radiotransmitter implantation, baseline blood pressure (BP) measurements were recorded. Afterward, mice were administered nitrite (25 mg/kg) via intraperitoneal injection and blood pressure was recorded for 2 h after injection which was plotted as pre and post nitrite injection (A-B). Nitrite administration decreased systolic BP in both WT and SMC-Mfn1^{-/-} mice (A) (mean BP ± SEM, n=5; two-way repeated measures ANOVA with Sidak's multiple comparisons test; **P<0.01). However, the difference from their respective baselines was not statically significant (C) (mean ΔBP ± SEM, n=5; unpaired t-test; P>0.05). Although not statistically significant, nitrite increased diastolic BP in WT mice, while diastolic BP was unchanged with nitrite in Mfn1^{-/-} mice (B) (mean BP ± SEM, n=5; two-way repeated measures ANOVA with Sidak's multiple comparisons test; P>0.05). The difference in diastolic BP from baseline due to nitrite was not statically significant (D) (mean ΔBP ± SEM, n=5; unpaired t-test; P>0.05).

4.3.3 SMC-specific KO of Mfn1 Alters Resistance but not Conduit Artery Vascular

Function

Though overall blood pressure was not altered with SMC deletion of Mfn1, it is possible that the contractile response of individual vessels is altered. Thus, we next determined the effects of SMC Mfn1 deletion on physiologic vessel function in three different vessels. Thoracic aortas, carotid arteries, and mesenteric arteries were isolated from WT and SMC-Mfn1^{-/-} mice and subjected to *ex vivo* wire myography experiments. Vessels were pre-constricted and then relaxed with increasing concentrations of acetylcholine (Ach) or sodium nitroprusside (SNP) to measure endothelial-dependent and independent dilation, respectively (**Figure 29A-C**). Deletion of Mfn1 in SMC did not affect vasodilation in response to either of these molecules in comparison to WT animals in the aorta, and no effect on aortic constriction by PGF was observed. Additionally, no significant difference was observed in carotid artery dilation or constriction in response to SNP or PE respectively between WT and SMC-Mfn1^{-/-} mice (**Figure 29D-E**). However, in mesenteric arteries, a small but significant decrease in sensitivity to Ach and SNP was observed in SMC-Mfn1^{-/-} vessels (**Figure 29F-H**). In sum, these data suggest that deletion of Mfn1 from SMC does not alter large vessel reactivity under physiologic conditions though it may have a small effect on smaller vessels.

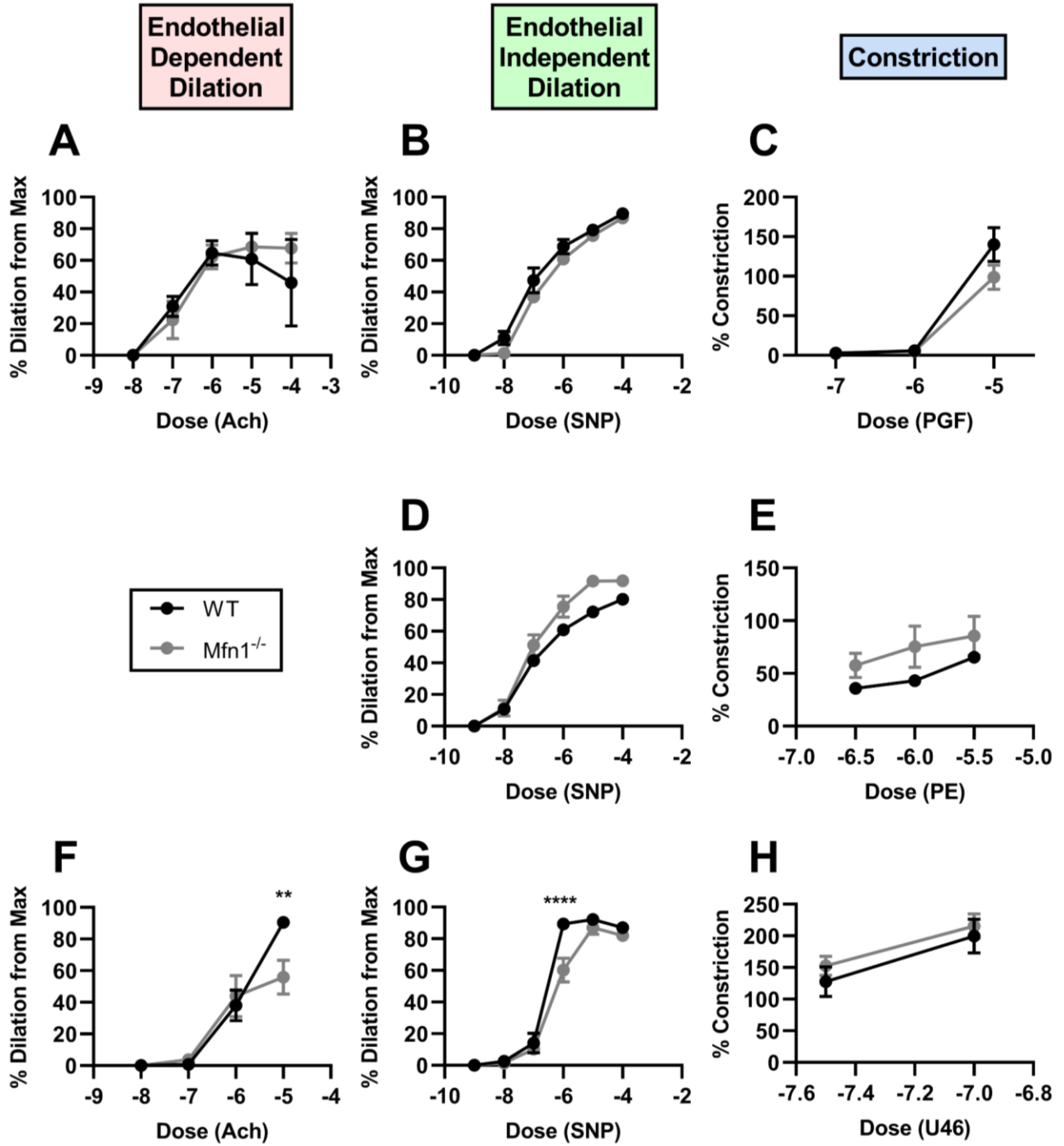


Figure 29: Conduit artery reactivity is unchanged with Mfn1 KO. Wire myography using arteries isolated from either wildtype (WT) or smooth muscle-specific Mfn1 knockout mice (SMC-Mfn1^{-/-}). Aortic ring vasodilation was measured in response to acetylcholine (Ach) to measure endothelial-dependent dilation (A) and sodium nitroprusside (SNP) to measure endothelial-independent dilation (B) (mean % dilation \pm SEM; n=3 WT; n=4

SMC-Mfn1^{-/-}; linear mixed model with Sidak's multiple comparisons test; P>0.05). Aortic constriction was measured in response to prostaglandin f2 α (PGF) (C) (mean % constriction \pm SEM; n=3 WT; n=4 SMC-Mfn1^{-/-}; linear mixed model with Sidak's multiple comparisons test; P>0.05). Carotid artery vasodilation was measured in response to SNP (D) (mean % dilation \pm SEM; n=2 ; two-way repeated measures ANOVA with Sidak's multiple comparisons test; P>0.05), while constriction was measured in response to phenylephrine (PE) (E) (mean % constriction \pm SEM; n=2 ; two-way repeated measures ANOVA with Sidak's multiple comparisons test; P>0.05) . Vasodilation of mesenteric arteries was measured in response to Ach (F) and SNP (G) (mean % dilation \pm SEM; n=5 WT; n=6 SMC-Mfn1^{-/-}; linear mixed model with Sidak's multiple comparisons test; **P<0.01; ***P<0.001). Vasoconstriction of mesenteric arteries was measured in response to prostaglandin H2 analogue U46619 (H) (mean % constriction \pm SEM; n=5 WT; n=6 SMC-Mfn1^{-/-}; linear mixed model with Sidak's multiple comparisons test; P>0.05).

To determine whether the small differences in vasoreactivity observed were due to differences in soluble guanylate cyclase (sGC) expression and activity, we genetically silenced Mfn1 in cultured RASMC for 48 h, after which we treated cells with modulators of sGC and measured cGMP production after 30 min. Mfn1 knockdown had no effect on sGC expression as measured by Western blot analysis (**Figure 30A-B**). Additionally, no significant difference in cGMP production was found between control and Mfn1 knockdown cells in response to Bay 58 or DEA NONOate (**Figure 30C-D**). To further investigate whether Mfn1 regulates sGC-cGMP signaling *in vivo*, mesenteric arteries from WT and SMC-Mfn1^{-/-} mice were isolated and basal cGMP concentrations were measured. No difference in cGMP production was observed between mice (**Figure 30E**). ROS is known to regulate sGC-cGMP signaling, such as through oxidation of sGC at its heme center (Shah et al.). To determine whether differences in mesenteric vasoreactivity may be due to ROS generation, we measured H₂O₂ production in isolated mesenteric arteries from these mice. Deletion of Mfn1 had no effect on H₂O₂ production compared to WT mice (**Figure**

30F). These data suggest Mfn1 does not regulate the sGC-cGMP pathway and is not required to maintain vessel function in the aorta. Additionally, these data suggest that the differences in mesenteric vasodilation between WT and SMC-Mfn1^{-/-} mice are not due to alterations in cGMP or ROS production.

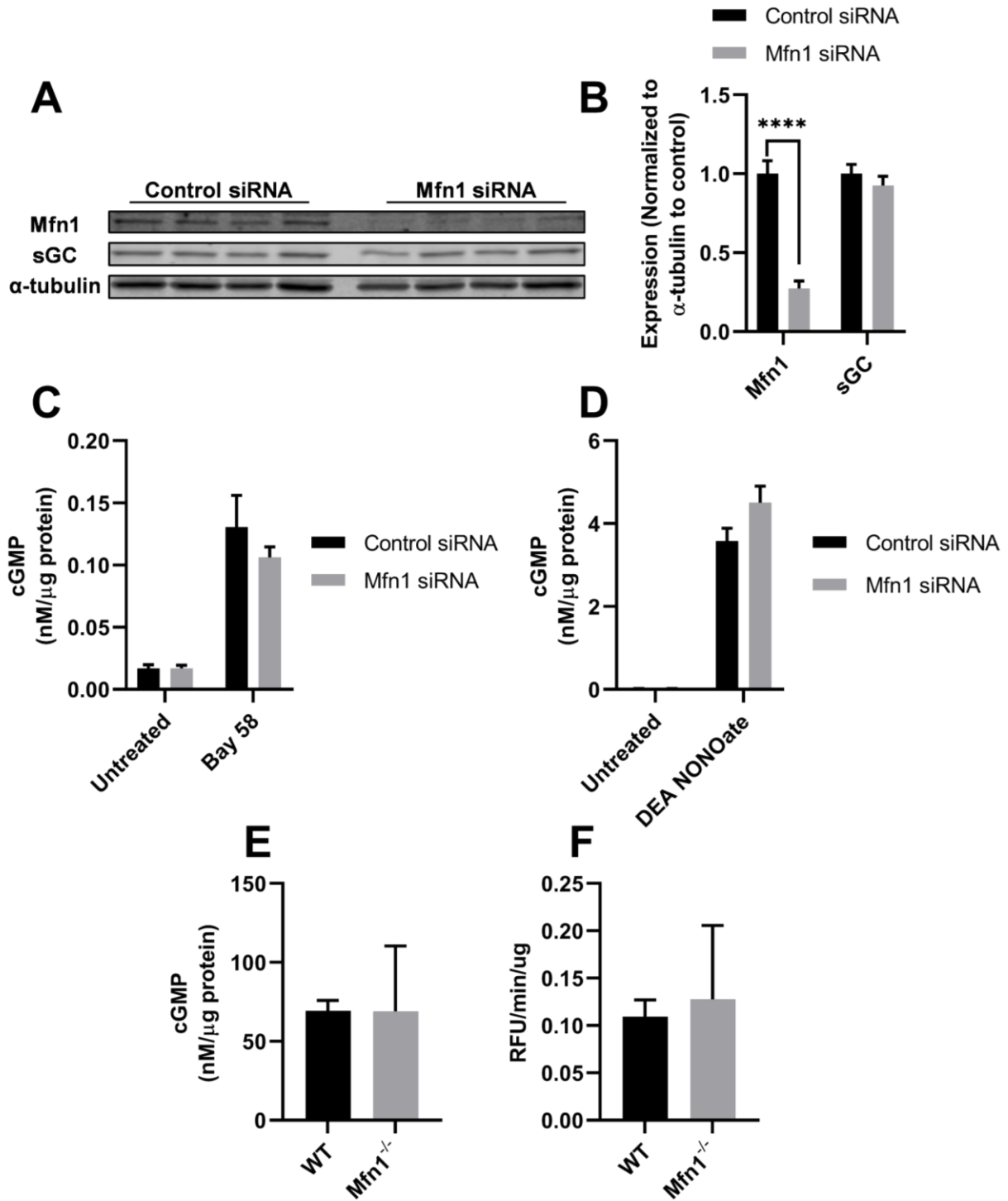


Figure 30: cGMP production is not regulated by Mfn1. RASMC were transfected with either control or Mfn1 siRNA for 48 h, after which cells were pretreated with IBMX (100 μ M) with or without Bay 41 (10 μ M). After

5 min, cells were then treated with Bay 58 (10 μ M) or DEA NONOate (10 μ M) for 20-30 min, after which cells were lysed. Production of cGMP in RASMC lysates was then measured via cGMP ELISA Kit (Cayman). Expression of sGC was unchanged with Mfn1 knockdown as measured by Western blot analysis (A) and quantification (B) (mean \pm SEM, n=4; two-way ANOVA with Sidak's multiple comparisons test; *P<0.0001). Silencing of Mfn1 had no effect cGMP production in response to DEA NONOate (C) or Bay 58 (D) (mean cGMP \pm SEM, n=3; two-way ANOVA with Sidak's multiple comparisons test; *P<0.05). (E) Mesenteric arteries from WT and SMC-Mfn1^{-/-} mice were isolated and subjected to cGMP measurement (mean cGMP \pm SEM, n=2; two-way ANOVA with Sidak's multiple comparisons test; P>0.05). (F) Measurement of H₂O₂ production in mesenteric arteries from WT and SMC-Mfn1^{-/-} mice using Amplex Red (mean RFU/min/ μ g \pm SEM, n=2 of triplicates; two-way ANOVA with Sidak's multiple comparisons test; *P<0.05).

4.3.4 Alterations in Response to Vascular Injury with SMC-specific KO of Mfn1

We showed that nitrite upregulates Mfn1 expression to inhibit RASMC proliferation *in vitro* but that nitrite promotes migration and phenotypic switching in an Mfn1 independent manner. However, the role of SMC Mfn1 in the pathogenesis of restenosis has not been tested. To address these questions, we subjected adult WT and SMC-Mfn1^{-/-} mice to partial carotid ligation injury, a well-established murine surgical procedure which models neointima hyperplasia similar to restenosis (Korshunov and Berk). Following ligation of the common carotid artery, WT and SMC-Mfn1^{-/-} mice were given either normal drinking water or nitrite supplemented drinking water (1.5 g/L) for 3 weeks after which mice were euthanized. Next, the injured arteries were isolated and subjected to histological studies in which neointimal hyperplasia was quantified as a ratio of intimal area to medial area. Deletion of Mfn1 significantly increased intimal to medial ratio compared to WT animals (**Figure 31E**). Nitrite administration similarly increased plasma nitrite levels in WT and SMC-Mfn1^{-/-} mice, although this increase was not statistically significant

compared to untreated animals (**Figure 31F**). Surprisingly, nitrite administration significantly reduced intima:media ratio in SMC-Mfn1^{-/-} but not WT mice (**Figure 31E**). In sum, these data demonstrate that the lack of SMC-Mfn1 potentiates restenosis and that nitrite-mediated protection does not require Mfn1 *in vivo*.

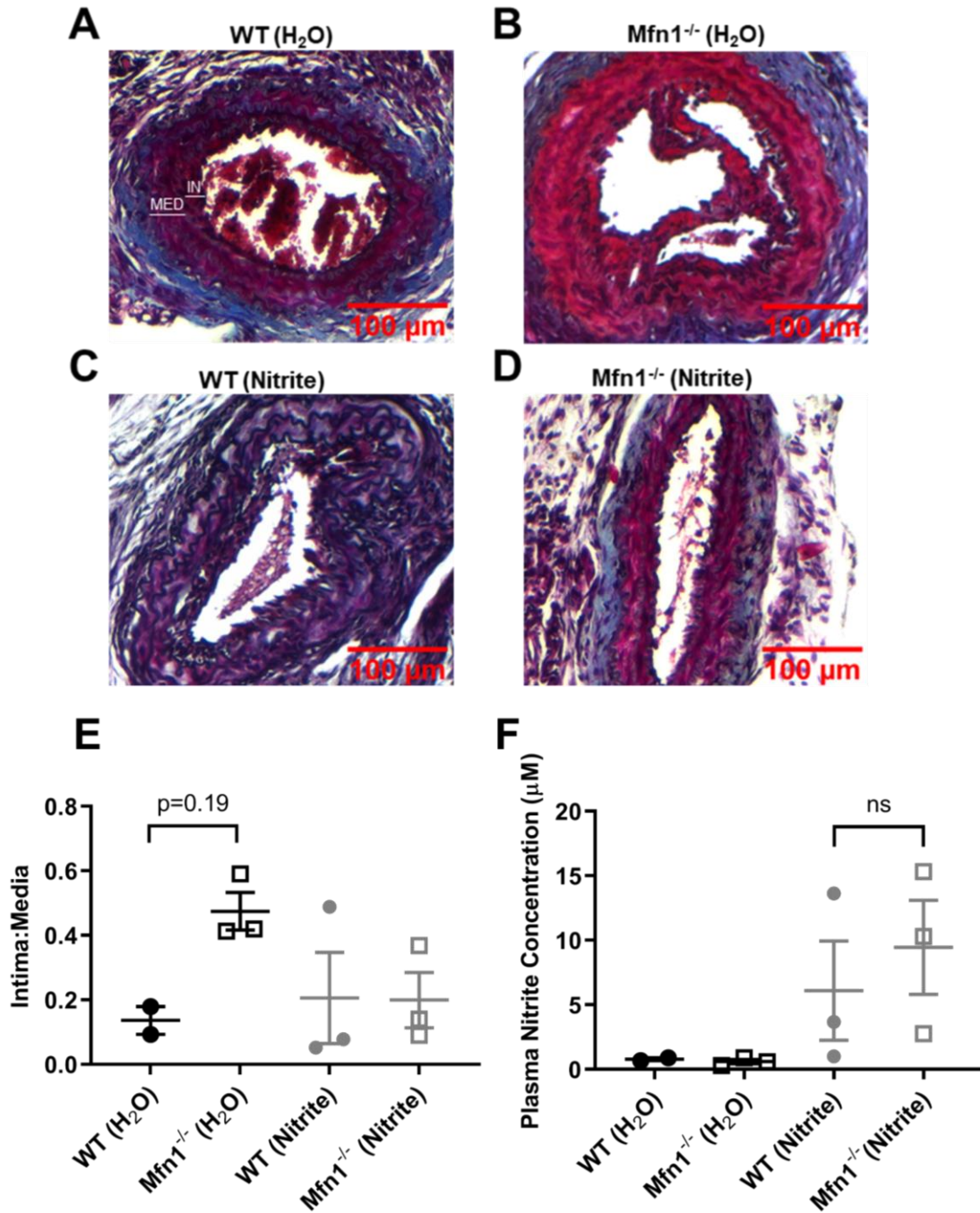


Figure 31: Nitrite attenuates neointimal hyperplasia in SMC-Mfn1^{-/-} mice. Masson trichrome stained carotid arteries subjected to carotid ligation injury from WT or SMC-Mfn1^{-/-} mice which were either given normal drinking water (H₂O) or nitrite supplemented drinking water (1.5 g/L, Nitrite) (A-D). Area of intimal (IN) and medial (MED) layers was quantified using ImageJ and expressed as ratio of intima:media (E) (mean ratio

intimal area:medial area \pm SEM, n=2-3; one-way ANOVA with Tukey's multiple comparisons test; $P>0.05$).
Plasma nitrite concentrations measured using Sievers 280i nitric oxide analyzer (F) (mean nitrite concentration \pm SEM, n=2-3; one-way ANOVA with Tukey's multiple comparisons test; $P>0.05$).

To assess the degree of cell proliferation, injured arteries from WT and SMC-Mfn1^{-/-} mice were stained with Ki67, a marker of cellular proliferation, as well as Acta2, which is expressed primarily in VSMC, and then imaged. Nitrite increased the percentage of Ki67 positive cells in both WT and SMC-Mfn1^{-/-} mice (**Figure 32B**). This included both the Acta2 positive cell population as well as other cells within the field of view. These data suggest that nitrite promotes cellular proliferation as measured by Ki67 staining within the vessel wall during vascular injury, both in terms of total cell number and Acta2 positive cells, and that nitrite likely inhibits neointimal hyperplasia in SMC-Mfn1^{-/-} mice not by inhibiting proliferation but through alternative mechanisms.

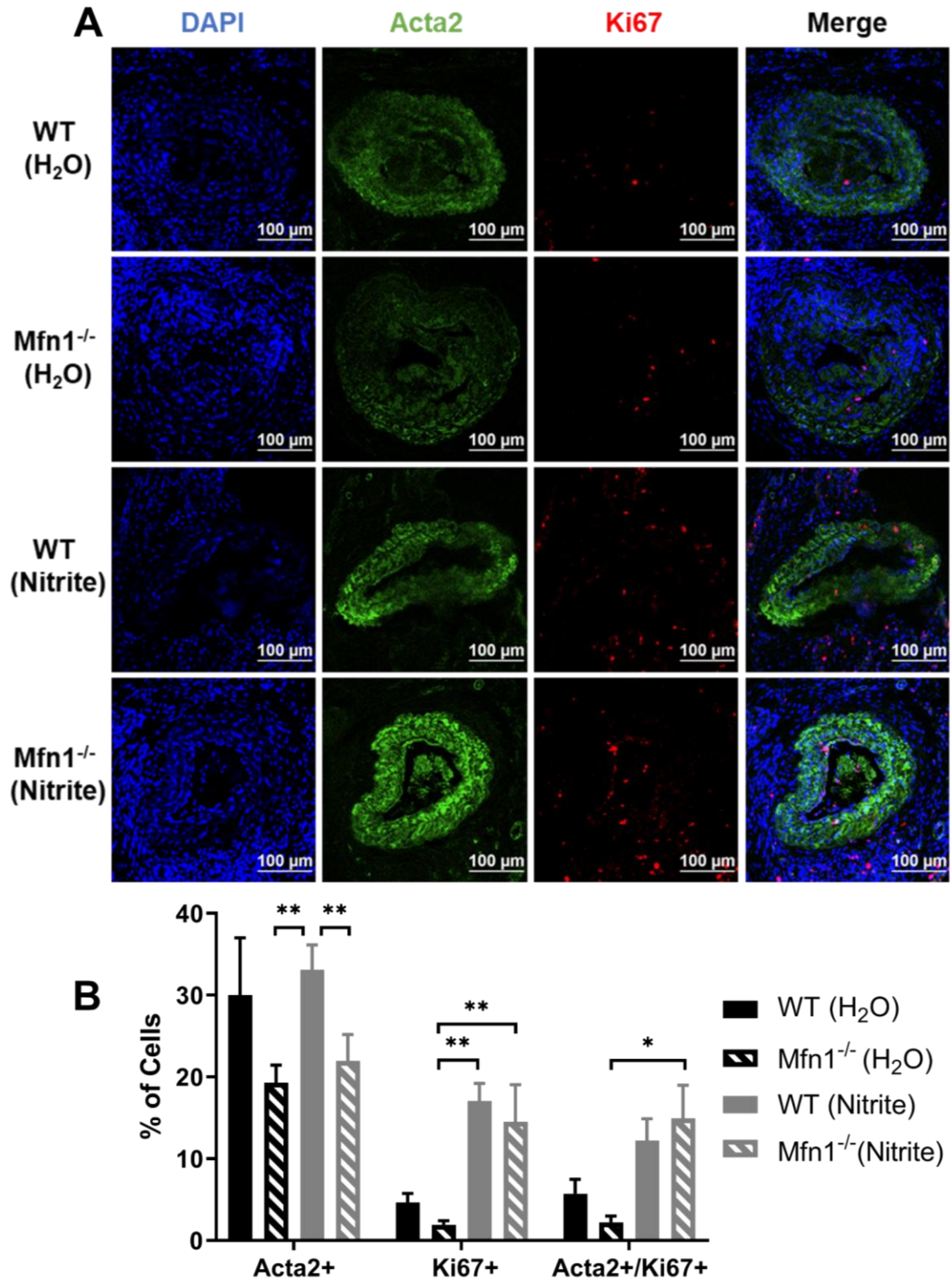


Figure 32: Nitrite increases vascular proliferation after carotid ligation *in vivo*. Confocal microscopy of 10 μ m carotid artery section subjected to carotid ligation injury from WT or SMC-Mfn1^{-/-} mice which were either

given normal drinking water (H₂O) or nitrite supplemented drinking water (1.5 g/L, Nitrite). Arteries were stained with DAPI to visualize all nuclei, Ki67 as a marker of cellular proliferation, and Acta2 to identify VSMC. Images were analyzed in Nikon Elements Software to quantify the percentage of Ki67 positive cells in view, percentage of Acta2 positive cells in view, and percentage of cells double positive for Ki67 and Acta2 (percent of cells \pm SEM, n=6; two-way ANOVA with Tukey's multiple comparisons test; *P<0.05; **P<0.01).

4.4 Discussion

In this study, we generated a smooth muscle specific Mfn1 knockout mouse and utilized it to examine the role of SMC-Mfn1 in regulating vascular physiology and pathological restenosis. Additionally, we were able to address our primary question of whether nitrite requires Mfn1 upregulation to inhibit VSMC proliferation and attenuate neointimal hyperplasia in restenosis. The major findings of this study is that SMC specific deletion of Mfn1 does not alter basal blood pressure regulation. However, it significantly worsens vascular injury after carotid artery ligation (**Figure 31**). Furthermore, nitrite administration decreased vascular injury in SMC-Mfn1^{-/-} mice. This effect was accompanied by a nitrite-dependent increase in Ki67 staining in the vessel wall of both WT and SMC-Mfn1^{-/-} mice.

Our data suggest that while there is no significant effect of SMC-Mfn1 on resting blood pressure, the effect of this protein on vessels with small diameters may be more subtle. Here, we show that deletion of Mfn1 in smooth muscle does not affect aortic constriction or endothelial dependent and independent dilation (**Figure 29**). In the mesenteric vessels, we observed a decrease in vasodilation in response to acetylcholine at the highest concentration tested as well as to SNP at approximately the EC₅₀ concentration. Thus under physiological conditions, the consequences of these differences on blood pressure and vasoreactivity *in vivo* may only be observed in specific

scenarios. Resistance arteries differ from larger conduit arteries like the aorta and carotids in various ways, such as lower basal NO production *in vivo* (Leloup et al.). Thus, it is possible that while in *ex vivo* myography experiments Mfn1^{-/-} mice have decrease sensitivity to SNP compared to WT, NO plays less of a role in regulating mesenteric artery tone *in vivo* and is not as physiologically relevant. The hypotensive effect of nitrite was similar in WT and Mfn1^{-/-} mice, suggesting that vasodilation in response to vasoactive compounds remains relatively unchanged with Mfn1 deletion, supporting this notion. In addition, these changes in mesenteric artery dilation could be due to loss of contractile gene expression which we observed when genetic silencing Mfn1 *in vitro*. We investigated whether Mfn1 deletion alters sGC-cGMP signaling and saw no differences compared to WT. It is also possible that other proteins which regulate vasodilation could be downregulated due to phenotypic switching only within muscular and smaller resistance vessels, such as PKG which can be modulated by VSMC phenotypic switching (Lincoln, Thomas).

The carotid ligation model herein demonstrates that SMC-Mfn1 has a much greater role in the modulation of intimal thickening after vascular injury. The finding that SMC-Mfn1, which likely increases mitochondrial fission, propagates vascular injury is consistent with prior studies in other models that show that decreased Mfn2 expression and increased Drp1-mediated fission leads to pathogenesis of vascular disease (Marsboom et al.; Salabei and Hill). These data are also consistent with our *in vitro* data in RASMC demonstrating that Mfn1 silencing increases cell migration and loss of contractile gene expression (**Section 3.0, Figure 18-Figure 19**). While we saw that Mfn1 deletion did not alter the percent of cells double positive for Acta2 and Ki67, SMC-Mfn1^{-/-} mice had less Acta2 positive cell within the field of view compared to WT mice SMC-Mfn1^{-/-} mice (**Figure 32**). In **Figure 9**, we observed that nitrite did not inhibit proliferation in Mfn1 knockdown RASMC. Also in that experiment, we observed that Mfn1 knockdown on its own did

not increase proliferation compared to control siRNA transfected cells. Thus, this decrease in Acta2 positive cells may be due to phenotypic switching which we observed with Mfn1 knockdown *in vitro*, suggesting phenotypic switching rather than proliferation may play a more significant role in this model of neointimal hyperplasia than we expected.

In addition to the effects of SMC-Mfn1, our data demonstrate that nitrite mediates protection after vascular injury even in the absence of Mfn1. This is contrary to our original hypothesis that Mfn1 upregulation is required for nitrite-mediated protection. This could be due to the fact that while nitrite requires Mfn1 to inhibit RASMC proliferation *in vitro*, nitrite-mediated phenotypic switching is Mfn1-independent. Thus, nitrite could promote phenotypic switching which is protective in SMC-Mfn1^{-/-} mice. Additionally, we observed that nitrite's phenotypic effects were dependent on ROS generation (**Figure 23**). If SMC-Mfn1^{-/-} mice are producing more ROS in the carotid arteries than WT, nitrite's effects could be potentiated, although measurement of ROS from mesenteric arteries does not support this hypothesis (**Figure 30F**). To further study the effects of nitrite on VSMC phenotypic switching, alternative strategies should be implemented as detection of VSMC which have decreased contractile gene expression poses a challenge. One potential model is a lineage tracing mouse which contains a reporter gene that is expressed upon Cre recombinase activity. Thus, upon tamoxifen injection, Mfn1 would be deleted in VSMC while expression of a reporter gene (YFP) is activated. Using such a method would allow us to distinguish VSMC from other cell types which may also express VSMC contractile markers, such as leukocytes and other inflammatory cells. It is possible that cells other than VSMC could be stained for markers such as Acta2, as it has been shown that cell types such as bone marrow derived cells can express markers of smooth muscle contractile phenotype and intravasate into the vessel wall.

During restenosis, inflammatory signaling initiates the cellular responses leading to increased VSMC proliferation and phenotypic switching in the vessel wall after injury. The partial carotid artery ligation model, which models restenosis through flow-induced shear stress, was used to promote neointima in this study and is known to produce similar inflammatory signaling events including increased levels of IL-1 β , IL-6, and PDGF as well as inflammatory cell infiltration into the intimal and medial layers of the affected vessel (Korshunov and Berk; Herring et al.; C. Y. Chen, Tsai, et al.). Many of the initial inflammatory signaling events in restenosis occurs in the first few days after injury, while constrictive remodeling occurs approximately 4 weeks later (Borhani et al.). Thus, it is also possible that the timepoint at which arteries were harvested may not represent the proliferation occurring in the weeks prior to euthanasia.

Furthermore, the effects of nitrite on neointimal hyperplasia *in vivo* may occur through mechanisms other than direct regulation of VSMC proliferation and phenotype, such as modulation of these inflammatory signaling near the site of vascular injury. It is known that nitrite administration decreases inflammation in various models of vascular diseases, including rat carotid artery balloon injury and in a high fat diet ApoE^{-/-} mouse model of atherosclerosis (Vavra et al.; Stokes et al.; Khambata et al.). While no one has specifically investigated the effects of nitrite in attenuation of inflammation due to partial carotid artery ligation injury, it is possible that nitrite could similarly inhibit inflammation in this model. Although outside the scope of this initial study, it is possible that the increase in vascular injury from carotid ligation in SMC-Mfn1^{-/-} mice is due to increased inflammation, such as phenotypic switching to inflammatory cell-like lineages or increased ROS production due to Mfn1 deletion. Through generation of a smooth muscle cell lineage tracing mouse, we hope to determine whether Mfn1 deletion alters phenotypic switching *in vivo* while investigating the role nitrite plays in these signaling mechanisms in the presence and

absence of Mfn1 in the smooth muscle. Additionally, we will be able to determine the effects of nitrite on monocyte and neutrophil infiltration to mediate inflammatory signaling by separating these cells from cells of smooth muscle cell origin. Also important to the propagation of restenosis is platelet activation and aggregation at the site of vessel injury (Chaabane et al.). Nitrite, through its reduction to NO to mediate cGMP, has been shown to be a potent inhibitor of platelet aggregation *in vivo* which could explain nitrite's effects in these models (Srihirun et al.; Apostoli et al.). As high shear stress is known to induce platelet aggregation, nitrite likely has similar effects on platelet thrombotic activity in the flow-induced model of neointimal hyperplasia that was performed in these experiments and should be addressed in future studies.

Notably, our study did not show a strong protective effect of nitrite in wildtype mice after carotid ligation. This is surprising based on prior data (Mo et al.; Alef et al.) and based on the fact that it was highly protective in SMC-Mfn1^{-/-} mice. One explanation for the lack of protection in wildtype mice is that levels of nitrite reached by supplementation were higher in Mfn1 KO mice and not high enough in WT mice. It has been shown that whether nitrite and NO *in vitro* inhibit or promote VSMC proliferation is highly dependent on concentration (Lehners et al.). Thus, alternative nitrite dosing or administration strategies could be implemented to address these concerns.

In sum, these data suggest that Mfn1 expression is protective in models of flow induced neointima formation. While Mfn1 is not crucial in regulating aortic vasoreactivity, we found that SMC-Mfn1^{-/-} mice have decreased mesenteric artery vasodilation compared to control animals. Future studies which measure mitochondrial function and morphology could reveal potential mechanisms by which Mfn1 elicits these effects, such as by decreasing ROS production, modulating ATP synthesis, or promoting mitochondrial hyperfusion to induce cell cycle arrest in

VSMC. Additionally, future studies using lineage tracing techniques could investigate the role of *Mfn1* in phenotypic switching to identify macrophage-like or osteochondrogenic-like VSMC in atherosclerotic plaques and neointima during restenosis.

5.0 General Discussion

5.1 Conclusions

The overarching goal of this thesis was to investigate the cross-talk between the vascular mediator nitrite and its regulation of mitochondrial dynamics to modulate vascular injury. Previous reports had shown that nitrite administration decreased neointima formation in rat carotid artery balloon injury models as well as data demonstrating that nitrite regulates mitochondrial dynamics proteins (Vavra et al.; Alef et al.; Mo et al.). However, whether nitrite regulates mitochondrial dynamics to attenuate restenosis was not known. Thus, we hypothesized that nitrite attenuates neointimal hyperplasia during restenosis by stimulating mitochondrial fusion through Mfn1 upregulation.

In the first two data chapters of this thesis, we investigated the effect of nitrite on VSMC function, demonstrating that nitrite has opposing effects on cellular proliferation versus phenotypic switching. The data in chapter 2 demonstrate that nitrite upregulates Mfn1 by inhibiting its degradation by March5, an outer mitochondrial membrane E3 ligase, establishing a new mechanism by which nitrite regulates Mfn1 and mitochondrial dynamics to modulate VSMC proliferation. In the next chapter, we defined a novel mechanism by which nitrite, independent of Mfn1, promotes VSMC migration and loss of contractile gene via ROS signaling.

In the final chapter, we investigated the role of nitrite and Mfn1 on VSMC function *in vivo* by generating a smooth muscle specific Mfn1 knockout mouse (SMC-Mfn1^{-/-}). We characterized vascular function of this new mouse strain by using *ex vivo* wire myography experiments and measuring blood pressure using radio telemetry, showing that at baseline these mice are similar to

wildtype mice in terms of cardiovascular function. We next subjected these mice to carotid artery ligation to investigate the role of Mfn1 in smooth muscle in neointima formation, and whether nitrite requires Mfn1 to inhibit neointima formation. As expected, Mfn1^{-/-} mice had more neointimal formation compared to wildtype animals. However, nitrite had decreased neointima formation in Mfn1^{-/-} but not wildtype mice, contrary to our hypothesis. These data demonstrate the antiproliferative role of Mfn1 in VSMC *in vivo* while suggesting that nitrite inhibits neointimal hyperplasia through alternative mechanisms.

5.2 Future Directions

5.2.1 How does nitrite inhibit March5-mediated ubiquitination to upregulate Mfn1?

March5 was first discovered in a human genome screen as a potential regulator of immune regulatory proteins and initially named mitochondrial ubiquitin ligase (MITOL) due to its localization to the outer mitochondrial membrane and targeted degradation of other outer mitochondrial membrane proteins (Yonashiro, Ishido, et al.). As a member of the membrane associated RING-CH-type (MARCH) finger domain ligase, its name has since been changed and its physiological role primarily in neurodegenerative disorders and breast cancer have recently been explored (Shiiba et al.). March5 performs ubiquitin transfer from its E2 ubiquitin conjugating enzyme directly to a substrate protein either through either K48 linkage to promote proteasomal degradation or K63 linkage to mediate signaling (Escobar-Henriques and Langer). March5 activity is regulated primarily by its relative expression level and is able to undergo rapid degradation by autoubiquitylation (Yonashiro, Ishido, et al.). Multiple molecular targets of March5 have been

identified in addition to Mfn1, including mitochondrial dynamics Drp1, Fis1, and Mfn2 (Yonashiro, Ishido, et al.; Nagashima et al.). It should be noted that while March5-mediated ubiquitination promotes proteasomal degradation of Mfn1, ubiquitylation of Mfn2 by March5 seems to be primarily involved in formation of mitochondria-ER contacts (Y-Y Park et al.; Sugiura et al.). Due to its localization to the outer mitochondrial membrane, recent evidence has also shown that March5-mediated ubiquitylation is involved in mitophagy through the PINK1/Parkin pathway and likely involves targeting of these molecular targets (Koyano et al.).

In chapter 2, we provided evidence that nitrite decreases ubiquitylation of Mfn1 by March5. Treatment with nitrite did not alter expression levels of March5, suggesting that nitrite is not promoting March5 autoubiquitylation to increase Mfn1. More likely, nitrite treatment is resulting in a post-translation modification of Mfn1 thereby affecting its interaction with March5. As described previously, we have suggested that this could be due to the acetylation status of Mfn1. Acetylation of Mfn1 on K491 potentiates binding to March5 resulting in ubiquitylation via K48 linkage and subsequent degradation of Mfn1 (Y-Y Park et al.). Recent evidence has shown that sirtuin 1 (SIRT1) specifically interacts with and deacetylates Mfn1 to increase its protein stability (Oanh et al.). Additionally, we and others have shown that nitrite increases deacetylase activity of SIRT1 and SIRT3, suggesting that nitrite could potentially upregulate Mfn1 through this pathway (Mo et al.; Lai et al.). Other modifications such as phosphorylation of Mfn1 by ERK which has been shown to decrease mitochondrial fusion could also interrupt Mfn1-March5 interactions (Pyakurel et al.). Preliminary data from our lab suggests that nitrite inhibits PDE4 to increase cAMP production and activate PKA. In some cells types, PKA has been shown to inhibit ERK signaling and attenuate cellular proliferation, which could be occurring in nitrite treated RASMC (Dumaz and Marais). A recent study also found that *S*-nitrosation of cytoskeletal protein

microtubule-associated protein 1B (MAP1B) modulates its ubiquitylation and degradation by March5 (Yonashiro, Kimijima, et al.). As Mfn1 has been shown to have a redox active cysteine, it is possible that Mfn1 could be undergoing *S*-nitrosation in the presence of nitrite which decreases its binding affinity to March5, thereby decreasing its degradation (Mattie et al.).

Future studies should investigate the molecular mechanisms which regulate Mfn1-March5 interactions. Additionally, the role of March5 in VSMC is almost entirely unexplored. A recent publication showed that overexpression of March5 in a breast cancer xenograft model promotes tumor growth and metastasis, suggesting March5 regulates cellular proliferation *in vivo* (Tang et al.). Targeting E3 ligases for therapeutic benefit is a relatively new approach in drug development and the pharmaceutical industry (Huang and Dixit). As the field progresses, the role of March5 and other E3 ligases in VSMC will likely be elucidated, and targeting of these enzymes could present as a new strategy for restenosis and other disorders involving hyperproliferative VSMC.

5.2.2 How do nitrite and Mfn1 regulate VSMC phenotypic switching?

We saw in chapter 3 that nitrite regulates VSMC phenotypic switching, promoting VSMC migration and decreased expression of the contractile genes we investigated. Additionally, we found that silencing of Mfn1 elicited similar effects. Emerging evidence suggests that VSMC phenotypic switching is regulated through epigenetic changes via histone modifications (Gomez, Swiatlowska, et al.). For example using chromatin immunoprecipitation (ChIP), KLF4 has been shown to recruit HDAC to highly enriched CARG regions upstream of VSMC contractile gene promoters, thereby decreasing their expression (McDonald et al.). More recently, DNA methylation decreases contractile gene expression in an atherosclerosis mouse model including myocardin and Tet2 (Zhuang et al.).

So what are potential mechanisms by which nitrite and Mfn1 regulate phenotypic switching through epigenetic regulation? Increasing evidence has linked oxidative stress to epigenetic changes, however many of these studies have only investigated global epigenetic changes and not at specific DNA loci (G. H. Kim et al.). As we saw that nitrite increased ROS production, it is possible that species such as hydroxyl radicals could oxidize DNA to block DNA methylation to inhibit transcription of contractile genes (Kietzmann et al.). As VSMC *in vivo* display a diverse heterogeneity in terms of contractile gene expression, new technologies such as single cell ChIP assays will be able to probe the epigenetic regulatory mechanisms underlying VSMC phenotypic switching and their dependence on ROS signaling (Gomez, Shankman, et al.).

In this chapter, we also investigated the metabolic changes associated with phenotypic switching. With nitrite treatment, we observed an increased in maximal mitochondrial respiration and reserve capacity. We have previously observed that long-term nitrite treatment in VSMC leads increased levels of PGC1- α , a transcription factor which promotes mitochondrial biogenesis (Mo et al.). In this study, we saw an increase number in mitochondrial content, indicative of increased mitochondrial biogenesis, thereby increasing maximal respiration. Other studies have also shown that PGC1- α overexpression attenuates neointimal hyperplasia, and that PGC1- α mitigates ROS production in VSMC (Qu et al.; Kadlec et al.). Future studies should investigate potential regulate of VSMC phenotype by PGC1- α and its dependence on ROS.

5.2.3 What are the roles of nitrite and Mfn1 in other vasculopathies?

In this study, we tested the effects of nitrite and Mfn1 on neointimal hyperplasia in large conduit vessels in response to flow-induced shear stress. From our *in vitro* studies, we observed that nitrite inhibited proliferation while promoting phenotypic switching in VSMC. *In vivo*, we

observed that chronic nitrite administration actually increased the amount of proliferating cells within the vasculature after injury. Although this is likely due to dosing or administration technique which will be addressed in future studies, this calls into question the long-term use of nitrite especially in a clinical setting. Nitrite is currently under clinical trials for treatment of PAH. Although nitrite seems to be well-tolerated in these studies, the long-term implications on VSMC proliferation and phenotypic switching are not entirely understood and should be addressed. Careful consideration may be recommended when using nitrite as a therapeutic, as nitrite may have differing effects on VSMC phenotype and function depending on the physiological environment of each patient especially within the vasculature. The endogenous levels of nitrite in each patient may also be crucial to the efficacy of nitrite in treatment of disease. As 40% of nitrite derives from dietary nitrates, nutrition guidelines may have to be altered when using nitrite long-term to ensure endogenous levels of nitrite remain in a safe physiological range.

As we are the first to generate a SMC-Mfn1^{-/-} mouse, there is an opportunity to study the effects of Mfn1 in other vascular disorders. To further investigate the role of Mfn1 in vascular injury, we subjected WT and SMC-Mfn1^{-/-} mice to a model of pulmonary hypertension (PH). Mice were placed in either normoxic conditions (21% O₂) or into temperature-humidity controlled hypoxia chamber (10% O₂). After 3 weeks, right ventricular systolic pressure (RVSP) was measured using a pressure catheter. As expected, hypoxia increased RVSP in WT mice compared to normoxic control mice indicative of PH, although this difference did not reach statistical significance (**Figure 33A**). Interestingly, deletion of smooth muscle Mfn1 further increased hypoxia-induced increase in RVSP. This increase in RVSP also correlated with Fulton index in these mice which also trended toward significance. Specifically, hypoxia increased Fulton index in WT mice which was exacerbated by Mfn1 deletion, consistent with worsened right ventricular

hypertrophy typically associated with PH (**Figure 33B**). In sum, these data show that Mfn1 protects against hypoxia-induced PH and provide further evidence that Mfn1 is protective in other mouse models of vascular injury. In the future, we hope to examine potential mechanisms by which vascular Mfn1 expression regulates these physiological effects, such as decreased vasodilatory function in resistance vessels (**Figure 29**).

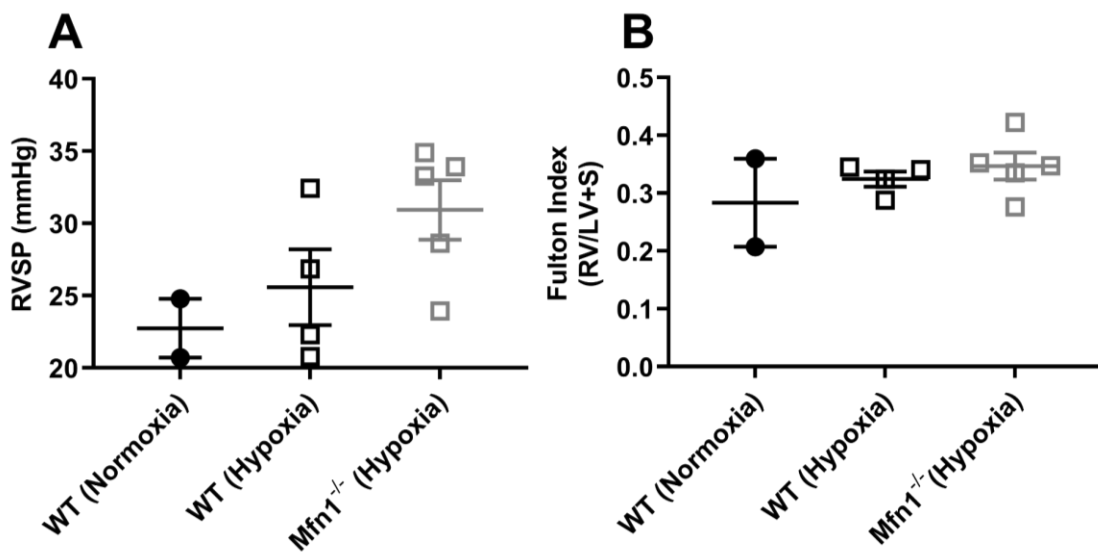
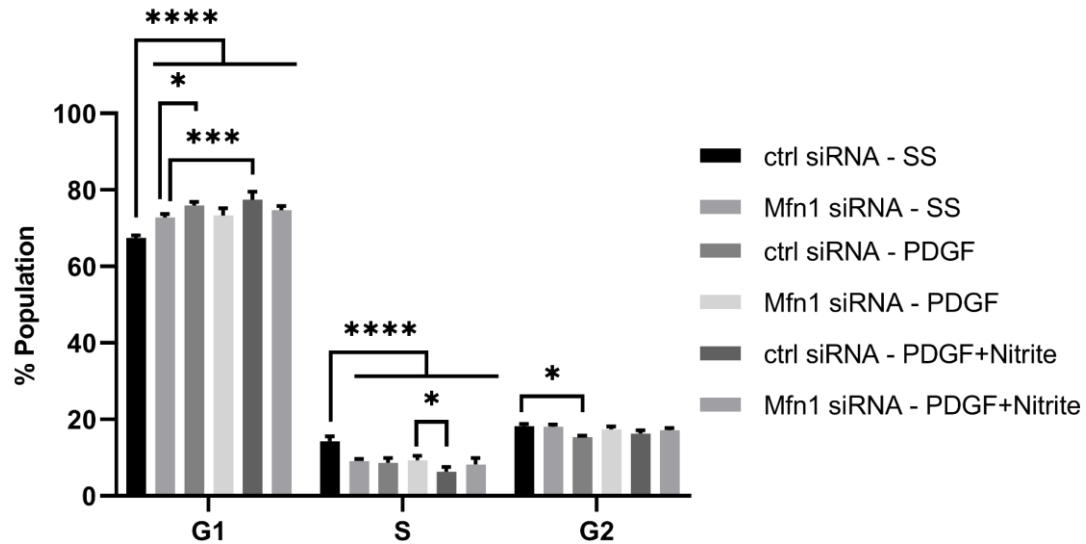


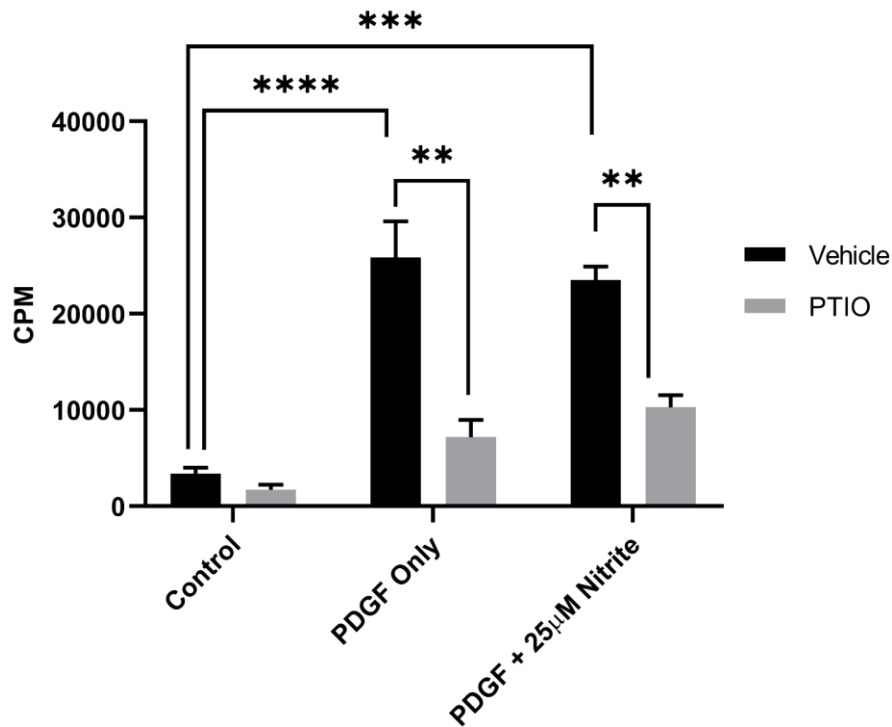
Figure 33: Mfn1^{-/-} mice are more susceptible to hypoxia-induced PH. WT and Mfn1^{-/-} mice were subjected to either normoxia (21% O₂) or placed into a temperature-humidity controlled hypoxia chamber (10% O₂) to model pulmonary hypertension (PH). After 3 weeks, mice were anesthetized with ketamine/xylazine and a pressure catheter was placed to measure right ventricular systolic pressure (A) (RVSP ± SEM, n=2; one-way ANOVA with Tukey's multiple comparisons test; P>0.05). After euthanasia, the heart was removed and weighed to measure Fulton index (B) (RV/LV+septum ± SEM, n=2; one-way ANOVA with Tukey's multiple comparisons test; P>0.05).

Appendix A Supplemental Figures

Appendix A.1 Chapter 2.0

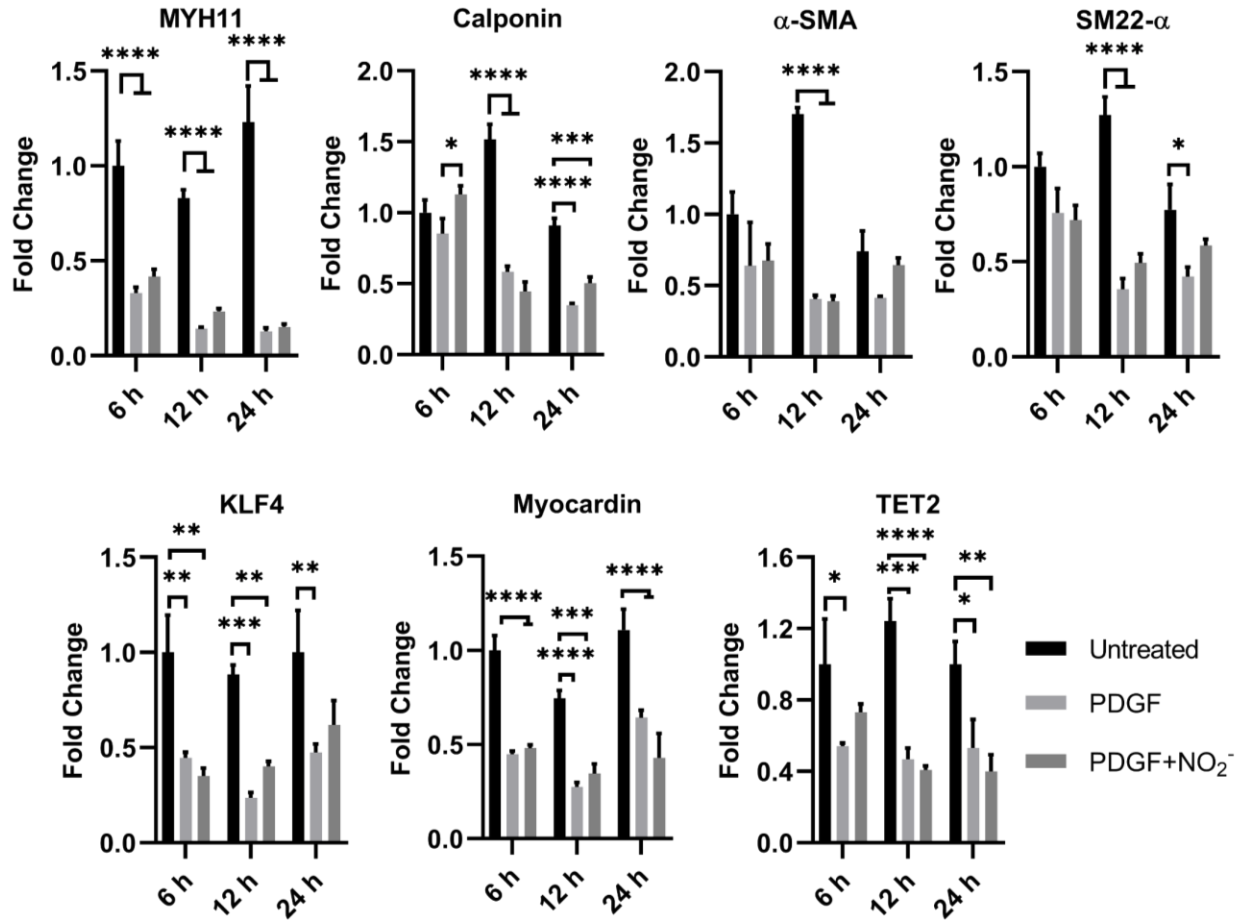


Appendix Figure 1: Nitrite does not inhibit PDGF-induced cell cycle progression after serum starvation. Cell cycle analysis by flow cytometry. RASMC were transfected with either control or Mfn1 siRNA followed by either serum starvation (SS) or treatment with PDGF in the presence or absence of nitrite. While Mfn1 knockdown resulted in more cells in G1 and less in S phase compared to control RASMC under serum starvation, no additional effect was observed in the presence of PDGF with or without addition of nitrite (% population \pm SEM, n=4 experiments; two-way ANOVA with Tukey's multiple comparisons test; *P<0.05, *P<0.001, ****P<0.0001).**



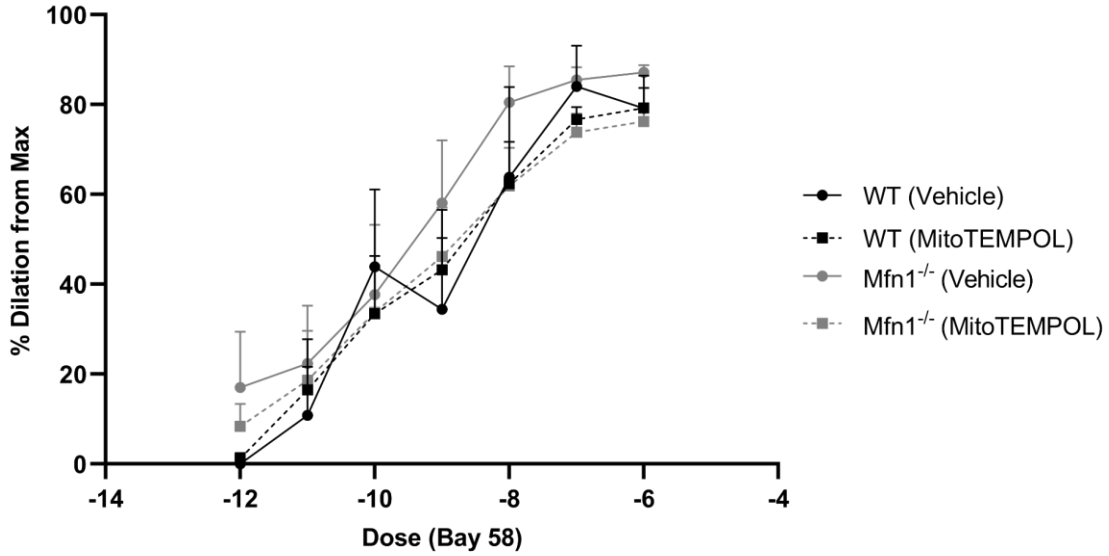
Appendix Figure 2: Anti-proliferative effects of nitrite in normoxia are NO-dependent. Anti-proliferative effects of nitrite in normoxia are NO-dependent. RASMC were stimulated into proliferation with PDGF in the presence or absence of nitrite with or without the addition of PTIO to scavenge NO in the cell media (gray bars). While nitrite did not inhibit proliferative as potently as previously observed, nitrite either had no effect or increased PDGF-induced proliferation when scavenging NO (proliferation \pm SEM, n=1 experiment of triplicates; two-way ANOVA with Sidak's multiple comparisons test; **P<0.01, ***P<0.001, ****P<0.0001).

Appendix A.2 Chapter 3.0

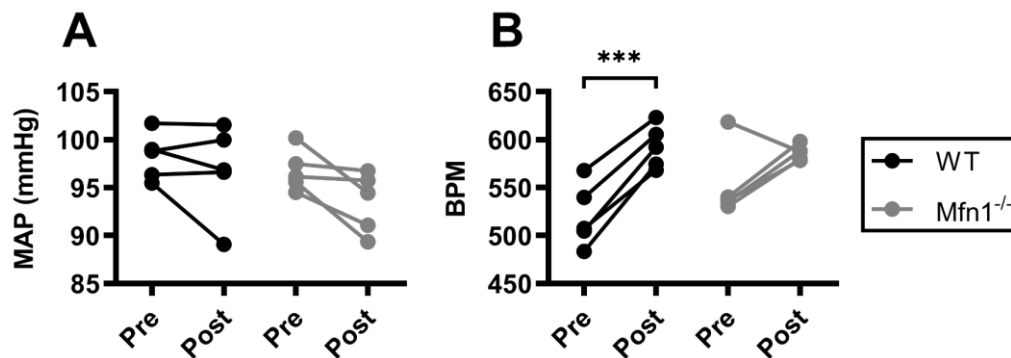


Appendix Figure 3: Nitrite does not prevent PDGF-induced decrease of RASMC contractile genes. RASMC were serum starved for 24-48 h after which they were pretreated with nitrite (25 μ M) followed by PDGF treatment (10 ng/mL). Cells were collected at the specified time points and the mRNA was extracted. Next, cDNA was synthesized and subjected to qPCR with primer pairs targeting various contractile genes. Levels of mRNA are expressed as fold change compared to 6 hour untreated control (mean \pm SEM, n=4 experimental replicates of triplicates; two-way ANOVA with Tukey's multiple comparisons test; *P<0.05, **P<0.01, ***P<0.001 ****P<0.0001).

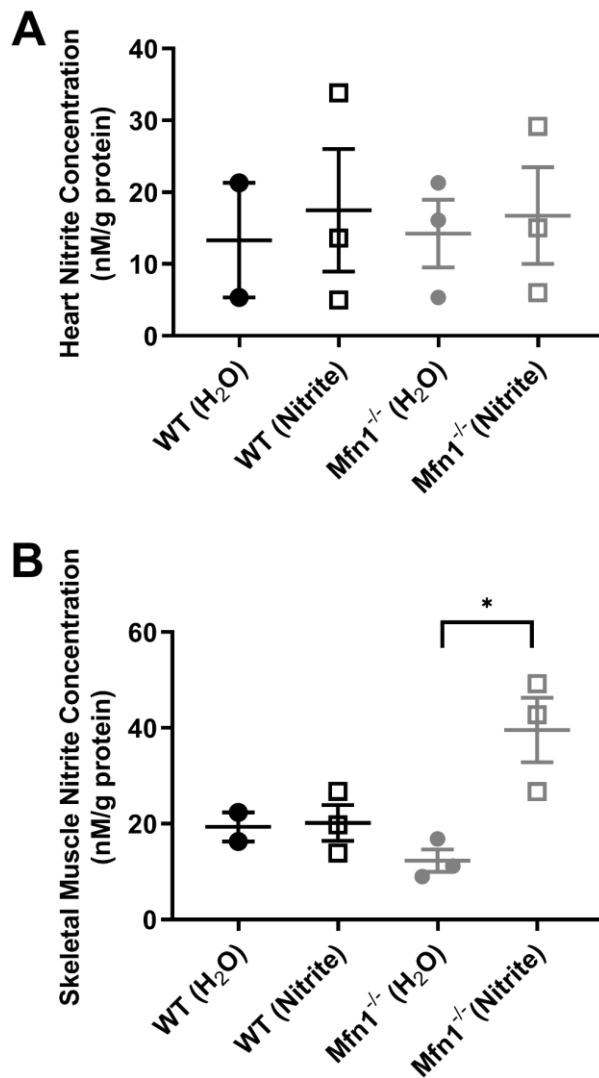
Appendix A.3 Chapter 4.0



Appendix Figure 4: Increase in Bay 58-stimulated mesenteric artery dilation in Mfn1^{-/-} mice is dependent on mitochondrial ROS. Wire myography performed using mesenteric arteries isolated from either wildtype (WT) or smooth-muscle specific Mfn1 knockout (Mfn1^{-/-}) mice with or without pretreatment using MitoTEMPOL to scavenge mitochondrial superoxide. Vasodilation was then assessed in response to Bay 58 (mean % dilation \pm SEM, n=3; two-way repeated measures ANOVA with Sidak's multiple comparisons test; P>0.05).



Appendix Figure 5: Deletion of smooth muscle Mfn1 alters MAP and HR. Wildtype (WT) and smooth muscle specific Mfn1 knockout mice (Mfn1^{-/-}) were subjected to radio telemetry for blood pressure measurement. Following recovery after radiotransmitter implantation, baseline blood pressure (BP) measurements were recorded. Baseline mean arterial pressure was unchanged in Mfn1^{-/-} mice compared to WT. Mice were then administered nitrite (25 mg/kg) via intraperitoneal injection and mean arterial pressure (MAP) and heart rate (HR) was recorded for 2 h after injection. No significant difference in MAP was observed at baseline (A, pre). MAP was decreased in both WT and Mfn1^{-/-} mice with nitrite, however the difference from their respective baseline was not statistically significant (A, post) (mean MAP \pm SEM, n=5; two-way repeated measures ANOVA with Sidak's multiple comparisons test; $P > 0.05$). HR (given as BPM) was significantly lower at baseline in Mfn1^{-/-} mice compared to WT (B, pre). Additionally, nitrite administration significantly increased HR in WT but not Mfn1^{-/-} mice (B, post) (mean BPM \pm SEM, n=5; two-way repeated measures ANOVA with Sidak's multiple comparisons test; *** $P < 0.001$)



Appendix Figure 6: Tissue Nitrite Concentrations. WT and Mfn1^{-/-} mice were subjected to carotid ligation injury receiving either normal drinking water (H₂O) or nitrite supplemented (1.5 g/L) drinking water (Nitrite). After 3 weeks at time of euthanasia, nitrite concentration in heart (A) and skeletal muscle (B) was measured using Sievers 280i nitric oxide analyzer and normalized to protein concentration (mean nitrite concentration ± SEM, n=2; one-way ANOVA with Tukey's multiple comparisons test; P<0.05).

Appendix A.3.1 Mouse Model of Pulmonary Hypertension

WT and *Mfn1^{-/-}* mice were subjected to 21 continuous days of normobaric hypoxia in a temperature-humidity controlled chamber (10% O₂, OxyCycler chamber, Biospherix Ltd.) as compared with normoxia (21% O₂). The mice were anesthetized with ketamine/xylazine and ventilated through a transtracheal catheter. The abdominal and thoracic cavities were opened, and a 1Fr pressure-volume catheter (Millar PVR-1035, Millar Instruments) was placed through the right ventricle apex to measure pressure. Following recording, the heart was rapidly removed and weighed after the right ventricle was dissected away from the septum and left ventricle.

Bibliography

- Adams, Ralf H., and Anne Eichmann. "Axon Guidance Molecules in Vascular Patterning." *Cold Spring Harbor Perspectives in Biology*, vol. 2, no. 5, 2010, pp. 1–19, doi:10.1101/cshperspect.a001875.
- Ahanchi, Sadaf S., et al. "The Role of Nitric Oxide in the Pathophysiology of Intimal Hyperplasia." *Journal of Vascular Surgery*, 2007, doi:10.1016/j.jvs.2007.02.027.
- Alef, Matthew J., et al. "Nitrite-Generated NO Circumvents Dysregulated Arginine/NOS Signaling to Protect against Intimal Hyperplasia in Sprague-Dawley Rats." *Journal of Clinical Investigation*, vol. 121, no. 4, Apr. 2011, pp. 1646–56, doi:10.1172/JCI44079.
- ALESSI, Dario, et al. "The Control of Protein Phosphatase-1 by Targetting Subunits. The Major Myosin Phosphatase in Avian Smooth Muscle Is a Novel Form of Protein Phosphatase-1." *European Journal of Biochemistry*, vol. 210, no. 3, Dec. 1992, pp. 1023–35, doi:10.1111/j.1432-1033.1992.tb17508.x.
- Allahverdian, Sima, et al. "Smooth Muscle Cell Fate and Plasticity in Atherosclerosis." *Cardiovascular Research*, vol. 114, no. 4, 2018, pp. 540–50, doi:10.1093/cvr/cvy022.
- Alzawahra, Wael F., et al. "Heme Proteins Mediate the Conversion of Nitrite to Nitric Oxide in the Vascular Wall." *American Journal of Physiology-Heart and Circulatory Physiology*, vol. 295, no. 2, Aug. 2008, pp. H499–508, doi:10.1152/ajpheart.00374.2008.
- Apostoli, G. L., et al. "Role of Inorganic Nitrate and Nitrite in Driving Nitric Oxide-CGMP-Mediated Inhibition of Platelet Aggregation in Vitro and in Vivo." *Journal of Thrombosis and Haemostasis*, vol. 12, no. 11, 2014, pp. 1880–89, doi:10.1111/jth.12711.
- Arnold, W. P., et al. "Nitric Oxide Activates Guanylate Cyclase and Increases Guanosine 3':5'-Cyclic Monophosphate Levels in Various Tissue Preparations." *Proceedings of the National Academy of Sciences of the United States of America*, vol. 74, no. 8, 1977, pp. 3203–07, doi:10.1073/pnas.74.8.3203.
- Ashrafi, G., and T. L. Schwarz. "The Pathways of Mitophagy for Quality Control and Clearance of Mitochondria." *Cell Death Differ*, vol. 20, no. 1, Nature Publishing Group, 2013, pp. 31–42, doi:10.1038/cdd.2012.81.
- Bacakova, Lucie, et al. "The Role of Vascular Smooth Muscle Cells in the Physiology and Pathophysiology of Blood Vessels." *Muscle Cell and Tissue - Current Status of Research Field*, vol. i, no. tourism, InTech, 2018, p. 13, doi:10.5772/intechopen.77115.

- Baker, John E., et al. "Nitrite Confers Protection against Myocardial Infarction: Role of Xanthine Oxidoreductase, NADPH Oxidase and KATP Channels." *Journal of Molecular and Cellular Cardiology*, vol. 43, 2007, pp. 437–44, doi:10.1016/j.yjmcc.2007.07.057.
- Ban, Tadato, et al. "Molecular Basis of Selective Mitochondrial Fusion by Heterotypic Action between OPA1 and Cardiolipin." *Nature Cell Biology*, vol. 19, no. 7, 2017, pp. 856–63, doi:10.1038/ncb3560.
- Bartolák-Suki, Erzsébet, et al. "Regulation of Mitochondrial Structure and Dynamics by the Cytoskeleton and Mechanical Factors." *International Journal of Molecular Sciences*, vol. 18, no. 8, 2017, pp. 7–11, doi:10.3390/ijms18081812.
- Batchelor, Andrew M., et al. "Exquisite Sensitivity to Subsecond, Picomolar Nitric Oxide Transients Conferred on Cells by Guanylyl Cyclase-Coupled Receptors." *Proceedings of the National Academy of Sciences of the United States of America*, vol. 107, no. 51, 2010, pp. 22060–65, doi:10.1073/pnas.1013147107.
- Bennett, Martin R., et al. "Vascular Smooth Muscle Cells in Atherosclerosis." *Circulation Research*, vol. 118, no. 4, 2016, pp. 692–702, doi:10.1161/CIRCRESAHA.115.306361.
- Bian, Ka, et al. "The Nature of Heme/Iron-Induced Protein Tyrosine Nitration." *Proceedings of the National Academy of Sciences of the United States of America*, vol. 100, no. 10, 2003, pp. 5712–17, doi:10.1073/pnas.0931291100.
- Boehm, Manfred, et al. "Bone Marrow–Derived Immune Cells Regulate Vascular Disease through a P27Kip1-Dependent Mechanism." *Journal of Clinical Investigation*, vol. 114, no. 3, Aug. 2004, pp. 419–26, doi:10.1172/JCI200420176.
- Boehme, Jason, et al. "Pulmonary Artery Smooth Muscle Cell Hyperproliferation and Metabolic Shift Triggered by Pulmonary Overcirculation." *American Journal of Physiology - Heart and Circulatory Physiology*, vol. 311, no. 4, 2016, pp. H944–57, doi:10.1152/ajpheart.00040.2016.
- Borhani, Setareh, et al. "Cardiovascular Stents: Overview, Evolution, and next Generation." *Progress in Biomaterials*, vol. 7, no. 3, Springer Berlin Heidelberg, 2018, doi:10.1007/s40204-018-0097-y.
- Bossy, Blaise, et al. "S-Nitrosylation of DRP1 Does Not Affect Enzymatic Activity and Is Not Specific to Alzheimer's Disease." *Journal of Alzheimer's Disease*, vol. 20, no. SUPPL.2, 2010, doi:10.3233/JAD-2010-100552.
- Boucher, Joshua, et al. "Molecular Pathways of Notch Signaling in Vascular Smooth Muscle Cells." *Frontiers in Physiology*, vol. 3 APR, no. April, 2012, pp. 1–13, doi:10.3389/fphys.2012.00081.

- Brandt, Tobias, et al. "A Mitofusin-Dependent Docking Ring Complex Triggers Mitochondrial Fusion in Vitro." *ELife*, vol. 5, no. JUNE2016, 2016, pp. 1–23, doi:10.7554/eLife.14618.
- Breitzig, Mason T., et al. "A Mitochondrial Delicacy: Dynamin-Related Protein 1 and Mitochondrial Dynamics." *American Journal of Physiology - Cell Physiology*, vol. 315, no. 1, 2018, pp. C80–90, doi:10.1152/ajpcell.00042.2018.
- Brennan, Marie Luise, et al. "A Tale of Two Controversies. Defining Both the Role of Peroxidases in Nitrotyrosine Formation in Vivo Using Eosinophil Peroxidase and Myeloperoxidase-Deficient Mice, and the Nature of Peroxidase-Generated Reactive Nitrogen Species." *Journal of Biological Chemistry*, vol. 277, no. 20, 2002, pp. 17415–27, doi:10.1074/jbc.M112400200.
- Brott, Thomas G., et al. "2011 ASA/ACCF/AHA/AANN/AANS/ACR/ASNR/CNS/SAIP/SCAI/SIR/SNIS/SVM/SVS Guideline on the Management of Patients with Extracranial Carotid and Vertebral Artery Disease: Executive Summary: A Report of the American College of Cardiology Foundation/American Heart." *Circulation*, vol. 124, no. 4, 2011, pp. 489–532, doi:10.1161/CIR.0b013e31820d8d78.
- Brown, Isola A. M., et al. "Vascular Smooth Muscle Remodeling in Conductive and Resistance Arteries in Hypertension." *Arteriosclerosis, Thrombosis, and Vascular Biology*, vol. 38, no. 9, 2018, pp. 1969–85, doi:10.1161/ATVBAHA.118.311229.
- Brozovich, F. V., et al. "Mechanisms of Vascular Smooth Muscle Contraction and the Basis for Pharmacologic Treatment of Smooth Muscle Disorders." *Pharmacological Reviews*, vol. 68, no. 2, 2016, pp. 476–532, doi:10.1124/pr.115.010652.
- Bryan, Nathan S., et al. "Nitrite Is a Signaling Molecule and Regulator of Gene Expression in Mammalian Tissues." *Nature Chemical Biology*, vol. 1, no. 5, 2005, pp. 290–97, doi:10.1038/nchembio734.
- Bueno, Marta, et al. "Nitrite Signaling in Pulmonary Hypertension: Mechanisms of Bioactivation, Signaling, and Therapeutics." *Antioxidants and Redox Signaling*, vol. 18, no. 14, 2013, pp. 1797–809, doi:10.1089/ars.2012.4833.
- Burtenshaw, Denise, et al. "Reactive Oxygen Species (ROS), Intimal Thickening, and Subclinical Atherosclerotic Disease." *Frontiers in Cardiovascular Medicine*, vol. 6, no. August, 2019, pp. 1–18, doi:10.3389/fcvm.2019.00089.
- Byon, Chang Hyun, et al. "Redox Signaling in Cardiovascular Pathophysiology: A Focus on Hydrogen Peroxide and Vascular Smooth Muscle Cells." *Redox Biology*, vol. 9, Elsevier, 2016, pp. 244–53, doi:10.1016/j.redox.2016.08.015.
- Cameron, Jenifer M., et al. "Polarized Cell Motility Induces Hydrogen Peroxide to Inhibit Cofilin via Cysteine Oxidation." *Current Biology*, vol. 25, no. 11, The Authors, June 2015, pp. 1520–25, doi:10.1016/j.cub.2015.04.020.

- Cao, Yu-Lu, et al. "MFN1 Structures Reveal Nucleotide-Triggered Dimerization Critical for Mitochondrial Fusion." *Nature*, vol. 542, no. 7641, Nature Publishing Group, 2017, pp. 1–5, doi:10.1038/nature21077.
- Castiglione, Nicoletta, et al. "Nitrite and Nitrite Reductases: From Molecular Mechanisms to Significance in Human Health and Disease." *Antioxidants and Redox Signaling*, vol. 17, no. 4, 2012, pp. 684–716, doi:10.1089/ars.2011.4196.
- Chaabane, Chiraz, et al. "Biological Responses in Stented Arteries." *Cardiovascular Research*, vol. 99, no. 2, 2013, pp. 353–63, doi:10.1093/cvr/cvt115.
- Chalmers, Susan, et al. "Mitochondrial Motility and Vascular Smooth Muscle Proliferation." *Arteriosclerosis, Thrombosis, and Vascular Biology*, vol. 32, no. 12, 2012, pp. 3000–11, doi:10.1161/ATVBAHA.112.255174.
- Chan, David C. "Fusion and Fission: Interlinked Processes Critical for Mitochondrial Health." *Annual Review of Genetics*, vol. 46, no. 1, Dec. 2012, pp. 265–87, doi:10.1146/annurev-genet-110410-132529.
- Chang, C. R., and C. Blackstone. "Cyclic AMP-Dependent Protein Kinase Phosphorylation of Drp1 Regulates Its GTPase Activity and Mitochondrial Morphology." *J Biol Chem*, vol. 282, no. 30, 2007, pp. 21583–87, doi:10.1074/jbc.C700083200.
- Chang, M. W., et al. "Adenovirus-Mediated over-Expression of the Cyclin/Cyclin-Dependent Kinase Inhibitor, P21 Inhibits Vascular Smooth Muscle Cell Proliferation and Neointima Formation in the Rat Carotid Artery Model of Balloon Angioplasty." *Journal of Clinical Investigation*, vol. 96, no. 5, Nov. 1995, pp. 2260–68, doi:10.1172/JCI118281.
- Chappell, Joel, et al. "Extensive Proliferation of a Subset of Differentiated, yet Plastic, Medial Vascular Smooth Muscle Cells Contributes to Neointimal Formation in Mouse Injury and Atherosclerosis Models." *Circulation Research*, vol. 119, no. 12, 2016, pp. 1313–23, doi:10.1161/CIRCRESAHA.116.309799.
- Chen, Chi Yu, Hsiao Ya Tsai, et al. "Deletion of the FHL2 Gene Attenuates Intima-Media Thickening in a Partially Ligated Carotid Artery Ligated Mouse Model." *Journal of Cellular and Molecular Medicine*, vol. 24, no. 1, 2020, pp. 160–73, doi:10.1111/jcmm.14687.
- Chen, Hsiuchen, J. Michael McCaffery, et al. "Mitochondrial Fusion Protects against Neurodegeneration in the Cerebellum." *Cell*, vol. 130, no. 3, 2007, pp. 548–62, doi:10.1016/j.cell.2007.06.026.
- Chen, Hsiuchen, Scott A. Detmer, et al. "Mitofusins Mfn1 and Mfn2 Coordinately Regulate Mitochondrial Fusion and Are Essential for Embryonic Development." *Journal of Cell Biology*, vol. 160, no. 2, 2003, pp. 189–200, doi:10.1083/jcb.200211046.

- Chen, Kuang-Hueih, et al. "Dysregulation of HSG Triggers Vascular Proliferative Disorders." *Nature Cell Biology*, 2004, doi:10.1038/ncb1161.
- Chen, Kuang Hueih, Asish Dasgupta, et al. "Role of Mitofusin 2 (Mfn2) in Controlling Cellular Proliferation." *FASEB Journal*, vol. 28, no. 1, 2014, pp. 382–94, doi:10.1096/fj.13-230037.
- Chettimada, Sukrutha, et al. "Contractile Protein Expression Is Upregulated by Reactive Oxygen Species in Aorta of Goto-Kakizaki Rat." *American Journal of Physiology-Heart and Circulatory Physiology*, vol. 306, no. 2, Jan. 2014, pp. H214–24, doi:10.1152/ajpheart.00310.2013.
- Chin, David, and Anthony R. Means. "Calmodulin: A Prototypical Calcium Sensor." *Trends in Cell Biology*, vol. 10, no. 8, 2000, pp. 322–28, doi:10.1016/S0962-8924(00)01800-6.
- Chiong, Mario, et al. "Mitochondrial Metabolism and the Control of Vascular Smooth Muscle Cell Proliferation." *Frontiers in Cell and Developmental Biology*, vol. 2, no. December, 2014, pp. 1–9, doi:10.3389/fcell.2014.00072.
- Cohen, Mickael M., and David Tareste. "Recent Insights into the Structure and Function of Mitofusins in Mitochondrial Fusion [Version 1; Referees: 2 Approved]." *F1000Research*, vol. 7, 2018, pp. 1–13, doi:10.12688/f1000research.16629.1.
- Cosby, Kenyatta, et al. "Nitrite Reduction to Nitric Oxide by Deoxyhemoglobin Vasodilates the Human Circulation." *Nature Medicine*, vol. 9, no. 12, 2003, pp. 1498–505, doi:10.1038/nm954.
- Daste, Frédéric, et al. "The Heptad Repeat Domain 1 of Mitofusin Has Membrane Destabilization Function in Mitochondrial Fusion." *EMBO Reports*, vol. 19, no. 6, 2018, p. e43637, doi:10.15252/embr.201643637.
- de Brito, Olga Martins, and Luca Scorrano. "Mitofusin 2 Tethers Endoplasmic Reticulum to Mitochondria." *Nature*, vol. 456, no. 7222, 2008, pp. 605–10, doi:10.1038/nature07534.
- De Lima Portella, Rafael, et al. "Nitrite Confers Preconditioning and Cytoprotection After Ischemia/Reperfusion Injury Through the Modulation of Mitochondrial Function." *Antioxidants & Redox Signaling*, vol. 23, no. 4, 2015, doi:10.1089/ars.2015.6260.
- Deaton, Rebecca A., et al. "Sp1-Dependent Activation of KLF4 Is Required for PDGF-BB-Induced Phenotypic Modulation of Smooth Muscle." *American Journal of Physiology-Heart and Circulatory Physiology*, vol. 296, no. 4, 2009, pp. H1027–37, doi:10.1152/ajpheart.01230.2008.
- Dejam, André, et al. "Erythrocytes Are the Major Intravascular Storage Sites of Nitrite in Human Blood." *Blood*, vol. 106, no. 2, 2005, pp. 734–39, doi:10.1182/blood-2005-02-0567.
- del Soldato, P., et al. "Role of the Arginine-Nitric Oxide Pathway in the Regulation of Vascular Smooth Muscle Cell Proliferation." *Proceedings of the National Academy of Sciences*, vol. 98, no. 7, 2002, pp. 4202–08, doi:10.1073/pnas.071054698.

- DeMartino, Anthony W., et al. "Nitrite and Nitrate Chemical Biology and Signalling." *British Journal of Pharmacology*, vol. 176, no. 2, 2019, pp. 228–45, doi:10.1111/bph.14484.
- Di Meo, Sergio, et al. "Role of ROS and RNS Sources in Physiological and Pathological Conditions." *Oxidative Medicine and Cellular Longevity*, vol. 2016, Hindawi Publishing Corporation, 2016, doi:10.1155/2016/1245049.
- Dorn, Gerald W. "Evolving Concepts of Mitochondrial Dynamics." *Annual Review of Physiology*, vol. 81, no. 1, 2018, pp. 1–17, doi:10.1146/annurev-physiol-020518-114358.
- Doyle, Michael P., and James W. Hoekstra. "Oxidation of Nitrogen Oxides by Bound Dioxygen in Hemoproteins." *Journal of Inorganic Biochemistry*, vol. 14, no. 4, 1981, pp. 351–58, doi:10.1016/S0162-0134(00)80291-3.
- Duband, Jean Loup, et al. "Calponin and SM22 as Differentiation Markers of Smooth Muscle: Spatiotemporal Distribution during Avian Embryonic Development." *Differentiation*, vol. 55, no. 1, International Society of Differentiation, 1993, pp. 1–11, doi:10.1111/j.1432-0436.1993.tb00027.x.
- Dumaz, Nicolas, and Richard Marais. "Integrating Signals between CAMP and the RAS/RAF/MEK/ERK Signalling Pathways: Based on the Anniversary Prize of the Gesellschaft Für Biochemie Und Molekularbiologie Lecture Delivered on 5 July 2003 at the Special FEBS Meeting in Brussels." *FEBS Journal*, vol. 272, no. 14, 2005, pp. 3491–504, doi:10.1111/j.1742-4658.2005.04763.x.
- Dungel, Peter, et al. "Impact of Mitochondrial Nitrite Reductase on Hemodynamics and Myocardial Contractility." *Scientific Reports*, vol. 7, no. 1, Springer US, 2017, pp. 1–13, doi:10.1038/s41598-017-11531-3.
- Durham, Andrew L., et al. "Role of Smooth Muscle Cells in Vascular Calcification: Implications in Atherosclerosis and Arterial Stiffness." *Cardiovascular Research*, vol. 114, no. 4, 2018, pp. 590–600, doi:10.1093/cvr/cvy010.
- Escobar-Henriques, M., and Thomas Langer. "Dynamic Survey of Mitochondria by Ubiquitin." *EMBO Reports*, vol. 15, no. 3, Mar. 2014, pp. 231–43, doi:10.1002/embr.201338225.
- Escobar-Henriques, Mafalda, and Mariana Joaquim. "Mitofusins: Disease Gatekeepers and Hubs in Mitochondrial Quality Control by E3 Ligases." *Frontiers in Physiology*, vol. 10, no. MAY, 2019, doi:10.3389/fphys.2019.00517.
- Evgenov, Oleg V., et al. "NO-Independent Stimulators and Activators of Soluble Guanylate Cyclase: Discovery and Therapeutic Potential." *Nature Reviews Drug Discovery*, vol. 5, no. 9, 2006, pp. 755–68, doi:10.1038/nrd2038.
- Feelisch, Martin, Takaaki Akaike, et al. "Long-Lasting Blood Pressure Lowering Effects of Nitrite Are NO-Independent and Mediated by Hydrogen Peroxide, Persulfides, and Oxidation of Protein Kinase G1 α Redox Signalling." *Cardiovascular Research*, vol. 116, no. 1, Jan. 2020, pp. 51–62, doi:10.1093/cvr/cvz202.

- Feelisch, Martin, Bernadette O. Fernandez, et al. "Tissue Processing of Nitrite in Hypoxia: An Intricate Interplay of Nitric Oxide-Generating and -Scavenging Systems." *Journal of Biological Chemistry*, vol. 283, no. 49, 2008, pp. 33927–34, doi:10.1074/jbc.M806654200.
- Feil, Susanne, et al. "Transdifferentiation of Vascular Smooth Muscle Cells to Macrophage-like Cells during Atherogenesis." *Circulation Research*, vol. 115, no. 7, 2014, pp. 662–67, doi:10.1161/CIRCRESAHA.115.304634.
- Filadi, Riccardo, et al. "Mitofusin 2 Ablation Increases Endoplasmic Reticulum-Mitochondria Coupling." *Proceedings of the National Academy of Sciences of the United States of America*, vol. 112, no. 17, 2015, pp. E2174–81, doi:10.1073/pnas.1504880112.
- Finkel, Toren. "Signal Transduction by Reactive Oxygen Species." *Journal of Cell Biology*, vol. 194, no. 1, 2011, pp. 7–15, doi:10.1083/jcb.201102095.
- Förstermann, Ulrich, and William C. Sessa. "Nitric Oxide Synthases: Regulation and Function." *European Heart Journal*, vol. 33, no. 7, 2012, pp. 829–37, doi:10.1093/eurheartj/ehr304.
- Francis, Sharron H., et al. "cGMP-Dependent Protein Kinases and cGMP Phosphodiesterases in Nitric Oxide and cGMP Action." *Pharmacological Reviews*, vol. 62, no. 3, 2010, pp. 525–63, doi:10.1124/pr.110.002907.
- Francis, Sharron H., and Jackie D. Corbin. "Molecular Mechanisms and Pharmacokinetics of Phosphodiesterase-5 Antagonists." *Current Urology Reports*, vol. 4, no. 6, 2003, pp. 457–65, doi:10.1007/s11934-003-0027-x.
- Franco, Antonietta, et al. "Correcting Mitochondrial Fusion by Manipulating Mitofusin Conformations." *Nature*, vol. 540, no. 7631, Nature Publishing Group, 2016, pp. 1–20, doi:10.1038/nature20156.
- Friedman, Jonathan R., et al. "ER Tubules Mark Sites of Mitochondrial Division." *Science*, vol. 334, no. 6054, 2011, pp. 358–62, doi:10.1126/science.1207385.
- Frismantiene, Agne, et al. "Smooth Muscle Cell-Driven Vascular Diseases and Molecular Mechanisms of VSMC Plasticity." *Cellular Signalling*, vol. 52, no. July, Elsevier, 2018, pp. 48–64, doi:10.1016/j.cellsig.2018.08.019.
- Fröhlich, Chris, et al. "Structural Insights into Oligomerization and Mitochondrial Remodelling of Dynamin 1-like Protein." *EMBO Journal*, vol. 32, no. 9, 2013, pp. 1280–92, doi:10.1038/emboj.2013.74.
- Furchgott, R. F., et al. "Endothelial Cells as Mediators of Vasodilation of Arteries." *Journal of Cardiovascular Pharmacology*, vol. 6, 1984, pp. S336–43, doi:10.1097/00005344-198406002-00008.

- Gabbiani, Giulio, et al. "Vascular Smooth Muscle Cells Differ from Other Smooth Muscle Cells: Predominance of Vimentin Filaments and a Specific Alpha-Type Actin." *Proceedings of the National Academy of Sciences*, vol. 78, no. 1, Jan. 1981, pp. 298–302, doi:10.1073/pnas.78.1.298.
- Galley, Joseph C., and Adam C. Straub. "Redox Control of Vascular Function." *Arteriosclerosis, Thrombosis, and Vascular Biology*, vol. 37, no. 12, 2017, pp. e178–84, doi:10.1161/ATVBAHA.117.309945.
- Ge, Yifan, et al. "Two Forms of Opal Cooperate to Complete Fusion of the Mitochondrial Inner-Membrane." *ELife*, vol. 9, 2020, pp. 1–22, doi:10.7554/eLife.50973.
- Gebhart, Verena, et al. "Site and Mechanism of Uncoupling of Nitric-Oxide Synthase: Uncoupling by Monomerization and Other Misconceptions." *Nitric Oxide - Biology and Chemistry*, vol. 89, no. March, Elsevier, 2019, pp. 14–21, doi:10.1016/j.niox.2019.04.007.
- Gegg, Matthew E., et al. "Mitofusin 1 and Mitofusin 2 Are Ubiquitinated in a PINK1/Parkin-Dependent Manner upon Induction of Mitophagy." *Human Molecular Genetics*, vol. 19, no. 24, 2010, pp. 4861–70, doi:10.1093/hmg/ddq419.
- Ghosh, Suborno M., et al. "Enhanced Vasodilator Activity of Nitrite in Hypertension: Critical Role for Erythrocytic Xanthine Oxidoreductase and Translational Potential." *Hypertension*, vol. 61, no. 5, 2013, pp. 1091–102, doi:10.1161/HYPERTENSIONAHA.111.00933.
- Gladwin, Mark T., et al. "The New Chemical Biology of Nitrite Reactions with Hemoglobin: R-State Catalysis, Oxidative Denitrosylation, and Nitrite Reductase/Anhydrase." *Accounts of Chemical Research*, vol. 42, no. 1, 2009, pp. 157–67, doi:10.1021/ar800089j.
- Gomes, Ligia C., et al. "During Autophagy Mitochondria Elongate, Are Spared from Degradation and Sustain Cell Viability." *Nature Cell Biology*, vol. 13, no. 5, Nature Publishing Group, 2011, pp. 589–98, doi:10.1038/ncb2220.
- Gomez, Delphine, Laura S. Shankman, et al. "Detection of Histone Modifications at Specific Gene Loci in Single Cells in Histological Sections." *Nature Methods*, vol. 10, no. 2, 2013, pp. 171–77, doi:10.1038/nmeth.2332.
- Gomez, Delphine, Pamela Swiatlowska, et al. "Epigenetic Control of Smooth Muscle Cell Identity and Lineage Memory." *Arteriosclerosis, Thrombosis, and Vascular Biology*, vol. 35, no. 12, 2015, pp. 2508–16, doi:10.1161/ATVBAHA.115.305044.
- Gomez, Delphine, and Gary K. Owens. "Smooth Muscle Cell Phenotypic Switching in Atherosclerosis." *Cardiovascular Research*, vol. 95, no. 2, 2012, pp. 156–64, doi:10.1093/cvr/cvs115.
- Gonzalez, F. M., et al. "Nitrite Anion Provides Potent Cytoprotective and Antiapoptotic Effects as Adjunctive Therapy to Reperfusion for Acute Myocardial Infarction." *Circulation*, vol. 117, no. 23, 2008, pp. 2986–94, doi:10.1161/CIRCULATIONAHA.107.748814.

- Guo, Xiaomei, et al. "Mitofusin 2 Triggers Vascular Smooth Muscle Cell Apoptosis via Mitochondrial Death Pathway." *Circulation Research*, vol. 101, no. 11, 2007, pp. 1113–22, doi:10.1161/CIRCRESAHA.107.157644.
- Guo, Yan hong, et al. "Overexpression of Mitofusin 2 Inhibited Oxidized Low-Density Lipoprotein Induced Vascular Smooth Muscle Cell Proliferation and Reduced Atherosclerotic Lesion Formation in Rabbit." *Biochemical and Biophysical Research Communications*, 2007, doi:10.1016/j.bbrc.2007.08.191.
- Halayko, Andrew J., and Julian Solway. "Molecular Mechanisms of Phenotypic Plasticity in Smooth Muscle Cells." *J. Appl. Physiol.*, vol. 90, no. 1, 2001, pp. 358–68, doi:10.1152/jappphysiol.00373.2011.
- Hassid, A., et al. "Nitric Oxide Selectively Amplifies FGF-2-Induced Mitogenesis in Primary Rat Aortic Smooth Muscle Cells." *American Journal of Physiology - Heart and Circulatory Physiology*, vol. 267, no. 3 36-3, 1994, doi:10.1152/ajpheart.1994.267.3.h1040.
- Hendgen-Cotta, U. B., et al. "Nitrite Reductase Activity of Myoglobin Regulates Respiration and Cellular Viability in Myocardial Ischemia-Reperfusion Injury." *Proceedings of the National Academy of Sciences*, vol. 105, no. 29, July 2008, pp. 10256–61, doi:10.1073/pnas.0801336105.
- Hendgen-Cotta, Ulrike B., et al. "Dietary Nitrate Supplementation Improves Revascularization in Chronic Ischemia." *Circulation*, vol. 126, no. 16, 2012, pp. 1983–92, doi:10.1161/CIRCULATIONAHA.112.112912.
- Herrera, Ana M., et al. "'Sarcomeres' of Smooth Muscle: Functional Characteristics and Ultrastructural Evidence." *Journal of Cell Science*, vol. 118, no. 11, 2005, pp. 2381–92, doi:10.1242/jcs.02368.
- Herring, B. Paul, et al. "Inflammation and Vascular Smooth Muscle Cell Dedifferentiation Following Carotid Artery Ligation." *Physiological Genomics*, vol. 49, no. 3, 2017, pp. 115–26, doi:10.1152/physiolgenomics.00095.2016.
- Hofmann, Franz. "The Biology of Cyclic GMP-Dependent Protein Kinases." *Journal of Biological Chemistry*, vol. 280, no. 1, 2005, pp. 1–4, doi:10.1074/jbc.R400035200.
- Hong, Zhigang, et al. "Role of Dynamin-Related Protein 1 (Drp1)-Mediated Mitochondrial Fission in Oxygen Sensing and Constriction of the Ductus Arteriosus." *Circulation Research*, vol. 112, no. 5, 2013, pp. 802–15, doi:10.1161/CIRCRESAHA.111.300285.
- Horman, Sandrine, et al. "AMP-Activated Protein Kinase Phosphorylates and Desensitizes Smooth Muscle Myosin Light Chain Kinase." *Journal of Biological Chemistry*, vol. 283, no. 27, 2008, pp. 18505–12, doi:10.1074/jbc.M802053200.
- House, Suzanne J., et al. "The Non-Excitable Smooth Muscle: Calcium Signaling and Phenotypic Switching during Vascular Disease." *Pflugers Archiv European Journal of Physiology*, vol. 456, no. 5, 2008, pp. 769–85, doi:10.1007/s00424-008-0491-8.

- Huang, Xiaodong, and Vishva M. Dixit. "Drugging the Undruggables: Exploring the Ubiquitin System for Drug Development." *Cell Research*, vol. 26, no. 4, Nature Publishing Group, 2016, pp. 484–98, doi:10.1038/cr.2016.31.
- Hudson, Claire, et al. "Dual Role of CREB in The Regulation of VSMC Proliferation: Mode of Activation Determines Pro- or Anti-Mitogenic Function." *Scientific Reports*, vol. 8, no. 1, Springer US, 2018, pp. 1–15, doi:10.1038/s41598-018-23199-4.
- Ignarro, L. J., et al. "Oxidation of Nitric Oxide in Aqueous Solution to Nitrite but Not Nitrate: Comparison with Enzymatically Formed Nitric Oxide from L-Arginine." *Proceedings of the National Academy of Sciences of the United States of America*, vol. 90, no. 17, 1993, pp. 8103–07, doi:10.1073/pnas.90.17.8103.
- Ignarro, Louis J., et al. "Activation of Purified Soluble Guanylate Cyclase by Protoporphyrin IX." *Proceedings of the National Academy of Sciences*, vol. 79, no. 9, May 1982, pp. 2870–73, doi:10.1073/pnas.79.9.2870.
- . "Haem-Dependent Activation of Guanylate Cyclase and Cyclic GMP Formation by Endogenous Nitric Oxide: A Unique Transduction Mechanism for Transcellular Signaling." *Pharmacology & Toxicology*, vol. 67, no. 1, 1990, pp. 1–7, doi:10.1111/j.1600-0773.1990.tb00772.x.
- Inoue, Teruo, et al. "Vascular Inflammation and Repair: Implications for Re-Endothelialization, Restenosis, and Stent Thrombosis." *JACC: Cardiovascular Interventions*, vol. 4, no. 10, Elsevier Inc., 2011, pp. 1057–66, doi:10.1016/j.jcin.2011.05.025.
- Ishihara, Naotada. "Mitofusin 1 and 2 Play Distinct Roles in Mitochondrial Fusion Reactions via GTPase Activity." *Journal of Cell Science*, vol. 117, no. 26, Dec. 2004, pp. 6535–46, doi:10.1242/jcs.01565.
- Jädert, Cecilia, et al. "Decreased Leukocyte Recruitment by Inorganic Nitrate and Nitrite in Microvascular Inflammation and NSAID-Induced Intestinal Injury." *Free Radical Biology and Medicine*, vol. 52, no. 3, Elsevier Inc., 2012, pp. 683–92, doi:10.1016/j.freeradbiomed.2011.11.018.
- Jeremy, J. Y., et al. "Effects of Sildenafil, a Type-5 CGMP Phosphodiesterase Inhibitor, and Papaverine on Cyclic GMP and Cyclic AMP Levels in the Rabbit Corpus Cavernosum in Vitro." *British Journal of Urology*, vol. 79, no. 6, 1997, pp. 958–63, doi:10.1046/j.1464-410x.1997.00206.x.
- Jukema, J. Wouter, et al. "Restenosis after PCI. Part 1: Pathophysiology and Risk Factors." *Nature Reviews Cardiology*, vol. 9, no. 1, Nature Publishing Group, 2012, pp. 53–62, doi:10.1038/nrcardio.2011.132.
- Kadlec, Andrew O., et al. "Role of PGC-1 α in Vascular Regulation: Implications for Atherosclerosis." *Arteriosclerosis, Thrombosis, and Vascular Biology*, vol. 36, no. 8, 2016, pp. 1467–74, doi:10.1161/ATVBAHA.116.307123.

- Kamm, K. E., and J. T. Stull. "The Function of Myosin and Myosin Light Chain Kinase Phosphorylation in Smooth Muscle." *Annual Review of Pharmacology and Toxicology*, vol. 25, no. 1, Apr. 1985, pp. 593–620, doi:10.1146/annurev.pa.25.040185.003113.
- Kapadia, Muneera R., et al. "Nitric Oxide and Nanotechnology: A Novel Approach to Inhibit Neointimal Hyperplasia." *Journal of Vascular Surgery*, vol. 47, no. 1, 2008, pp. 173–82, doi:10.1016/j.jvs.2007.09.005.
- Karbowski, Mariusz, et al. "The Mitochondrial E3 Ubiquitin Ligase MARCH5 Is Required for Drp1 Dependent Mitochondrial Division." *Journal of Cell Biology*, vol. 178, no. 1, 2007, pp. 71–84, doi:10.1083/jcb.200611064.
- Kashatus, Jennifer A., et al. "Erk2 Phosphorylation of Drp1 Promotes Mitochondrial Fission and MAPK-Driven Tumor Growth." *Molecular Cell*, vol. 57, no. 3, Elsevier Inc., 2015, pp. 537–52, doi:10.1016/j.molcel.2015.01.002.
- Keszler, Agnes, et al. "The Reaction between Nitrite and Oxyhemoglobin: A Mechanistic Study." *Journal of Biological Chemistry*, vol. 283, no. 15, 2008, pp. 9615–22, doi:10.1074/jbc.M705630200.
- Khambata, Rayomand S., et al. "Antiinflammatory Actions of Inorganic Nitrate Stabilize the Atherosclerotic Plaque." *Proceedings of the National Academy of Sciences*, vol. 114, no. 4, 2017, pp. E550–59, doi:10.1073/pnas.1613063114.
- Khoo, Nicholas K. H., et al. "Nitrite Augments Glucose Uptake in Adipocytes through the Protein Kinase A-Dependent Stimulation of Mitochondrial Fusion." *Free Radical Biology and Medicine*, vol. 70, 2014, pp. 45–53, doi:10.1016/j.freeradbiomed.2014.02.009.
- Kietzmann, Thomas, et al. "The Epigenetic Landscape Related to Reactive Oxygen Species Formation in the Cardiovascular System." *British Journal of Pharmacology*, vol. 174, no. 12, 2017, pp. 1533–54, doi:10.1111/bph.13792.
- Kim-Shapiro, Daniel B., and Mark T. Gladwin. "Mechanisms of Nitrite Bioactivation." *Nitric Oxide - Biology and Chemistry*, vol. 38, no. 1, Elsevier Inc., 2014, pp. 58–68, doi:10.1016/j.niox.2013.11.002.
- Kim, Gene H., et al. "The Role of Redox Signaling in Epigenetics and Cardiovascular Disease." *Antioxidants and Redox Signaling*, vol. 18, no. 15, 2013, pp. 1920–36, doi:10.1089/ars.2012.4926.
- Kim, Jun-Sub, et al. "Reactive Oxygen Species Regulate a Slingshot-Cofilin Activation Pathway." *Molecular Biology of the Cell*, edited by Jonathan Chernoff, vol. 20, no. 11, June 2009, pp. 2650–60, doi:10.1091/mbc.e09-02-0131.
- Kim, Michael S., and Larry S. Dean. "In-Stent Restenosis." *Cardiovascular Therapeutics*, vol. 29, no. 3, 2011, pp. 190–98, doi:10.1111/j.1755-5922.2010.00155.x.

- Klemm, Dwight J., et al. "cAMP Response Element-Binding Protein Content Is a Molecular Determinant of Smooth Muscle Cell Proliferation and Migration." *Journal of Biological Chemistry*, vol. 276, no. 49, 2001, pp. 46132–41, doi:10.1074/jbc.M104769200.
- Komalavilas, Padmini, et al. "Activation of Mitogen-Activated Protein Kinase Pathways by Cyclic GMP and Cyclic GMP-Dependent Protein Kinase in Contractile Vascular Smooth Muscle Cells." *Journal of Biological Chemistry*, vol. 274, no. 48, 1999, pp. 34301–09, doi:10.1074/jbc.274.48.34301.
- Korshunov, Vyacheslav A., and Bradford C. Berk. "Flow-Induced Vascular Remodeling in the Mouse: A Model for Carotid Intima-Media Thickening." *Arteriosclerosis, Thrombosis, and Vascular Biology*, vol. 23, no. 12, 2003, pp. 2185–91, doi:10.1161/01.ATV.0000103120.06092.14.
- Koyano, Fumika, et al. "Parkin Recruitment to Impaired Mitochondria for Nonselective Ubiquitylation Is Facilitated by MITOL." *Journal of Biological Chemistry*, vol. 294, no. 26, 2019, pp. 10300–14, doi:10.1074/jbc.RA118.006302.
- Kuhn, Michaela. "Molecular Physiology of Membrane Guanylyl Cyclase Receptors." *Physiological Reviews*, vol. 96, no. 2, 2016, pp. 751–804, doi:10.1152/physrev.00022.2015.
- Kumar, Dinesh, et al. "Chronic Sodium Nitrite Therapy Augments Ischemia-Induced Angiogenesis and Arteriogenesis." *Proceedings of the National Academy of Sciences of the United States of America*, vol. 105, no. 21, 2008, pp. 7540–45, doi:10.1073/pnas.0711480105.
- Lai, Yen Chun, et al. "SIRT3-AMP-Activated Protein Kinase Activation by Nitrite and Metformin Improves Hyperglycemia and Normalizes Pulmonary Hypertension Associated with Heart Failure with Preserved Ejection Fraction." *Circulation*, vol. 133, no. 8, 2016, pp. 717–31, doi:10.1161/CIRCULATIONAHA.115.018935.
- Larsen, F. J., et al. "Effects of Dietary Nitrate on Oxygen Cost during Exercise." *Acta Physiologica*, vol. 191, no. 1, 2007, pp. 59–66, doi:10.1111/j.1748-1716.2007.01713.x.
- Leboucher, Guillaume P., et al. "Stress-Induced Phosphorylation and Proteasomal Degradation of Mitofusin 2 Facilitates Mitochondrial Fragmentation and Apoptosis." *Molecular Cell*, vol. 47, no. 4, Elsevier, 2012, pp. 547–57, doi:10.1016/j.molcel.2012.05.041.
- Lee, Duk shin, and Ji Eun Kim. "PDI-Mediated S-Nitrosylation of DRP1 Facilitates DRP1-S616 Phosphorylation and Mitochondrial Fission in CA1 Neurons." *Cell Death and Disease*, vol. 9, no. 9, 2018, doi:10.1038/s41419-018-0910-5.
- Lee, Hakjoo, et al. "The Short Variant of the Mitochondrial Dynamin OPA1 Maintains Mitochondrial Energetics and Cristae Structure." *Journal of Biological Chemistry*, vol. 292, no. 17, 2017, pp. 7115–30, doi:10.1074/jbc.M116.762567.

- Lee, Joo-Yong, et al. “MFN1 Deacetylation Activates Adaptive Mitochondrial Fusion and Protects Metabolically Challenged Mitochondria.” *Journal of Cell Science*, vol. 127, no. 22, 2014, pp. 4954–63, doi:10.1242/jcs.157321.
- Lehners, Moritz, et al. “cGMP Signaling and Vascular Smooth Muscle Cell Plasticity.” *Journal of Cardiovascular Development and Disease*, vol. 5, no. 2, Apr. 2018, p. 20, doi:10.3390/jcdd5020020.
- Leloup, Arthur J. A., et al. “Elastic and Muscular Arteries Differ in Structure, Basal NO Production and Voltage-Gated Ca²⁺-Channels.” *Frontiers in Physiology*, vol. 6, no. DEC, 2015, pp. 1–9, doi:10.3389/fphys.2015.00375.
- Levine, Glenn N., et al. “2011 ACCF/AHA/SCAI Guideline for Percutaneous Coronary Intervention: Executive Summary: A Report of the American College of Cardiology Foundation/American Heart Association Task Force on Practice Guidelines and the Society for Cardiovascular Angiography A.” *Catheterization and Cardiovascular Interventions*, vol. 79, no. 3, 2012, pp. 453–95, doi:10.1002/ccd.23438.
- Liao, Xing Hua, et al. “VEGF-A Stimulates STAT3 Activity via Nitrosylation of Myocardin to Regulate the Expression of Vascular Smooth Muscle Cell Differentiation Markers.” *Scientific Reports*, vol. 7, no. 1, Springer US, 2017, pp. 1–11, doi:10.1038/s41598-017-02907-6.
- Libby, Peter. “Inflammation in Atherosclerosis.” *Arteriosclerosis, Thrombosis, and Vascular Biology*, vol. 32, no. 9, 2012, pp. 2045–51, doi:10.1161/ATVBAHA.108.179705.
- Liesa, Marc, and Orian S. Shirihai. “Mitochondrial Dynamics in the Regulation of Nutrient Utilization and Energy Expenditure.” *Cell Metabolism*, vol. 17, no. 4, Elsevier Inc., 2013, pp. 491–506, doi:10.1016/j.cmet.2013.03.002.
- Lilly, Brenda. “We Have Contact: Endothelial Cell-Smooth Muscle Cell Interactions.” *Physiology*, vol. 29, no. 4, 2014, pp. 234–41, doi:10.1152/physiol.00047.2013.
- Lim, Soyeon, et al. “Regulation of Mitochondrial Morphology by Positive Feedback Interaction Between PKC δ and Drp1 in Vascular Smooth Muscle Cell.” *Journal of Cellular Biochemistry*, vol. 116, no. 4, 2015, pp. 648–60, doi:10.1002/jcb.25016.
- Lincoln, Thomas, M. “Regulation of Vascular Smooth Muscle Cell Phenotype by Cyclic GMP and Cyclic GMP-Dependent Protein Kinase.” *Frontiers in Bioscience*, vol. 11, no. 1, 2006, p. 356, doi:10.2741/1803.
- Liu, Mingjun, and Delphine Gomez. “Smooth Muscle Cell Phenotypic Diversity.” *Arteriosclerosis, Thrombosis, and Vascular Biology*, vol. 39, no. 9, 2019, pp. 1715–23, doi:10.1161/ATVBAHA.119.312131.
- Liu, Renjing, et al. “Ten-Eleven Translocation-2 (TET2) Is a Master Regulator of Smooth Muscle Cell Plasticity.” *Circulation*, vol. 128, no. 18, 2013, pp. 2047–57, doi:10.1161/CIRCULATIONAHA.113.002887.

- Liu, Yan, et al. “Kruppel-like Factor 4 Abrogates Myocardin-Induced Activation of Smooth Muscle Gene Expression.” *Journal of Biological Chemistry*, vol. 280, no. 10, 2005, pp. 9719–27, doi:10.1074/jbc.M412862200.
- Long, Xiaochun, et al. “Myocardin Is Sufficient for a Smooth Muscle-like Contractile Phenotype.” *Arteriosclerosis, Thrombosis, and Vascular Biology*, vol. 28, no. 8, 2008, pp. 1505–10, doi:10.1161/ATVBAHA.108.166066.
- Losón, Oliver C., et al. “Fis1, Mff, MiD49, and MiD51 Mediate Drp1 Recruitment in Mitochondrial Fission.” *Molecular Biology of the Cell*, edited by Donald D. Newmeyer, vol. 24, no. 5, Mar. 2013, pp. 659–67, doi:10.1091/mbc.e12-10-0721.
- Lundberg, Jon O., et al. “Metabolic Effects of Dietary Nitrate in Health and Disease.” *Cell Metabolism*, vol. 28, no. 1, 2018, pp. 9–22, doi:10.1016/j.cmet.2018.06.007.
- Lundberg, Jon O, et al. “The Nitrate-Nitrite-Nitric Oxide Pathway in Physiology and Therapeutics.” *Nature Reviews Drug Discovery*, vol. 7, no. 8, Aug. 2008, pp. 710–710, doi:10.1038/nrd2466-c2.
- Ma, Yibao, et al. “Fatty Acid Oxidation: An Emerging Facet of Metabolic Transformation in Cancer.” *Cancer Letters*, vol. 435, no. August, Elsevier, 2018, pp. 92–100, doi:10.1016/j.canlet.2018.08.006.
- MacArthur, Peter H., et al. “Measurement of Circulating Nitrite and S-Nitrosothiols by Reductive Chemiluminescence.” *Journal of Chromatography B: Analytical Technologies in the Biomedical and Life Sciences*, vol. 851, no. 1–2, 2007, pp. 93–105, doi:10.1016/j.jchromb.2006.12.012.
- Mack, Christopher P. “Signaling Mechanisms That Regulate Smooth Muscle Cell Differentiation.” *Arteriosclerosis, Thrombosis, and Vascular Biology*, vol. 31, no. 7, July 2011, pp. 1495–505, doi:10.1161/ATVBAHA.110.221135.
- Macmillan-Crow, L. A., et al. “Nitration and Inactivation of Manganese Superoxide Dismutase in Chronic Rejection of Human Renal Allografts.” *Proceedings of the National Academy of Sciences of the United States of America*, vol. 93, no. 21, 1996, pp. 11853–58, doi:10.1073/pnas.93.21.11853.
- Maleknia, Mohsen, et al. “Inflammatory Growth Factors and In-Stent Restenosis: Effect of Cytokines and Growth Factors.” *SN Comprehensive Clinical Medicine*, vol. 2, no. 4, SN Comprehensive Clinical Medicine, 2020, pp. 397–407, doi:10.1007/s42399-020-00240-0.
- Manabe, Ichiro, and Gary K. Owens. “Recruitment of Serum Response Factor and Hyperacetylation of Histones at Smooth Muscle-Specific Regulatory Regions during Differentiation of a Novel P19-Derived in Vitro Smooth Muscle Differentiation System.” *Circulation Research*, vol. 88, no. 11, 2001, pp. 1127–34, doi:10.1161/hh1101.091339.

- Marsboom, Glenn, et al. "Dynamamin-Related Protein 1-Mediated Mitochondrial Mitotic Fission Permits Hyperproliferation of Vascular Smooth Muscle Cells and Offers a Novel Therapeutic Target in Pulmonary Hypertension." *Circulation Research*, vol. 110, no. 11, May 2012, pp. 1484–97, doi:10.1161/CIRCRESAHA.111.263848.
- Martin, Faye, et al. "Structure of Cinaciguat (BAY 58-2667) Bound to Nostoc H-NOX Domain Reveals Insights into Heme-Mimetic Activation of the Soluble Guanylyl Cyclase." *Journal of Biological Chemistry*, vol. 285, no. 29, 2010, pp. 22651–57, doi:10.1074/jbc.M110.111559.
- Marx, Steven O., et al. "Vascular Smooth Muscle Cell Proliferation in Restenosis." *Circulation: Cardiovascular Interventions*, 2011, doi:10.1161/CIRCINTERVENTIONS.110.957332.
- Mattie, Sevan, et al. "A New Mitofusin Topology Places the Redox-Regulated C Terminus in the Mitochondrial Intermembrane Space." *The Journal of Cell Biology*, vol. 217, no. 2, Feb. 2018, pp. 507–15, doi:10.1083/jcb.201611194.
- McCarron, John G., et al. "From Structure to Function: Mitochondrial Morphology, Motion and Shaping in Vascular Smooth Muscle." *Journal of Vascular Research*, vol. 50, no. 5, 2013, pp. 357–71, doi:10.1159/000353883.
- McDonald, Oliver G., et al. "Control of SRF Binding to CARG Box Chromatin Regulates Smooth Muscle Gene Expression in Vivo." *Journal of Clinical Investigation*, vol. 116, no. 1, 2006, pp. 36–48, doi:10.1172/JCI26505.
- Miano, Joseph M. "Myocardin in Biology and Disease." *Journal of Biomedical Research*, vol. 29, no. 1, 2015, pp. 3–19, doi:10.7555/JBR.29.20140151.
- . "Smooth Muscle Myosin Heavy Chain Exclusively Marks the Smooth Muscle Lineage during Mouse Embryogenesis." *Circulation Research*, vol. 75, no. 5, 1994, pp. 803–12, doi:10.1161/01.RES.75.5.803.
- Mitra, Kasturi, et al. "A Hyperfused Mitochondrial State Achieved at G1-S Regulates Cyclin E Buildup and Entry into S Phase." *Proceedings of the National Academy of Sciences of the United States of America*, vol. 106, no. 29, 2009, pp. 11960–65, doi:10.1073/pnas.0904875106.
- . "Mitochondrial Fission-Fusion as an Emerging Key Regulator of Cell Proliferation and Differentiation." *BioEssays*, vol. 35, no. 11, Nov. 2013, pp. 955–64, doi:10.1002/bies.201300011.
- Mizuno, Yusuke, et al. "Myosin Light Chain Kinase Activation and Calcium Sensitization in Smooth Muscle in Vivo." *American Journal of Physiology - Cell Physiology*, vol. 295, no. 2, 2008, pp. 358–64, doi:10.1152/ajpcell.90645.2007.
- Mo, Li, et al. "Nitrite Activates AMP Kinase to Stimulate Mitochondrial Biogenesis Independent of Soluble Guanylate Cyclase." *Free Radical Biology and Medicine*, vol. 53, no. 7, 2012, pp. 1440–50, doi:10.1016/j.freeradbiomed.2012.07.080.

- Moncada, S., and E. A. Higgs. "The Discovery of Nitric Oxide and Its Role in Vascular Biology." *British Journal of Pharmacology*, vol. 147, no. SUPPL. 1, 2006, pp. 193–201, doi:10.1038/sj.bjp.0706458.
- Montfort, William R., et al. "Structure and Activation of Soluble Guanylyl Cyclase, the Nitric Oxide Sensor." *Antioxidants and Redox Signaling*, vol. 26, no. 3, 2017, pp. 107–21, doi:10.1089/ars.2016.6693.
- Monzani, Enrico, et al. "Mechanistic Insight into the Peroxidase Catalyzed Nitration of Tyrosine Derivatives by Nitrite and Hydrogen Peroxide." *European Journal of Biochemistry*, vol. 271, no. 5, 2004, pp. 895–906, doi:10.1111/j.1432-1033.2004.03992.x.
- Mulvany, Michael J. "Small Artery Remodelling in Hypertension." *Basic and Clinical Pharmacology and Toxicology*, vol. 110, no. 1, 2012, pp. 49–55, doi:10.1111/j.1742-7843.2011.00758.x.
- Nagashima, Shun, et al. "Roles of Mitochondrial Ubiquitin Ligase MITOL/MARCH5 in Mitochondrial Dynamics and Diseases." *Journal of Biochemistry*, vol. 155, no. 5, 2014, pp. 273–79, doi:10.1093/jb/mvu016.
- Nakamura, Nobuhiro, et al. "MARCH-V Is a Novel Mitofusin 2- and Drp1-Binding Protein Able to Change Mitochondrial Morphology." *EMBO Reports*, vol. 7, no. 10, 2006, pp. 1019–22, doi:10.1038/sj.embor.7400790.
- Nguyen, Emily K., et al. "CaMKII (Ca²⁺/Calmodulin-Dependent Kinase II) in Mitochondria of Smooth Muscle Cells Controls Mitochondrial Mobility, Migration, and Neointima Formation." *Arteriosclerosis, Thrombosis, and Vascular Biology*, vol. 38, no. 6, 2018, pp. 1333–45, doi:10.1161/ATVBAHA.118.310951.
- Oanh, Nguyen Thi Kim, et al. "Mitochondria Elongation Is Mediated through SIRT1-Mediated MFN1 Stabilization." *Cellular Signalling*, vol. 38, no. April, Elsevier, 2017, pp. 67–75, doi:10.1016/j.cellsig.2017.06.019.
- Otera, Hidenori, et al. "Mff Is an Essential Factor for Mitochondrial Recruitment of Drp1 during Mitochondrial Fission in Mammalian Cells." *Journal of Cell Biology*, vol. 191, no. 6, 2010, pp. 1141–58, doi:10.1083/jcb.201007152.
- Owens, Gary K., et al. "Molecular Regulation of Vascular Smooth Muscle Cell Differentiation in Development and Disease." *Physiological Reviews*, vol. 84, no. 3, 2004, pp. 767–801, doi:10.1152/physrev.00041.2003.
- Palmer, Catherine S., et al. "MiD49 and MiD51, New Components of the Mitochondrial Fission Machinery." *EMBO Reports*, vol. 12, no. 6, Nature Publishing Group, 2011, pp. 565–73, doi:10.1038/embor.2011.54.

- Pan, Jie, et al. “The Molecular Mechanism of Heme Loss from Oxidized Soluble Guanylate Cyclase Induced by Conformational Change.” *Biochimica et Biophysica Acta - Proteins and Proteomics*, vol. 1864, no. 5, Elsevier B.V., 2016, pp. 488–500, doi:10.1016/j.bbapap.2016.02.012.
- Park, S. Y., et al. “Cardiac, Skeletal, and Smooth Muscle Mitochondrial Respiration: Are All Mitochondria Created Equal?” *AJP: Heart and Circulatory Physiology*, vol. 307, no. 3, 2014, pp. H346–52, doi:10.1152/ajpheart.00227.2014.
- Park, Y-Y, et al. “MARCH5-Mediated Quality Control on Acetylated Mfn1 Facilitates Mitochondrial Homeostasis and Cell Survival.” *Cell Death & Disease*, vol. 5, no. 4, Nature Publishing Group, Apr. 2014, pp. e1172–e1172, doi:10.1038/cddis.2014.142.
- Park, Yong-Yea, Seungmin Lee, et al. “Loss of MARCH5 Mitochondrial E3 Ubiquitin Ligase Induces Cellular Senescence through Dynamin-Related Protein 1 and Mitofusin 1.” *Journal of Cell Science*, vol. 123, no. Pt 4, 2010, pp. 619–26, doi:10.1242/jcs.061481.
- Park, Yong-Yea, Hyeseong Cho, et al. “Mitofusin 1 Is Degraded at G2/M Phase through Ubiquitylation by MARCH5.” *Cell Division*, vol. 7, no. 1, 2012, p. 25, doi:10.1186/1747-1028-7-25.
- Parker, D. J., et al. “A New Mitochondrial Pool of Cyclin E, Regulated by Drp1, Is Linked to Cell-Density-Dependent Cell Proliferation.” *Journal of Cell Science*, vol. 128, no. 22, 2015, pp. 4171–82, doi:10.1242/jcs.172429.
- Pearce, Charles G., et al. “Beneficial Effect of a Short-Acting NO Donor for the Prevention of Neointimal Hyperplasia.” *Free Radical Biology and Medicine*, vol. 44, no. 1, 2008, pp. 73–81, doi:10.1016/j.freeradbiomed.2007.09.010.
- Peleli, M., et al. “Dietary Nitrate Attenuates High-Fat Diet-Induced Obesity via Mechanisms Involving Higher Adipocyte Respiration and Alterations in Inflammatory Status.” *Redox Biology*, vol. 28, no. October 2019, Elsevier B.V., 2020, p. 101387, doi:10.1016/j.redox.2019.101387.
- Perez, Jessica, et al. “Role of Cellular Bioenergetics in Smooth Muscle Cell Proliferation Induced by Platelet-Derived Growth Factor.” *Biochemical Journal*, vol. 428, no. 2, June 2010, pp. 255–67, doi:10.1042/BJ20100090.
- Pipes, G. C. Te., et al. “The Myocardin Family of Transcriptional Coactivators: Versatile Regulators of Cell Growth, Migration, and Myogenesis.” *Genes and Development*, vol. 20, no. 12, 2006, pp. 1545–56, doi:10.1101/gad.1428006.
- Pride, Christelle Kamga, et al. “Nitrite Activates Protein Kinase A in Normoxia to Mediate Mitochondrial Fusion and Tolerance to Ischaemia/Reperfusion.” *Cardiovascular Research*, vol. 101, no. 1, Jan. 2014, pp. 57–68, doi:10.1093/cvr/cvt224.

- Pyakurel, Aswin, et al. “Extracellular Regulated Kinase Phosphorylates Mitofusin 1 to Control Mitochondrial Morphology and Apoptosis.” *Molecular Cell*, vol. 58, no. 2, The Authors, 2015, pp. 244–54, doi:10.1016/j.molcel.2015.02.021.
- Qian, W., et al. “Mitochondrial Hyperfusion Induced by Loss of the Fission Protein Drp1 Causes ATM-Dependent G2/M Arrest and Aneuploidy through DNA Replication Stress.” *Journal of Cell Science*, vol. 125, no. 23, 2012, pp. 5745–57, doi:10.1242/jcs.109769.
- Qu, Aijuan, et al. “PGC-1 α Attenuates Neointimal Formation via Inhibition of Vascular Smooth Muscle Cell Migration in the Injured Rat Carotid Artery.” *American Journal of Physiology - Cell Physiology*, vol. 297, no. 3, 2009, pp. 645–53, doi:10.1152/ajpcell.00469.2008.
- Radi, Rafael. “Protein Tyrosine Nitration: Biochemical Mechanisms and Structural Basis of Functional Effects.” *Accounts of Chemical Research*, vol. 46, no. 2, 2013, pp. 550–59, doi:10.1021/ar300234c.
- Ramani, Gautam V., and Myung H. Park. “Update on the Clinical Utility of Sildenafil in the Treatment of Pulmonary Arterial Hypertension.” *Drug Design, Development and Therapy*, vol. 4, 2010, pp. 61–70, doi:10.2147/dddt.s6208.
- Regan, Christopher P., et al. “Molecular Mechanisms of Decreased Smooth Muscle Differentiation Marker Expression after Vascular Injury.” *Journal of Clinical Investigation*, vol. 106, no. 9, 2000, pp. 1139–47, doi:10.1172/JCI10522.
- Rocha, Agostinho G., et al. “MFN2 Agonists Reverse Mitochondrial Defects in Preclinical Models of Charcot-Marie-Tooth Disease Type 2A.” *Science*, vol. 360, no. 6386, 2018, pp. 336–41, doi:10.1126/science.aao1785.
- Rodriguez, Andres I., et al. “MEF2B-Nox1 Signaling Is Critical for Stretch-Induced Phenotypic Modulation of Vascular Smooth Muscle Cells.” *Arteriosclerosis, Thrombosis, and Vascular Biology*, vol. 35, no. 2, 2015, pp. 430–38, doi:10.1161/ATVBAHA.114.304936.
- Rudzka, Dominika A., et al. “Reactive Oxygen Species and Hydrogen Peroxide Generation in Cell Migration.” *Communicative & Integrative Biology*, vol. 8, no. 5, Sept. 2015, p. e1074360, doi:10.1080/19420889.2015.1074360.
- Ryan, John, et al. “Mitochondrial Dynamics in Pulmonary Arterial Hypertension.” *Journal of Molecular Medicine*, vol. 93, no. 3, 2015, pp. 229–42, doi:10.1007/s00109-015-1263-5.
- Rybalkin, Sergei D., et al. “Cyclic GMP Phosphodiesterases and Regulation of Smooth Muscle Function.” *Circulation Research*, vol. 93, no. 4, 2003, pp. 280–91, doi:10.1161/01.RES.0000087541.15600.2B.
- Safar, Michel E., et al. “Current Perspectives on Arterial Stiffness and Pulse Pressure in Hypertension and Cardiovascular Diseases.” *Circulation*, vol. 107, no. 22, 2003, pp. 2864–69, doi:10.1161/01.CIR.0000069826.36125.B4.

- Salabei, Joshua K., et al. "PDGF-Mediated Autophagy Regulates Vascular Smooth Muscle Cell Phenotype and Resistance to Oxidative Stress." *The Biochemical Journal*, vol. 451, no. 3, 2013, pp. 375–88, doi:10.1042/BJ20121344.
- Salabei, Joshua K., and Bradford G. Hill. "Mitochondrial Fission Induced by Platelet-Derived Growth Factor Regulates Vascular Smooth Muscle Cell Bioenergetics and Cell Proliferation." *Redox Biology*, vol. 1, no. 1, 2013, pp. 542–51, doi:10.1016/j.redox.2013.10.011.
- San Martín, Alejandra, and Kathy K. Griendling. "Redox Control of Vascular Smooth Muscle Migration." *Antioxidants and Redox Signaling*, vol. 12, no. 5, 2010, pp. 625–40, doi:10.1089/ars.2009.2852.
- Sandner, Peter, et al. *Soluble Guanylate Cyclase Stimulators and Activators*. 2018, doi:10.1007/164_2018_197.
- Sarti, Paolo, et al. "Cytochrome c Oxidase and Nitric Oxide in Action: Molecular Mechanisms and Pathophysiological Implications." *Biochimica et Biophysica Acta - Bioenergetics*, vol. 1817, no. 4, Elsevier B.V., 2012, pp. 610–19, doi:10.1016/j.bbabi.2011.09.002.
- Savage, Michael P., et al. "Efficacy of Coronary Stenting versus Balloon Angioplasty in Small Coronary Arteries." *Journal of the American College of Cardiology*, vol. 31, no. 2, Elsevier Masson SAS, 1998, pp. 307–11, doi:10.1016/S0735-1097(97)00511-1.
- Schrepfer, Emilie, and Luca Scorrano. "Mitofusins, from Mitochondria to Metabolism." *Molecular Cell*, vol. 61, no. 5, Elsevier Ltd, Mar. 2016, pp. 683–94, doi:10.1016/j.molcel.2016.02.022.
- Sellers, J. R., and R. S. Adelstein. "The Mechanism of Regulation of Smooth Muscle Myosin by Phosphorylation." *Current Topics in Cellular Regulation*, vol. 27, 1985, pp. 51–62, doi:10.1016/b978-0-12-152827-0.50012-8.
- Shah, Rohan C., et al. "Redox Regulation of Soluble Guanylyl Cyclase." *Nitric Oxide - Biology and Chemistry*, vol. 76, no. February, Elsevier, 2018, pp. 97–104, doi:10.1016/j.niox.2018.03.013.
- Sharma, Rameshwar K., and Teresa Duda. "Membrane Guanylate Cyclase, a Multimodal Transduction Machine: History, Present, and Future Direction." *Frontiers in Molecular Neuroscience*, vol. 7, no. JULY, 2014, pp. 1–20, doi:10.3389/fnmol.2014.00056.
- Shiiba, Isshin, et al. "Overview of Mitochondrial E3 Ubiquitin Ligase MITOL/MARCH5 from Molecular Mechanisms to Diseases." *International Journal of Molecular Sciences*, vol. 21, no. 11, 2020, doi:10.3390/ijms21113781.
- Shiva, Sruti, Xunde Wang, et al. "Ceruloplasmin Is a NO Oxidase and Nitrite Synthase That Determines Endocrine NO Homeostasis." *Nature Chemical Biology*, vol. 2, no. 9, 2006, pp. 486–93, doi:10.1038/nchembio813.

- Shiva, Sruti. “Nitrite: A Physiological Store of Nitric Oxide and Modulator of Mitochondrial Function.” *Redox Biology*, vol. 1, no. 1, 2013, pp. 40–44, doi:10.1016/j.redox.2012.11.005.
- Shiva, Sruti, Michael N. Sack, et al. “Nitrite Augments Tolerance to Ischemia/Reperfusion Injury via the Modulation of Mitochondrial Electron Transfer.” *The Journal of Experimental Medicine*, vol. 204, no. 9, 2007, pp. 2089–102, doi:10.1084/jem.20070198.
- Shiva, Sruti, Tienush Rassaf, et al. “The Detection of the Nitrite Reductase and NO-Generating Properties of Haemoglobin by Mitochondrial Inhibition.” *Cardiovascular Research*, vol. 89, no. 3, 2011, pp. 566–73, doi:10.1093/cvr/cvq327.
- Skulachev, Vladimir P. “Mitochondrial Filaments and Clusters as Intracellular Power-Transmitting Cables.” *Trends in Biochemical Sciences*, vol. 26, no. 1, 2001, pp. 23–29, doi:10.1016/S0968-0004(00)01735-7.
- Son, M. J., et al. “Mitofusins Deficiency Elicits Mitochondrial Metabolic Reprogramming to Pluripotency.” *Cell Death and Differentiation*, vol. 22, no. 12, Nature Publishing Group, 2015, pp. 1957–69, doi:10.1038/cdd.2015.43.
- Song, Moshi, et al. “Mitochondrial Fission and Fusion Factors Reciprocally Orchestrate Mitophagic Culling in Mouse Hearts and Cultured Fibroblasts (with Supplemental Figures).” *Cell Metabolism*, vol. 21, no. 2, Elsevier Inc., 2015, pp. 273–85, doi:10.1016/j.cmet.2014.12.011.
- Soonpaa, M. H., et al. *S-Nitrosylation of Drp1 Mediates β -Amyloid – Related Mitochondrial Fission and Neuronal Injury*. no. April, 2009, pp. 102–06.
- Sorianello, Eleonora, et al. “The Promoter Activity of Human Mfn2 Depends on Sp1 in Vascular Smooth Muscle Cells.” *Cardiovascular Research*, vol. 94, no. 1, 2012, pp. 38–47, doi:10.1093/cvr/cvs006.
- Srihirun, Sirada, et al. “Platelet Inhibition by Nitrite Is Dependent on Erythrocytes and Deoxygenation.” *PLoS ONE*, vol. 7, no. 1, 2012, pp. 1–9, doi:10.1371/journal.pone.0030380.
- Stasch, Johannes Peter, et al. “No- and Haem-Independent Activation of Soluble Guanylyl Cyclase: Molecular Basis and Cardiovascular Implications of a New Pharmacological Principle.” *British Journal of Pharmacology*, vol. 136, no. 5, 2002, pp. 773–83, doi:10.1038/sj.bjp.0704778.
- Stokes, Karen Y., et al. “Dietary Nitrite Prevents Hypercholesterolemic Microvascular Inflammation and Reverses Endothelial Dysfunction.” *American Journal of Physiology-Heart and Circulatory Physiology*, vol. 296, no. 5, May 2009, pp. H1281–88, doi:10.1152/ajpheart.01291.2008.
- Stuehr, Dennis J. “Enzymes of the L-Arginine to Nitric Oxide Pathway.” *The Journal of Nutrition*, vol. 134, no. 10, Oct. 2004, pp. 2748S–2751S, doi:10.1093/jn/134.10.2748S.

- Sugiura, Ayumu, et al. "MITOL Regulates Endoplasmic Reticulum-Mitochondria Contacts via Mitofusin2." *Molecular Cell*, vol. 51, no. 1, Elsevier Inc., 2013, pp. 20–34, doi:10.1016/j.molcel.2013.04.023.
- Sutendra, Gopinath, et al. "Fatty Acid Oxidation and Malonyl-CoA Decarboxylase in the Vascular Remodeling of Pulmonary Hypertension." *Science Translational Medicine*, vol. 2, no. 44, 2010, doi:10.1126/scitranslmed.3001327.
- Sweet, David R., et al. "Krüppel-Like Factors in Vascular Inflammation: Mechanistic Insights and Therapeutic Potential." *Frontiers in Cardiovascular Medicine*, vol. 5, no. February, 2018, pp. 1–17, doi:10.3389/fcvm.2018.00006.
- Taguchi, Naoko, et al. "Mitotic Phosphorylation of Dynamin-Related GTPase Drp1 Participates in Mitochondrial Fission." *Journal of Biological Chemistry*, vol. 282, no. 15, 2007, pp. 11521–29, doi:10.1074/jbc.M607279200.
- Takahashi, Yu, et al. "Spatial and Temporal Pattern of Smooth Muscle Cell Differentiation during Development of the Vascular System in the Mouse Embryo." *Anatomy and Embryology*, vol. 194, no. 5, 1996, pp. 515–26, doi:10.1007/BF00185997.
- Tang, Haili, et al. "MARCH5 Overexpression Contributes to Tumor Growth and Metastasis and Associates with Poor Survival in Breast Cancer." *Cancer Management and Research*, vol. 11, 2019, pp. 201–15, doi:10.2147/CMAR.S190694.
- Tilokani, Lisa, et al. "Mitochondrial Dynamics: Overview of Molecular Mechanisms." *Essays in Biochemistry*, vol. 62, no. 3, 2018, pp. 341–60, doi:10.1042/EBC20170104.
- Totzeck, Matthias, et al. "Nitrite Circumvents Canonical CGMP Signaling to Enhance Proliferation of Myocyte Precursor Cells." *Molecular and Cellular Biochemistry*, vol. 401, no. 1–2, 2014, pp. 175–83, doi:10.1007/s11010-014-2305-y.
- Tourneau, Thierry Le, et al. "Role of Nitric Oxide in Restenosis after Experimental Balloon Angioplasty in the Hypercholesterolemic Rabbit: Effects on Neointimal Hyperplasia and Vascular Remodeling." *Journal of the American College of Cardiology*, vol. 33, no. 3, 1999, pp. 876–82, doi:10.1016/S0735-1097(98)00621-4.
- Uebelhoer, Melanie, and M. Luisa Iruela-Arispe. "Cross-Talk between Signaling and Metabolism in the Vasculature." *Vascular Pharmacology*, vol. 83, no. 2016, Elsevier Inc., 2016, pp. 4–9, doi:10.1016/j.vph.2016.06.002.
- Vallée, Alexandre, et al. "Metabolic Reprogramming in Atherosclerosis: Opposed Interplay between the Canonical WNT/ β -Catenin Pathway and PPAR γ ." *Journal of Molecular and Cellular Cardiology*, vol. 133, no. March, 2019, pp. 36–46, doi:10.1016/j.yjmcc.2019.05.024.
- van der Blik, a M., et al. "Mechanisms of Mitochondrial Fission and Fusion." *Cold Spring Harb Perspect Biol*, vol. 5, no. 6, 2013, pp. 1–16, doi:10.1101/cshperspect.a011072.

- Van Der Vliet, Albert, et al. "Formation of Reactive Nitrogen Species during Peroxidase-Catalyzed Oxidation of Nitrite: A Potential Additional Mechanism of Nitric Oxide-Dependent Toxicity." *Journal of Biological Chemistry*, vol. 272, no. 12, 1997, pp. 7617–25, doi:10.1074/jbc.272.12.7617.
- Vanin, A. F., et al. "Nitric Oxide Synthase Reduces Nitrite to NO under Anoxia." *Cellular and Molecular Life Sciences*, vol. 64, no. 1, 2007, pp. 96–103, doi:10.1007/s00018-006-6374-2.
- Vasquez-Trincado, César, et al. "Mitochondrial Dynamics, Mitophagy and Cardiovascular Disease." *The Journal of Physiology*, vol. 3, 2015, pp. 509–25, doi:10.1113/JP271301.
- Vavra, Ashley K., et al. "Insights into the Effect of Nitric Oxide and Its Metabolites Nitrite and Nitrate at Inhibiting Neointimal Hyperplasia." *Nitric Oxide - Biology and Chemistry*, vol. 25, no. 1, 2011, pp. 22–30, doi:10.1016/j.niox.2011.04.013.
- Wales, Jessica A., et al. "Discovery of Stimulator Binding to a Conserved Pocket in the Heme Domain of Soluble Guanylyl Cyclase." *Journal of Biological Chemistry*, vol. 293, no. 5, 2018, pp. 1850–64, doi:10.1074/jbc.RA117.000457.
- Wall, Valerie Z., et al. "Smooth Muscle Glucose Metabolism Promotes Monocyte Recruitment and Atherosclerosis in a Mouse Model of Metabolic Syndrome." *JCI Insight*, vol. 3, no. 11, 2018, doi:10.1172/jci.insight.96544.
- Walters, C. L., and A. Mc M. Taylor. "The Reduction of Nitrite by Skeletal-Muscle Mitochondria." *BBA Section Nucleic Acids And Protein Synthesis*, vol. 96, no. 3, 1965, pp. 522–24, doi:10.1016/0005-2787(65)90570-8.
- Wang, Li, et al. "Decreasing Mitochondrial Fission Diminishes Vascular Smooth Muscle Cell Migration and Ameliorates Intimal Hyperplasia." *Cardiovascular Research*, vol. 106, no. 2, 2015, pp. 272–83, doi:10.1093/cvr/cvv005.
- Wang, Ling, et al. "Normoxic Cyclic GMP-Independent Oxidative Signaling by Nitrite Enhances Airway Epithelial Cell Proliferation and Wound Healing." *Nitric Oxide - Biology and Chemistry*, vol. 26, no. 4, Elsevier Inc., 2012, pp. 203–10, doi:10.1016/j.niox.2012.03.002.
- Wasser, Katrin, et al. "Inflammation and In-Stent Restenosis: The Role of Serum Markers and Stent Characteristics in Carotid Artery Stenting." *PLoS ONE*, vol. 6, no. 7, 2011, pp. 3–8, doi:10.1371/journal.pone.0022683.
- Wassif, Heba, and Frederick G. P. Welt. "Restenosis." *SCAI Interventional Cardiology Board Review: Second Edition*, 2013, pp. 10–15, doi:10.1161/circinterventions.110.959882.
- Weitzberg, Eddie, and Jon O. Lundberg. "Novel Aspects of Dietary Nitrate and Human Health." *Annual Review of Nutrition*, vol. 33, no. 1, 2013, pp. 129–59, doi:10.1146/annurev-nutr-071812-161159.

- Westermann, Benedikt. "Bioenergetic Role of Mitochondrial Fusion and Fission." *Biochimica et Biophysica Acta - Bioenergetics*, vol. 1817, no. 10, Elsevier B.V., 2012, pp. 1833–38, doi:10.1016/j.bbabi.2012.02.033.
- . "Mitochondrial Fusion and Fission in Cell Life and Death." *Nature Reviews. Molecular Cell Biology*, vol. 11, 2010, pp. 872–84, doi:10.1038/nrm3013.
- Willems, Peter H. G. M., et al. "Redox Homeostasis and Mitochondrial Dynamics." *Cell Metabolism*, vol. 22, no. 2, Elsevier Inc., 2015, pp. 207–18, doi:10.1016/j.cmet.2015.06.006.
- Xiao, Qingzhong, et al. "Embryonic Stem Cell Differentiation into Smooth Muscle Cells Is Mediated by Nox4-Produced H₂O₂." *American Journal of Physiology - Cell Physiology*, vol. 296, no. 4, 2009, pp. 711–23, doi:10.1152/ajpcell.00442.2008.
- Xu, Qian, et al. "Redox Regulation of the Actin Cytoskeleton and Its Role in the Vascular System." *Free Radical Biology and Medicine*, vol. 109, no. February, 2017, pp. 84–107, doi:10.1016/j.freeradbiomed.2017.03.004.
- Xu, Zhonghui, et al. "SOX9 and Myocardin Counteract Each Other in Regulating Vascular Smooth Muscle Cell Differentiation." *Biochemical and Biophysical Research Communications*, vol. 422, no. 2, 2012, pp. 285–90, doi:10.1016/j.bbrc.2012.04.149.
- Yonashiro, Ryo, Satoshi Ishido, et al. "A Novel Mitochondrial Ubiquitin Ligase Plays a Critical Role in Mitochondrial Dynamics." *EMBO Journal*, vol. 25, no. 15, 2006, pp. 3618–26, doi:10.1038/sj.emboj.7601249.
- Yonashiro, Ryo, Yuya Kimijima, et al. "Mitochondrial Ubiquitin Ligase MITOL Blocks S-Nitrosylated MAP1B-Light Chain 1-Mediated Mitochondrial Dysfunction and Neuronal Cell Death." *Proceedings of the National Academy of Sciences of the United States of America*, vol. 109, no. 7, Feb. 2012, pp. 2382–87, doi:10.1073/pnas.1114985109.
- Youle, Richard J., and Derek P. Narendra. "Mechanisms of Mitophagy." *Nat Rev Mol Cell Biol*, vol. 12, no. 1, Nature Publishing Group, 2011, pp. 9–14, doi:10.1038/nrm3028.
- Yu, Tianzheng, et al. "Increased Production of Reactive Oxygen Species in Hyperglycemic Conditions Requires Dynamic Change of Mitochondrial Morphology." *Proceedings of the National Academy of Sciences of the United States of America*, vol. 103, no. 8, 2006, pp. 2653–58, doi:10.1073/pnas.0511154103.
- Zhai, Kui, et al. "β-Adrenergic cAMP Signals Are Predominantly Regulated by Phosphodiesterase Type 4 in Cultured Adult Rat Aortic Smooth Muscle Cells." *PLoS ONE*, vol. 7, no. 10, 2012, pp. 1–13, doi:10.1371/journal.pone.0047826.
- Zhang, Zhi, et al. "Human Xanthine Oxidase Converts Nitrite Ions into Nitric Oxide (NO)." *Biochemical Society Transactions*, vol. 25, no. 3, Aug. 1997, pp. 524S-524S, doi:10.1042/bst025524s.

- Zhao, Y., et al. "Inhibition of Soluble Guanylate Cyclase by ODQ." *Biochemistry*, vol. 39, no. 35, 2000, pp. 10848–54, doi:10.1021/bi9929296.
- Zheng, Bin, et al. "Role of Krüppel-like Factor 4 in Phenotypic Switching and Proliferation of Vascular Smooth Muscle Cells." *IUBMB Life*, vol. 62, no. 2, 2010, pp. 132–39, doi:10.1002/iub.298.
- Zhou, Wei, et al. "Mutation of the Protein Kinase A Phosphorylation Site Influences the Anti-Proliferative Activity of Mitofusin 2." *Atherosclerosis*, vol. 211, no. 1, Elsevier Ireland Ltd, 2010, pp. 216–23, doi:10.1016/j.atherosclerosis.2010.02.012.
- Zhuang, Jianhui, et al. "The Yin-Yang Dynamics of DNA Methylation Is the Key Regulator for Smooth Muscle Cell Phenotype Switch and Vascular Remodeling." *Arteriosclerosis, Thrombosis, and Vascular Biology*, vol. 37, no. 1, 2017, pp. 84–97, doi:10.1161/ATVBAHA.116.307923.
- Zollbrecht, Christa, et al. "Nitrite-Mediated Reduction of Macrophage NADPH Oxidase Activity Is Dependent on Xanthine Oxidoreductase-Derived Nitric Oxide but Independent of S-Nitrosation." *Redox Biology*, vol. 10, no. September, Elsevier, 2016, pp. 119–27, doi:10.1016/j.redox.2016.09.015.
- Zorova, Ljubava D., et al. "Mitochondrial Membrane Potential." *Analytical Biochemistry*, vol. 552, Elsevier Inc, 2018, pp. 50–59, doi:10.1016/j.ab.2017.07.009.
- Zuckerbraun, Brian S., et al. "Nitrite Potently Inhibits Hypoxic and Inflammatory Pulmonary Arterial Hypertension and Smooth Muscle Proliferation via Xanthine Oxidoreductase-Dependent Nitric Oxide Generation." *Circulation*, vol. 121, no. 1, Jan. 2010, pp. 98–109, doi:10.1161/CIRCULATIONAHA.109.891077.